Norwegian University of Life Sciences

Master's Thesis 2020 **60 ECTS**

Department of Medical Genetics, Oslo University Hospital, Ullevål

THE ROLE OF COAGULATION FACTOR V IN BREAST CANCER: EFFECT ON TREATMENT RESPONSE

Sara Marie Lind
Biotechnology

THE ROLE OF COAGULATION FACTOR V IN BREAST CANCER: EFFECT ON TREATMENT RESPONSE

Oslo University Hospital,
Department of Medical Genetics

and

The Norwegian University of Life Sciences,
Faculty of Chemistry, Biotechnology and Food Sciences

Acknowledgements

The work described in this thesis was performed at the Department of Medical Genetics, Oslo University Hospital Ullevål as a part of the master program in Biotechnology at the Norwegian University of Life Science (NMBU) at the Faculty of Chemistry, Biotechnology and Food Science (KBM) from August 2020 to June 2021.

I would like to direct my gratitude to my supervisor Dr. Philos Nina Iversen for the opportunity to participate in this project and for all the support and guidance throughout the year. I would like to thank Department Engineer Marit Sletten for all help and guidance in the laboratory. I would also like to thank Ph.D Mari Tinholt for all advices and constructive feedback. I would like to thank Scientist Xavier Tekpli for providing me datasets and advises for analyzing them. Finally, I would like to thank my internal supervisor at NMBU, Prof. Harald Carlsen, at the Faculty of Chemistry, Biotechnology and Food Science.

Moreover, I would like to acknowledge with gratitude, the support, encouragement and love from my family through the work with this thesis. I especially want to thank my two boys, Luka and William, for being patient with me and continually providing requisite breaks filled with love and joy.

June 2021

Sara Marie Lind

Sammendrag

Sammenhengen mellom kreft og koagulasjon er vel etablert og det er kjent at kreftpasienter har en økt risiko for å utvikle trombose. Kreftceller kan ofte uttrykke koagulasjonsfaktorer som fører til ubalanse i hemostasen og som igjen kan føre til en protrombotisk tilstand. Det er oppdaget at koagulasjonsfaktor V (FV) uttrykkes i brystkrefttumorer, men hvilke mekanismer den har i kreftprogresjon er fremdeles ikke kjent. Ved å få en bedre forståelse av de molekylære mekanismene bak sammenhengen mellom kreft og koagulasjon kan en mer individuell behandling for både kreft og trombose i kreftpasienter bli mulig.

Målet for denne oppgaven var å få en bedre forståelse for mekanismene til FV i kreftprogresjon. Behandlingsrespons til neoadjuvant kjemoterapi i brystkreftpasienter ble studert gjennom analyser av kliniske datamaterialer. Effekten til kjemoterapi på koagulasjonsfaktor V mRNA (*F5*)-uttrykket, reguleringen av *F5* og de funksjonelle effektene til FV ble studert *in vitro* i brystkreftcellelinjer.

Analysene av de kliniske datamaterialene avslørte en assosiasjon mellom økt *F5*-utrykk og behandlingsrespons til neoadjuvant kjemoterapi i to av pasientkohortene. I begge kohortene hadde pasientene blitt behandlet med kjemoterapi bestående av en kombinasjon av 5-fluorouracil, epirubicin og cyclophosphamide. I brystkreftcellelinjer førte separat behandling med 5-fluorouracil, epirubicin og doxorubicin til økt *F5*-uttrykk. Blant virkningsmekanismene til kjemoterapiene som ble assosiert med økt *F5*-uttrykk er induksjon av tumorprotein p53 (p53) aktivitet involvert. Rollen til p53 i reguleringen av *F5* ble derfor studert. Både hemming av p53 og nedslåing av p53 genet resulterte i reduksjon av doxorubicin-indusert *F5*-utrykk. Mutasjoner i to mulige p53 bindingsseter i *F5*-promoteren i et luciferaseplasmid førte til en redusert luciferaseaktivitet i celler behandlet med doxorubicin. De funksjonelle effektene til FV på apoptose og proliferasjon ble studert i MDA-MB-231 celler. FV alene forårsaket økt apoptose og FV kombinert med aktivert protein C førte til redusert proliferasjon. Dette indikerte at FV hadde en antitumor effekt og at en av mekanismene bak kunne være gjennom hemming av vevsfaktor-mediert proteaseaktivert reseptor 2-aktivering. I tillegg forsterket FV effekten til doxorubicin ytterligere i brystkreftceller og kan da være involvert i effekten av økt *F5*-uttrykk på behandlingsrespons som ble funnet i de kliniske datamaterialene.

Resultatene indikerer en assosiasjon mellom FV og behandlingsrespons til neoadjuvant kjemoterapi, en induksjon av *F5* ved behandling med flere typer kjemoterapi, en rolle for p53 i reguleringen av *F5*, en antitumor effekt for FV og støttet at effekten til FV kunne være gjennom det postulerte hemmingskomplekset for T vevsfaktor-mediert proteaseaktivert reseptor 2-aktivering.

Abstract

The link between cancer and coagulation is well established and it is documented that cancer patients have an increased risk for developing thrombosis. Cancer cells themselves often express coagulation factors, which causes imbalances in hemostasis resulting in a prothrombotic condition. Coagulation factor V (FV) is found to be expressed in breast cancer tumors, but the mechanisms of FV in cancer progression are not yet determined. By understanding the molecular mechanisms behind the link between cancer and coagulation, it may be possible to provide a more individualized treatment for both cancer and thrombosis in cancer patients.

The aim of this thesis was to gain a better understanding of the mechanisms of FV in the context of cancer progression. Treatment response to neoadjuvant chemotherapy in breast cancer patients was studied by analyses of clinical data materials. The effect of chemotherapy on coagulation factor V mRNA (*F5*) expression, the regulation of *F5* and the functional effects of FV were studied in *in vitro* experiments in breast cancer cell lines.

Analyses of the clinical data material revealed an association between an elevated *F5* expression and treatment response to neoadjuvant chemotherapy in two cohorts. In both cohorts the patients received a combination chemotherapy with 5-fluorouracil, epirubicin and cyclophosphamide. Separate treatment with 5-fluorouracil, epirubicin and doxorubicin resulted in an increased expression of *F5* in breast cancer cell lines. The mechanism of action of the chemotherapies associated with increased expression of *F5* is involved in induction of p53 activity. The role of p53 in the regulation of *F5* was thus studied. Inhibition of p53 and knockdown of the coagulation factor V gene resulted in a reduction in doxorubicin induced *F5* expression. Mutation of two putative p53 sites in the *F5* promoter in a luciferase plasmid, resulted in a reduction in luciferase activity in cells treated with doxorubicin. The functional effects of FV were studied on apoptosis and proliferation in MDA-MB-231 cells. FV alone caused an increase in apoptosis and FV combined with activated protein C led to a decrease in proliferation. This indicated an antitumor effect of FV, and one mechanism involved may be the inhibition of tissue factor-induced protease activated receptor 2 activation. Moreover, FV facilitated the doxorubicin effect in breast cancer cells further which may also be involved in

the treatment response in patients with elevated *F5* expression documented in the clinical data materials.

The results indicated an association between FV and treatment response to neoadjuvant chemotherapy, an induction of *F5* by several chemotherapies, a role of p53 in the regulation of *F5*, an antitumor effect of FV and supported the effect of FV through the postulated inhibition complex of tissue factor-induced protease activated receptor 2 activation.

Abbreviations

APC	Activated Protein C
asTF	Alternatively Spliced Tissue Factor
Bp	Base Pair
cDNA	Complementary DNA
ddNTP	Dideoxyribonucleotide Triphosphate
DNA	Deoxyribonucleic Acid
dNTP	Deoxyribonucleotide Triphosphate
dsRNA	Double Stranded RNA
dTMP	Deoxythymidine Monophosphate
dUMP	Deoxyuridine Monophosphate
ELISA	Enzyme-Linked Immunosorbent Assay
EPCR	Endothelial Cell Protein C Receptor
ER	Estrogen Receptor
F5	Coagulation Factor V Gene
FBS	Fetal Bovine Serum
FdUDP	Fluorodeoxyuridine Diphosphate
FdUMP	Fluorodeoxyuridine Monophosphate
FIXa	Activated Coagulation Factor IX
flTF	Full-Length Tissue Factor
FUDP	Fluorouridine Diphosphate
FUDR	Fluorodeoxyuridine
FUMP	Fluorouridine Monophosphate
FV	Coagulation Factor V
FVa	Activated Coagulation Factor V
FVII	Coagulation Factor VII
FVIIa	Activated Coagulation Factor VII
FVIII	Coagulation Factor VIII
FX	Coagulation Factor X
FXa	Activated Coagulation Factor X
FXIa	Activated Coagulation Factor XI
FXIIa	Activated Coagulation Factor XII
GAPDH	Glyceraldehyde-3-Phosphate Dehydrogenase
HER2	Human Epidermal Growth Factor Receptor 2
HPRT1	Hypoxanthine Phosphoribosyltransferase
IGF-1	Insulin-like Growth Factor-1
IL-8	Interleukin-8
Kb	Kilo Bases
kDA	Kilodalton
LAR II	Luciferase Assay Reagent II

LB	Lysogeny Broth
MDM2	Murine Double Minute-2
Microparticle	MP
miRNA	MicroRNA
OPRT	Orotate Phosphoribosyltransferase
p53	Tumor Protein p53
PAR	Protease-Activated Receptors
PCR	Polymerase Chain Reaction
pCR	Pathologic Complete Response
PLB	Passive Lysis Buffer
PR	Progesterone Receptor
PS	Protein S
RIPA	Radioimmunoprecipitation Assay
RISC	RNA-Induced Silencing Complex
RNA	Ribonucleic Acid
RNAi	RNA Interference
RT-qPCR	Real Time Quantitative Transcription Polymerase Chain Reaction
siRNA	Small Interfering RNA
SNP	Single Nucleotide Polymorphism
TF	Tissue Factor
TFPI	Tissue Factor Pathway Inhibitor
TP53	Tumor Protein p53 Gene
TS	Thymidylate Synthase
UK	Uridine Kinase
UP	Uridine Phosphorylase
VEGF	Vascular Endothelial Growth Factor
VEGF-A	Vascular Endothelial Growth Factor A
VEGF-B	Vascular Endothelial Growth Factor B
VEGFR-2	Vascular Endothelial Growth Factor Receptor 2
vWF	Von Willebrand Factor
gDNA	Genomic DNA

Table of contents

1. INTRODUCTION

1.1 CANCER

With over 18 million new cases of cancer worldwide and about 9.6 million deaths in 2018, cancer is the second leading cause to death in the world (WHO, 2019). It is predicted that if recent trends in cancer incidents and population growth continues, there will be about 27.5 million new cases of cancer worldwide by 2040 each year (WHO, 2019).

1.1.1 HALLMARKS OF CANCER

Normal cells communicate closely with each other and have a collective behavior for tissue-specific functions. The interaction enables a tightly regulated balance between cell proliferation and cell death. Cancer cells, on the other hand, are cells where this balance is not properly working, leading to uncontrolled behavior and proliferation. The cells form a tumor, and if the tumor gain the ability to invade neighboring tissue, it is malignant and thus called cancer. Malignant cancer cells can also metastasize to distant organs in the body (Weinberg, 2014).

Cancer cells gradually undergo alterations which provides new characteristics that differ from the tissue they are a part of. The changes enable survival, tumor growth and metastatic dissemination despite the malfunction of the cells. The alteration is carried out by eight biologic capabilities which cancer cells acquire. The eight hallmarks of cancer consists of sustaining proliferative signaling, evading growth suppressors, avoiding immune destruction, enabling replicative immortality, activating invasion and metastasis, inducing angiogenesis, resisting cell death and deregulating cellular energetics (Figure 1) (Hanahan & Weinberg, 2015).

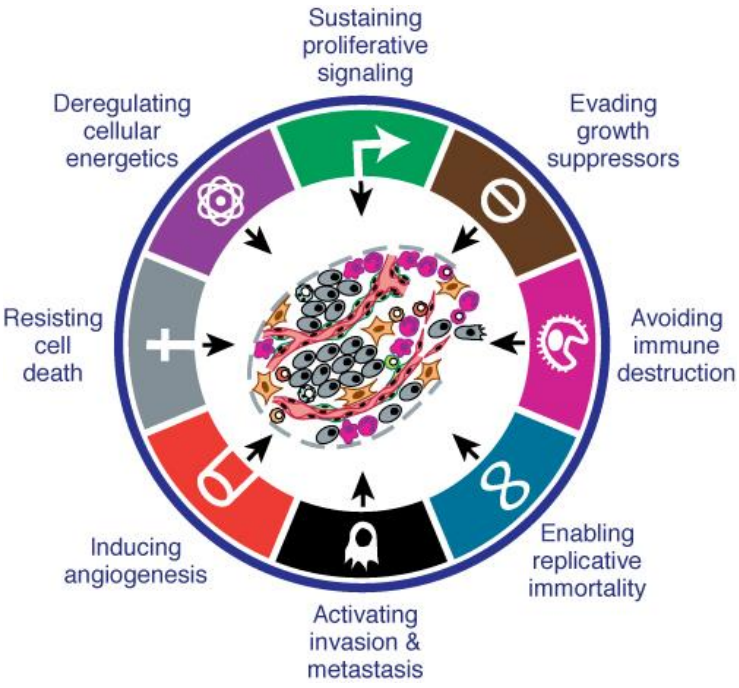

Figure 1: The hallmarks of cancer *(Hanahan & Weinberg, 2015)*

Sustaining proliferative signaling involves the ability for the cancer cells to chronic proliferate by manipulate the regulation system. This can be performed by increasing the number of receptor proteins for growth factor ligands and growth factors, or generation of structural alterations in the receptor molecule leading to ligand-independent firing (Hanahan & Weinberg, 2015).

Evading growth suppressors involves the ability to circumvent negative regulation of cell proliferation. For example, evading the tumor protein p53 (p53), which is encoded by a prototypical suppressor gene and have a central role in deciding whether cells should proliferate or undergo growth arrest, apoptosis or senescence, is advantageous for tumor progression (Hanahan & Weinberg, 2015).

Avoiding immune destruction is performed to avoiding being detected by the immune system or reduce the scope of immunological killing. Cancer cells can prevent natural killer cells and cytotoxic T lymphocytes by generating and secreting immunosuppressive factors and ligands (Hanahan & Weinberg, 2015).

Enabling replicative immortality involves the property of cancer cells to have an unlimited number of replications. It is indicated that telomeres, which are expressed in cancer cells, are involved in the replicative immortality by protecting the chromosome ends and thus prevent crisis (Hanahan & Weinberg, 2015).

Activation of invasion and metastasis are initiated with local invasion by cancer cells and may eventually end in colonization and growth to a macroscopic tumor. This is possible due to alteration of cancer cells, like the loss of the cell-to-cell adhesion molecule E-cadherin which is an antagonist of invasion and metastasis (Hanahan & Weinberg, 2015).

Inducing angiogenesis is necessary for the supply of oxygen and nutrition as well as remove carbon dioxide and metabolic wastes for all cells in the body. In tumor cells, angiogenesis is almost consistently switched on which allows the expanding growth of the tumor. For example,

vascular endothelial growth factor-A (VEGF-A) is a prototype for inducing angiogenesis (Hanahan & Weinberg, 2015).

Resisting cell death is performed in cancer cells by attenuation or inactivation of the latent apoptotic cell-death program. The most common strategy for cancer cells to resist cell death is loss of p53 function, or damage of sensors in the apoptose inducing circuitry (Hanahan & Weinberg, 2015).

Deregulating cellular energetics includes the adjustment in the energy metabolism, which is necessary to supply sufficient energy to support cell growth and division of cancer cells. By favoring aerobic glycolysis and increase the level of glucose transporters, cancer cells ensure increased amounts of glycolytic intermediates which are needed in biosynthetic pathways (Hanahan & Weinberg, 2015).

1.1.2 BREAST CANCER

Breast cancer is the most common cancer type for women, and the among the two most common cancer types generally (Momenimovahed & Salehiniya, 2019; WHO, 2019).

Breast cancer is a disease with great biological diversity and molecular complexity. It consists of heterogenic group of lesions which can vary in pathological features, clinical presentation and prognosis (Breastcancer.org, 2020). Molecular analyses with gene expression profiling conducted in several studies, have classified breast cancer into different subtypes (Perou et al., 2000; Sørlie et al., 2001). It has also been using techniques like immunohistochemistry for defining breast cancer subtypes, as well as gene expression profiling (Fragomeni et al., 2018). The major subgroups determined includes luminal A type, luminal B type, triple negative/basal-like type, human epidermal growth factor receptor 2 (HER2)-enriched type and normal-like type (Breastcancer.org, 2020). Stratification of the various cancer subtypes has become critical for characterization of the disease (Fragomeni et al., 2018).

Subgroup characterizing is partly determined of the status of HER2 and hormone-receptors. If the estrogen-receptor or/and the progesterone-receptor are present the cell is considered as

hormone-receptor positive, and if none of the two are present the cell is considered as hormone-receptor negative (Breastcancer.org, 2020; Yersal & Barutca, 2014).

Luminal A type of breast cancer is HER2 negative and hormone-receptor positive. It has low levels of protein Ki-67 which is involved in the growth rate of the cells. This subtype has slow growth, which makes it a low-grade cancer with the best prognosis of the subtypes (Breastcancer.org, 2020).

Luminal B type of breast cancer is either HER2 negative or HER2 positive and hormone-receptor positive. It has high levels of protein Ki-67 and has a growth rate slightly faster than the luminal A subtype as well as a slightly worse prognosis (Breastcancer.org, 2020).

Triple-negative/basal-like type of breast cancer is HER2 negative and hormone-receptor negative. This subtype is associated with mutations in breast cancer gene 1 (Breastcancer.org, 2020).

HER2-enriched type of breast cancer is HER2 positive and hormone-receptor negative. This subtype commonly has a more rapid cell growth and a worse prognosis than the luminal subtypes. Treatment of this cancer subtype is often successfully achieved with targeted therapies against the HER2 protein (Breastcancer.org, 2020).

Normal-like type of breast cancer is, similar to luminal A subtype, HER2 negative and hormone-receptor positive as well as low levels of protein Ki-67. The prognosis is slightly worse than the luminal A subtype prognosis (Breastcancer.org, 2020).

1.1.3 CANCER AND THROMBOSIS

The fact that cancer patients have an increased risk of developing thrombosis has been known for over a century. The risk of developing venous thrombosis is measured to be four- to sevenfold, but the risk of developing all other types of thrombotic events is also increased. Cancer patients suffering from venous thrombosis, often develope the illness within three months after diagnosis (Soff, 2019). Cancer patients with venous thrombosis have a poor

prognosis, and deaths caused by thromboembolism is one of the most common among cancer patients (Khorana et al., 2007; Königsbrügge et al., 2014).

The increased risk for thrombosis is caused by a complex composition of various components. This consists of general and biologic clinical risk factors, which are present in both cancer and non-cancer patients, in addition to the disease specific general and biological risk factors in patients with malignancy. Cancer cells often express several procoagulant properties like microparticles (MPs), procoagulant proteins, fibrinolysis proteins and coagulation factors. This causes imbalances in the hemostasis, which leads towards a prothrombotic condition (Soff, 2019).

Different types of cancers have different risks for developing thrombosis. Hematological, lung, gastrointestinal and brain cancer are associated with a high risk of thrombosis, while prostate and breast cancer are associated with a low risk of thrombosis. Despite the low risk in prostate and breast cancers, it is common to observe thrombosis in these cancer types because they are the most common cancer types worldwide (Fernandes et al., 2019).

It is clinically relevant to prevent the development for thrombosis in cancer patients for reducing morbidity, hospitalizations and mortality (Soff, 2019). In addition to this it is also relevant in an economical aspect.

1.2 Chemotherapy in cancer treatment

1.2.1 Chemotherapy

Traditional cancer therapies, like surgery, chemotherapy and radiation, are still the most common therapies despite the emergence of new promising treatments (Arruebo et al., 2011). Unfortunately, both surgery and chemotherapy pose a major risk for developing both venous thrombosis and bleeding in cancer patients (Kwaan & Vicuna, 2007; Königsbrügge et al., 2014).

Chemotherapy had its origin in the early 20th century. In the 1930s, chemotherapy used for treatment of cancer began. Since then, there has been developed several different

chemotherapy drugs for fighting different types of cancer and it is used as primary- as well as neoadjuvant and adjuvant treatment (Arruebo et al., 2011).

Chemotherapy is an aggressive drug, targeting rapidly proliferating cells in the body. It is suitable in cancer treatment, because cancer cells proliferate faster than most healthy cells in the body. Chemotherapy is a systemic treatment, which means that it is transported through the bloodstream and easily can reach almost all tissues in the body (Corrie, 2007).

A major drawback is the non-specificity of chemotherapy agents (Corrie, 2007). Although cancer cells proliferate faster than most healthy cells, chemotherapy will also affect healthy tissue. In particularly this applies to the continuously dividing cells with rapid turnover like the skin, hair, bone marrow, mucous membrane cells and the lining of the digestive system (CancerResearchUK, 2020; Khleif et al., 2016).

1.2.2 CHEMOTHERAPY – MECHANISM OF ACTION

1.2.2.1 Doxorubicin:

Doxorubicin is a part of the anthracycline group of chemotherapy agents and is a systemic medication used in cancer treatment. It is considered to have a great treatment potential, as well as one of the most potent chemotherapeutic drugs approved by the Food and Drug Administration (Carvalho et al., 2009). The effectivity of doxorubicin has been appreciated for several decades (Tacar et al., 2013).

At the cellular level, doxorubicin has several functions. Generation of free radicals, leading to damage of deoxyribonucleic acid (DNA) strands and oxidation of membrane lipids, causes damages at the cell. Intercalation of doxorubicin between nitric bases of the DNA helix, causes inhibition of DNA-dependent DNA and ribonucleic acid (RNA) polymerases which in turn results in damage to the repair mechanisms of DNA and suppression of RNA and DNA synthesis. It can also interference with helicase and DNA unwinding activity, inhibit of the enzymes in the respiratory chain in mitochondria, and inhibition of topoisomerase II which results in the induction of apoptosis. Additionally, doxorubicin is known to induce p53 activity, which facilitates the death of cancer cells. The mechanisms are summarized in Figure 2 (Czeczuga-Semeniuk et al., 2004; Pilco-Ferreto & Calaf, 2016).

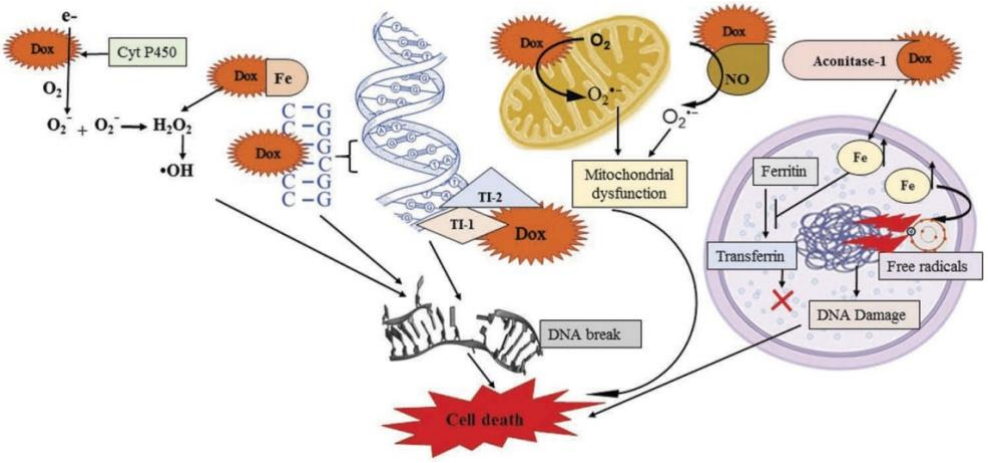

Figure 2: Doxorubicin – Mechanisms of action (Aniogo et al., 2017).

1.2.2.2 Epirubicin:

Epirubicin is a 4´-epimer of doxorubicin. Similar to doxorubicin, epirubicin is also a part of anthracycline group of chemotherapy agents and functions through the same mechanisms as doxorubicin. The molecular difference between the drugs is the epimerization of the hydroxyl group located in the fourth position in the daunosamine ring (Figure 3). It is suggested that the efficiency for the drugs is similar, but epirubicin has been shown to have a more favorable toxicity profile, making it possible to use higher doses in cancer treatment compared to doxorubicin (Khasraw et al., 2012).

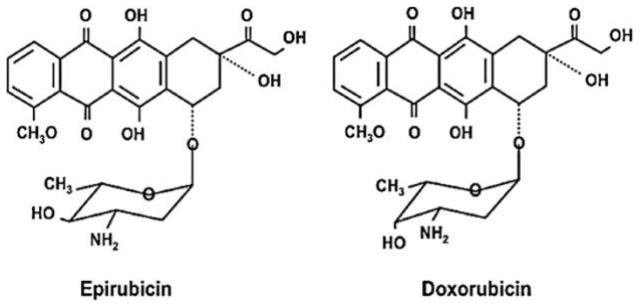

Figure 3: The molecular structure of epirubicin and doxorubicin (Khasraw et al., 2012).

1.2.2.3 5-fluorouracil:

5-fluorouracil is an antimetabolite drug, commonly used in treatment of several cancer types including breast cancer. Inside the cell, 5-fluorouracil can have several outcomes. The thymidine phosphorylase (TP) can convert 5-fluorouracil to fluorodeoxyuridine (FUDR) which

again can be converted to fluorodeoxyuridine monophosphate (FdUMP) by thymidine kinase (TK). FdUMP inhibits the nucleotide synthetic enzyme thymidylate synthase (TS). TS acts as a catalyzer for the reductive methylation of deoxyuridine monophosphate (dUMP) to deoxythymidine monophosphate (dTMP). This is the only de novo source of thymidylate which is critical for replication and repair of DNA (Caminiti et al., 2020; Longley et al., 2003).

5-fluorouracil can also be converted to fluorouridine monophosphate (FUMP) directly by orotate phosphoribosyltransferase (OPRT) or indirectly via conversion to fluorouridine by uridine phosphorylase (UP) and to FUMP by uridine kinase (UK). Phosphorylation converts FUMP to fluorouridine diphosphate (FUDP) which can be incorporated into RNA leading to RNA damage. FUDP can also be converted to fluorodeoxyuridine diphosphate (FdUDP) by ribonucleotide reductase (RR) and can either be incorporated into DNA and cause DNA damage or be converted to FdUMP and lead to TS inhibition (Caminiti et al., 2020; Longley et al., 2003). The mechanisms are summarized in Figure 4. Additionally, 5-fluorouracil is known to induce p53 activity, which facilitates the death of cancer cells.

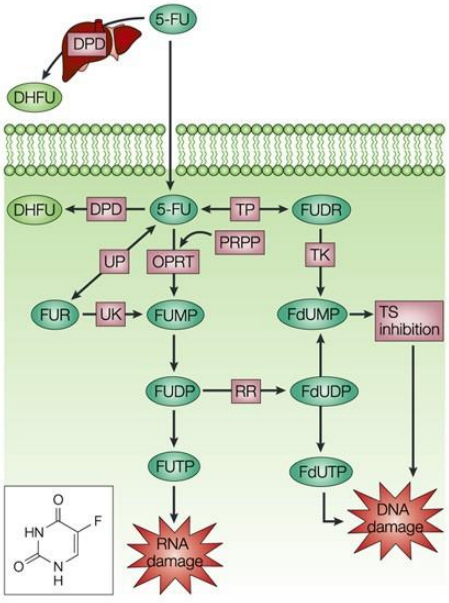

Figure 4: 5-fluorouracil – Mechanisms of action (Longley et al., 2003).

1.2.2.4 Cyclophosphamide:

Cyclophosphamide is used as chemotherapy for a wide range of cancer types. It is an alkylating agent of the nitrogen mustard type which alkylates DNA, causing in cross-linking of DNA or RNA strands and thereby inhibition of protein synthesis (BC Cancer Agency Cancer Drug Manual©,

2013). Cyclophosphamide is activated by hydroxylation to 4-hydroxycyclophosphamide by the liver enzymes like cytochrome P450 2B. 4-hydroxycyclophosphamide is metabolized to aldophosphamide which subsequently is cleaved and converted to the toxic, alkylating agents phosphoramide mustard and acrolein (Ogino & Tadi, 2020). The mechanisms are summarized in Figure 5.

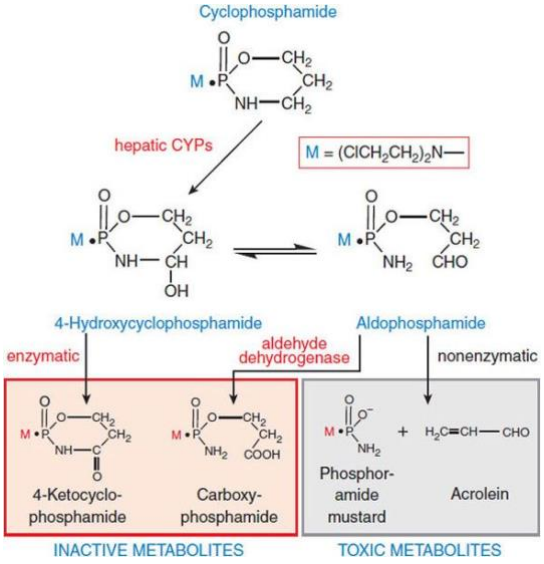

Figure 5: Cyclophosphamide – Mechanisms of action (PHARMACY, 2016).

1.2.2.5 Bevacizumab:

Cancer cells are highly metabolic active and angiogenesis, the generation of new capillary blood vessels, is crucial to cover the need for oxygen and nutrition in the growing tumor. Bevacizumab can be used in combination with chemotherapy and is a monoclonal antibody targeting VEGF-A (Montero et al., 2012). VEGF-A is a cytokine produced by benign stromal cells and cancer cells and is especially induced by the transcription factor hypoxia-inducible factor-1 in conditions of decreased access to oxygen. Binding to the extracellular endothelial tyrosine kinase receptor vascular endothelial growth factor receptor 2 (VEGFR-2), VEGF-A induce dimerization and autophosphorylation which initiates the intracellular downstream signal-transduction pathways (Figure 6). The vascular endothelial growth factor (VEGF) pathways result in, among other things, vascular permeability, survival, proliferation, migration and angiogenesis. Bevacizumab inhibits this process by binding to the most critical initiator, VEGF-A (Kanat & Ertas, 2019; Kazazi-Hyseni et al., 2010).

Other members of the VEGF family like vascular endothelial growth factor B (VEGF-B) and placental growth factor and their specific VEGF receptor has supportive roles in the angiogenesis process.

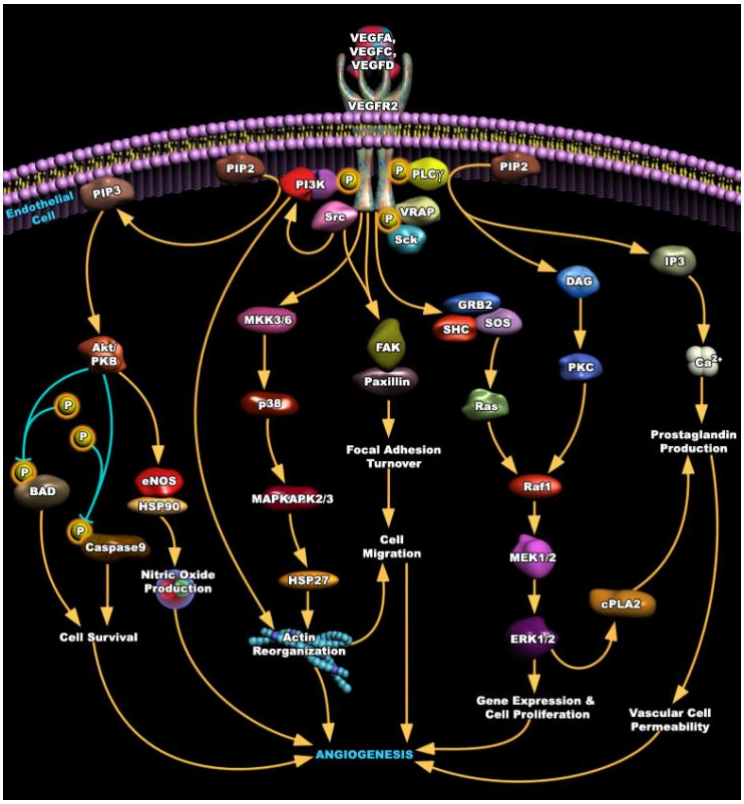

Figure 6: Overview of the VEGFR-2 pathway (BioLegend, 2008).

1.2.3 Chemotherapy and p53

p53 is a tumor suppressor and is often called "the guardian of the genome". It has an important role in inhibition of proliferation in malfunctional cells (Weinberg, 2014). Several of the genotoxic drugs used in cancer treatment activates p53 (Fritsche et al., 1993; Kastan et al., 1991; Zhan et al., 1993). The activated p53 plays an important role in the killing of cancer cells.

Normal and healthy cells usually have low levels of p53, due to rapid degradation of the protein. The p53 level is increased under several pathological conditions like DNA damage, hypoxia, oxidative stress, osmotic stress and shortening or loss of telomers. It is suggested that the levels of p53 may also be increased by intense and uncoordinated regulatory signals, so strong that the cells normal limit is reached, resulting in breakdown of the control mechanisms

and coordination of the cell. Under these circumstances, p53 can either induce temporary cell arrest for reparation of the damage, permanent cell arrest (senescence), or apoptosis. In this way, p53 is responsible for preventing damaged cells to proliferate (Alberts et al., 2015).

Cancer cells often acquire properties to avoid the p53-pathway. p53 acts primarily as a transcription regulator. It binds to the p53-bindings sites at the DNA as a tetramer, and a mutation in just one of the subunits can potentially by enough to inhibit its functions (Alberts et al., 2015). Mutations in the tumor protein p53 gene (*TP53*) are found in approximately 50% of all cancer incidents, which are the highest proportion among known cancer-critical genes (Alberts et al., 2015). A large part of the other cancer incidents lacks expression of the ADP-ribosylation factor protein, which normally binds and inhibit murine double minute-2 (Mdm2). The role of Mdm2 is to inhibit p53, and the lack of inhibition of Mdm2 results in decreased activity of p53 (Figure 7) (Weinberg, 2014). Cancer cells may also use strategies like overexpression of Mdm2 or mislocation of p53 to the cytoplasm where it cannot function as a transcription regulator (Weinberg, 2014).

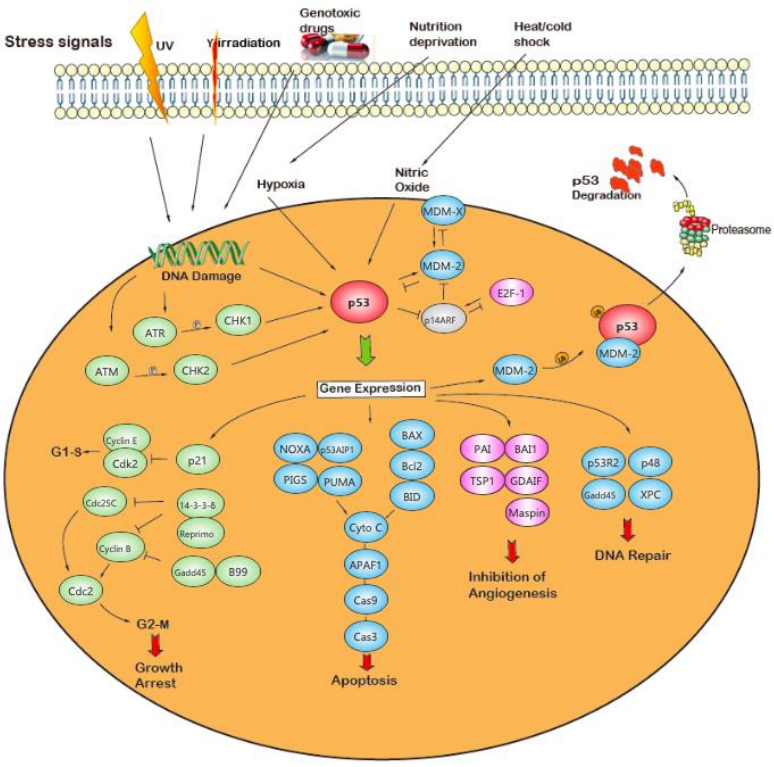

Figure 7: Overview of the p53 signaling pathway (Creative Diagnostics).

In chemotherapy treatment of several cancer types, the status of p53 seems to be important for treatment response. Wildtype p53 increases the sensitivity to chemotherapeutic agents by inducing apoptosis by both transcription independent mechanisms, and transcriptional mechanisms like activation of apoptotic genes. In contrast, p53 may also decrease the sensitivity by induction of growth arrest, DNA repair and differentiation, as well as transcriptional mechanisms by activation of antiapoptotic genes (Weller, 1998).

The sensitivity to chemotherapeutic agents varies, among other things, due to single-nucleotide polymorphisms (SNPs) in *TP53*. Several studies have demonstrated that a SNP in *TP53* exon 4, which results in either arginine (72R) or proline (72P) in codon 72, has significant impact of sensitivity of several chemotherapeutic agents *in vitro* and *in vivo* (Sullivan et al., 2004; Xu et al., 2005). Several studies have found that the 72P type of p53 mainly causes cell cycle arrest, while the 72R type causes extensive apoptosis in cancer cells (Dumont et al., 2003; Sullivan et al., 2004).

TP53 is the gene with the highest frequency of mutations in human cancers (Hollstein et al., 1997). Many studies have pinpointed that mutation in p53 results in decreased sensitivity to therapy (Lowe & Jacks, 1997; Rusch et al., 1995; Wattel et al., 1994). This can be explained by the loss of p53 activity. Nevertheless, a study conducted by Blandino et al. (1999) showed that some of the mutations in p53 actually constituted a protective effect against apoptosis induced by chemotherapeutic agents in a drug- and mutation-specific matter. These p53 gain of function mutations may contribute to a decreased response to chemotherapy (Blandino et al., 1999).

1.3 Chemotherapy and coagulation

Chemotherapy is the main therapy in several cancer types, and it is well established that chemotherapeutic agents may lead to coagulation disturbances resulting in coagulation disorders in cancer patients (Kvolik et al., 2010).

Chemotherapeutic agents can affect the functions of the liver, causing a decrease in production of both anticoagulant and procoagulant factors and thus a disturbance in the

coagulation system which could lead to bleeding or thrombosis (Kvolik et al., 2010). The platelet synthesis is affected in most of chemotherapeutic treatments by diminished platelet synthesis, which leads to thrombocytopenia and thus an increased risk for bleeding (Kuter, 2015).

Injury of endothelial cells caused by chemotherapeutic agents may lead to a loss of antithrombotic properties, and it is suggested that this may play a role in the increased risk for venous thrombosis. Although the side effects of chemotherapeutic treatment are reversible, the endothelial lesions caused by chemotherapeutic agents may last for several years (Kvolik et al., 2010).

Chemotherapeutic agents also leads to increased expression of procoagulant tissue factor (TF), phosphatidylserine and circulating MPs which are important factors to promote coagulation (Falanga et al., 2013).

1.4 Hemostasis and coagulation

Hemostasis is the cascade of events that prevent bleeding after injury. A complex balance between the pro coagulation pathway and mechanisms that inhibit the same pathway, is necessary for maintaining an appropriate and regulated hemostasis (Palta et al., 2014). The different components which promotes hemostasis, consist of a heterogeneous and complex group of procoagulants like glycosaminoglycans, platelets, as well as plasma-borne and cell-associated proteins (Crawley, 2011). Abnormalities in the coagulation pathway regulation can lead to either bleeding or thrombosis (Palta et al., 2014).

1.4.1 Primary hemostasis

The primary hemostasis is the first step in hemostasis. This involves the formation of the initial platelet plug as a result of multiple complex interactions between the vessel wall, platelets and several adhesive proteins (Palta et al., 2014).

1.4.2 The cascade model of coagulation

The cascade model of coagulation is based on a series of proenzymes which activates downstream enzymes (Palta et al., 2014). This is due to enzymes that cleaves zymogen substrates and activates the next enzyme in the cascade (Smith, 2009).

The coagulation cascade can be affected by the intrinsic or the extrinsic pathway. The extrinsic pathway is initiated with a tissue trauma, either by a trauma to the vascular wall or the extravascular tissue. This leads to the release of TF. The intrinsic pathway is initiated by factors which causes trauma to the blood cells, or the exposure of blood cells to collagen. Both pathways leads to activation of coagulation factor X (FX). This causes the conversion from prothrombin to thrombin followed by the conversion of fibrinogen to fibrin (Adams & Bird, 2009). Fibrin acts as a molecular scaffold, which strengthens the platelet plug and allows the other repair mechanisms to operate (Crawley, 2011). An overview of the coagulation pathway is shown in Figure 8.

The cascade model is useful for understanding plasma-based *in vitro* coagulation. Still, it has deficiencies and is not sufficient for understanding coagulation *in vivo* (Smith, 2009).

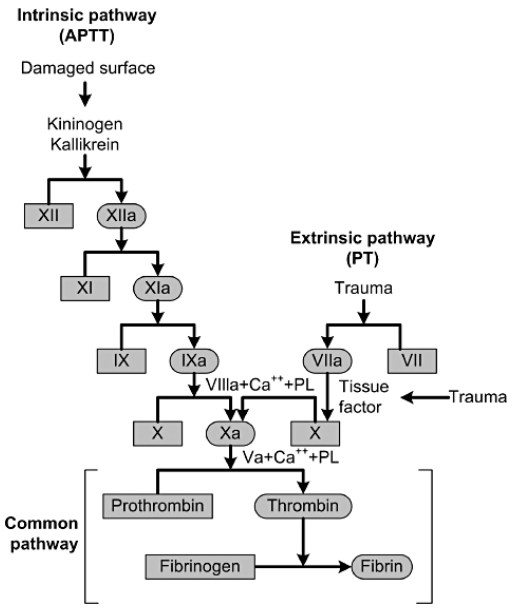

Figure 8: The coagulation pathway (From Adams & Bird, 2009).

1.4.3 Secondary hemostasis / the cell-based model of coagulation

The secondary hemostasis involves the coagulation process, which contributes to strengthen the platelet plug made in the primary coagulation. The cell-based model of coagulation is more suitable than the cascade model for understanding the coagulation *in vivo*, as it takes into account the contribution of the cells. The cells involved are TF-bearing cells, often located outside the vasculature, and platelets (Smith, 2009).

The cell-based model consists of three phases: the initiation phase, the amplification phase and the propagation phase. Thrombin is generated in the overlapping phases. The initiation phase begins when TF bearing cells are exposed to the flowing blood after injury. Activated coagulation factor VII (FVIIa) is the only activated coagulation protein circulating in the blood (the rest of the coagulation factors exist as zymogens in the bloodstream) and will bind to TF immediately. This generates activated coagulation factor IX (FIXa) and thrombin which migrates to the platelets. In the amplification phase, the generated thrombin activates the platelets which in turn releases von Willebrand factor (vWF). This activates FX, coagulation factor VIII (FVIII) and coagulation factor V (FV). The propagation phase is the last phase, where the enzymes from the two earlier phases migrates to the activated platelets. The platelets membrane surfaces are procoagulant, and the enzymes leads to the formation of intrinsic tenase. This generates activated coagulation factor X (FXa) on the surface of the platelets, which leads to the formation of prothrombinase complexes. The prothrombinase complexes boosts the generation of thrombin which leads to a large amount of thrombin on the platelets (Smith, 2009). An overview of the cell-based model of coagulation is shown in Figure 9.

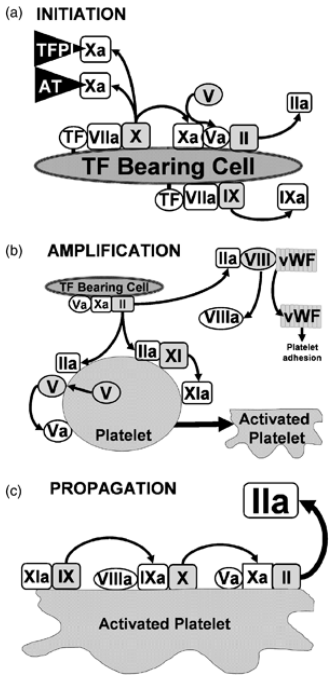

Figure 9: The cell-based model of coagulation (From Smith, 2009).

1.4.4 REGULATION

Regulation of coagulation is essential to avoid excessive and unnecessary coagulation and development of thrombosis. Thrombosis causes a series of diseases like strokes, heart attacks, pulmonary emboli and venous thrombosis (Esmon, 2000). Thus, a better understanding of the regulation processes of coagulation is important in a clinical- as well as a basic point of view.

The regulation of coagulation is performed of several types of inhibitors in anticoagulant pathways. Important inhibitors of the coagulation process includes tissue factor pathway inhibitor (TFPI), protein C and antithrombin (Crawley, 2011).

TFPI is the inhibitor of the TF-mediated initiation in the extrinsic pathway of coagulation. TFPI is mainly produced in endothelial cells, but is also produced in monocytes, vascular smooth muscle cells, fibroblasts, megakaryocytes/platelets and cardiomyocytes. TFPI is expressed under normal conditions and is circulating in plasma as well as being present on the surface of the TFPI-producing cells. TFPI binds to FXa and inhibits its function. The TFPI-FXa complex binds to and inhibits the TF-FVIIa complex, resulting in a negative feedback loop. The initiation of the coagulation process can then be turned off, and the uncontrolled thrombin generation is hindered (Crawley, 2011).

Protein C anticoagulant pathway occurs when protein C is bound to the endothelial cell protein C receptor (EPCR) and subsequently is activated by the integral membrane protein thrombomodulin bound to thrombin. Activated protein C (APC) binds to protein S (PS) and can thereafter inactivate activated coagulation factor V (FVa) and activated coagulation factor FVIII (FVIIIa) by proteolysis. Thrombomodulin is produced by intact endothelium, unlike injured endothelium, which enables a shift between an anticoagulant and coagulant function relative to the location of the site of injury (Crawley, 2011; Esmon, 2000).

The antithrombin anticoagulant pathway ensures rapid inactivation of thrombin in plasma. Antithrombin is a serine protease inhibitor located in plasma and circulating in the blood stream. It acts by mimicking its target enzyme substrates and has a wide specificity that allows it to bind to several different unbound target enzymes. The major target enzymes are thrombin and FXa, but FIXa activated coagulation factor XI (FXIa) and activated coagulation factor XII (FXIIa) are also inhibited by antithrombin. This inhibition results in an anticoagulant function (Crawley, 2011).

1.5 Cancer and coagulation

The role of the proteins in the hemostatic system and tumor progression are closely linked. The ability to promote neoangiogenesis and metastasis are crucial for the cancer cells to be able to maintain cell growth and increased aggressiveness. Several of the components in the hemostatic system have been documented in these processes, and both coagulation dependent- and coagulation independent mechanisms have been examined (Falanga et al., 2013).

1.5.1 Coagulation dependent mechanisms for tumor progression

Fibrin located in the tumor vasculature, forms a scaffold which both physically facilitates neoangiogenesis as well as binding and sequestering several growth factors including VEGF, basic fibroblast growth factor, and insulin-like growth factor-1 (IGF-1). The sequestering protects the growth factors from degradation by proteolysis. In addition, fibrinogen can

promote metastasis by stabilizing adhesion of the tumor cells, or tumor cell embolism to the endothelium (Falanga et al., 2013).

The fibrinolytic system is constantly working with the deposition and dissolution of fibrin in tumor tissue. This is necessary for eventually replacing the fibrin with mature connective tissue stroma. Expression of the components in the fibrinolytic system in cancer cells are therefore crucial for motility and mobility of neoplastic cells, and deficiency of the system can reduce metastasis in some cancer types (Falanga et al., 2013).

Platelets can be activated by tumor cells and facilitate metastasis. The activation occurs when cancer cells produce and release pro-aggregating substances or cell-to-cell adhesion mechanisms, which enables the escape from the innate immune cells (Falanga et al., 2013).

1.5.2 Coagulation independent mechanisms for tumor progression

TF and thrombin are promoting tumor progression by interacting with protease-activated receptors (PARs). PARs are expressed in several cell types, including tumor cells, vascular smooth muscle cells, platelets, endothelial cells, and macrophages (Falanga et al., 2013).

Thrombin can cleave PAR-1, which in turn stimulates chemokines, growth factors and extracellular protein release. This promotes proliferation and migration of tumor cells. Thrombin is responsible for upregulation of genes involved in angiogenesis in endothelial cells, and platelets activated by thrombin results in the release of granule content with several proangiogenic factors (Falanga et al., 2013).

TF is involved in several mechanisms to promote tumor progression. TF can bind to coagulation factor VII (FVII), resulting in activating of several signaling cascades. This can increase endothelial cell adhesion and migration. A complex composed of TF, FVIIa and FXa can activate PARs like PAR-2, which stimulates PAR2 signaling (Falanga et al., 2013). TF-mediated PAR2 signaling has been shown to induce protumor effects like stimulation of anti-apoptosis, angiogenesis, proliferation, migration and metastasis (Figure 10) (Ruf et al., 2011; Schaffner & Ruf, 2009; Wojtukiewicz et al., 2015). At the protein level, TF exists in two isoforms, full-length tissue factor (flTF) and alternatively spliced tissue factor (asTF) (Pan et al., 2019). flTF is

membrane bound, and is the main isoform of TF (Pan et al., 2019). asTF exists as a soluble protein, and is associated with tumor growth, metastasis, angiogenesis and cell growth (Pan et al., 2019). Increasing evidence also suggests that both TF and PAR2 are overexpressed in human triple-negative breast cancer (Su et al., 2009; Zhang et al., 2017).

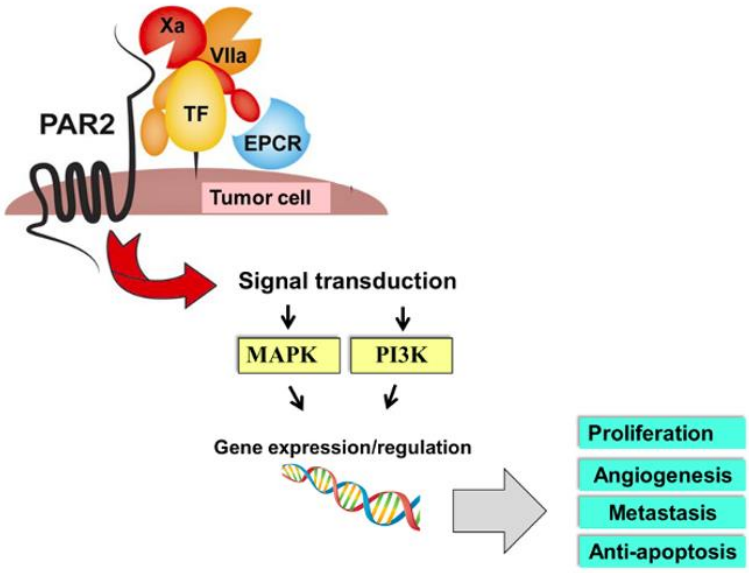

Figure 10: Overview of the stimulation of PAR2 by TF, FVIIa, EPCR and FXa. *Figure modified from Ruf (2014).*

Studies conducted in the research group has illustrated that TFPI has a role in inhibiting tumor progression. These antitumor characteristics of TFPI occurs through a decrease in adhesion and migration (Pollen, 2014). A study by Stavik et al. (2011) also found an association between TFPI and inhibition of tumor progression in breast cancer cells by a decrease in cell growth, migration and invasion.

Platelet-derived MPs contributes to proangiogenic activity due to angiogenesis-stimulating agents released from platelet alpha-granules, expression of adhesion substances, and stimulate tumor cells to release pro-angiogenic factors. Cancer cells can also transfer MPs to each other intracellularly, leading to a coordinated expression of oncogenes (Falanga et al., 2013).

Leucocytes can be involved in cancer progression by promote tumor growth and metastasis. Inflammatory mediators can activate neutrophiles, resulting in the ability to adhere to tumor cells and facilitate the crossing of the endothelial membrane and favor the motility of cancer cells (Falanga et al., 2013).

1.6 COAGULATION FACTOR V

FV is a non-enzymatic clotting cofactor, which is a central part of the coagulation process and is crucial for rapid generation of thrombin (Asselta et al., 2006). FV is a plasma single-chain glycoprotein of 330 kilodalton (kDa), homologous with FVIII. FV is synthetized in the liver, mainly of megakaryocytes and hepatocytes, and is present in the blood circulation as an inactive precursor at a concentration of approximately 10 µg/ml (Lam & Moosavi, 2020; Neuenschwander, 2006). FV can have a coagulant as well as an anticoagulant function and defects which affects the expression or activity level can therefore result in either hemorrhagic or thrombotic events (Lam & Moosavi, 2020; Segers et al., 2007).

1.6.1 GENE AND PROTEIN STRUCTURE

The factor V gene (*F5*) is located at chromosomal region 1.q24.2 and consists of 25 exons within a range of 80 kb. The FV protein is made of 2224 amino acids and includes a 28-residue leader peptide. It is assembled on a distinctive and recognizable way throughout the A1-A2-B-A3-C1-C2 domain structure (Figure 11). The A domains are similar to ceruloplasmin, a copper-carrying protein, while the C domains are like lipid-binding discoidin-like proteins. In contrast, the B domain has no similarity to any known proteins. It is composed of two tandem repeats of seventeen amino acids and thirty-one tandem repeats of nine amino acids. The FV protein undergoes several post-translational modifications like phosphorylation, glycosylation and sulfation (Asselta et al., 2006).

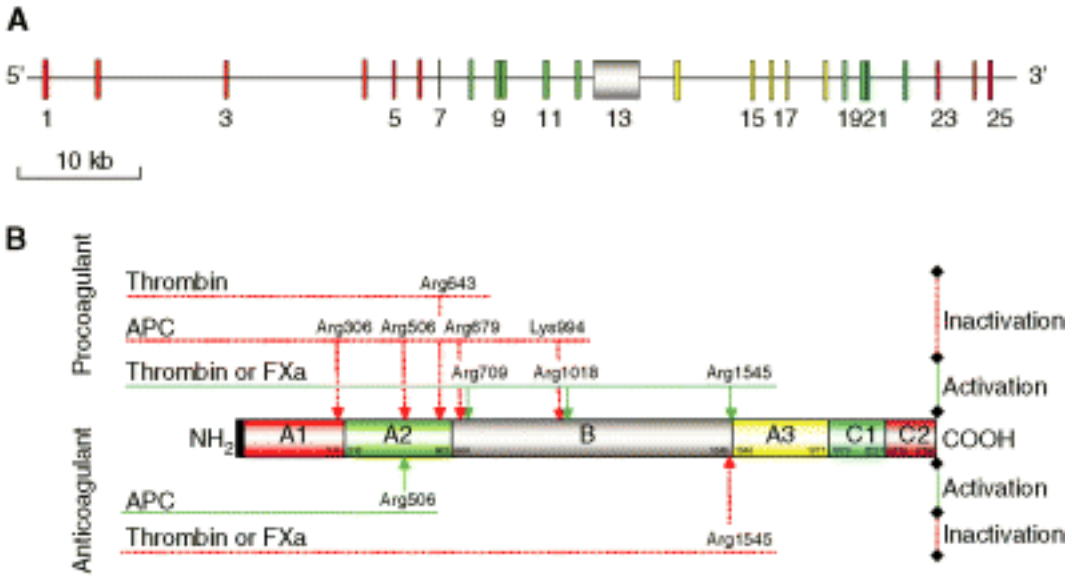

Figure 11: Overview of the F5 gene. A) Structure of the F5 gene with exons (boxes) and introns (lines). B) Organization of the domains in the single chain 330-kDa FV with an overview of the proteolytic cleavage sites involved in activation and inactivation of F5 (Asselta et al., 2006).

1.6.2 PROCOAGULANT FUNCTION

The activation of the procoagulant properties of FV, which transforms it to FVa, is triggered by proteolysis mediated by FXa or thrombin (Asselta et al., 2006). The activation process results in the B domain being cleaved of and assembles in the Ca^{2+}-dependent prothrombinase complex that converts prothrombin to thrombin (Asselta et al., 2006; Segers et al., 2007). This increases the rate of prothrombin activation by as much as 300 000-fold (Asselta et al., 2006).

Precisely in which way FVa acts in the prothrombinase complex is not fully known, but it is observed that the presence of FVa increases the affinity of the interaction between FXa and phospholipid surface with approximately 100-fold. In addition, the catalytic activity of FXa is increased by 1000-fold in the presence of FVa. It is therefore suggested that FVa may act as a receptor of FXa (Segers et al., 2007).

The procoagulant function of FVa can be downregulated by APC-mediated proteolysis at three cleavage sites on the protein (Asselta et al., 2006; Segers et al., 2007). The first cleavage at Arg506 in the FVa protein, resulting in a poorer cofactor activity as well as a reduction in the affinity for FXa (Asselta et al., 2006; Segers et al., 2007). The next cleavage at Arg306 results in

a complete inhibition of FVa (Asselta et al., 2006; Segers et al., 2007). Inactivation may also be performed with cleavage by thrombin or plasmin (Asselta et al., 2006).

1.6.3 Anticoagulant function

The anticoagulant role of FV occurs by acting as a cofactor for APC and facilitate inactivation of FVIIIa (Segers et al., 2007).

The anticoagulant properties of FV appears after cleavage at Arg506 by APC (Asselta et al., 2006; Segers et al., 2007). The cleavage occurs at the surface of negatively charged phospholipids (Asselta et al., 2006). This deprives FV of its procoagulant properties and changes it into an activated anticoagulant FV protein (Asselta et al., 2006). The anticoagulant activity of FV is most likely located at the B-domain because cleaving of this domain is associated with activation of the procoagulant properties of FV (Segers et al., 2007).

1.6.4 Role in cancer and inflammation

Inability to control or express FV can lead to disorders and diseases. Because FV has both a procoagulant and anticoagulant function, malfunction can lead to either thromboembolic disease or bleeding (Segers et al., 2007). Increasing evidences suggests that the procoagulant state is advantageous for tumor progression (Tinholt et al., 2018).

Genetics changes often affects the balance towards the coagulation pathway. An example is the FV Leiden mutation, which causes abolishment of the APC cleavage site on FV. This creates resistance against APC and leads to a deficient downregulation of FV (Segers et al., 2007). The FV Leiden mutation is related to cancer by a 5.8-fold increased risk for developing colorectal cancer for homozygote carriers compared to non-carriers of the mutation (Vossen et al., 2011).

A study by Tinholt et al. (2014) illustrated an association between four single nucleotide polymorphisms (SNPs), elevated expression of *F5* and breast cancer. Another study by Tinholt et al. (2018) revealed that FV could function as a marker for aggressive breast cancer types like basal and HER2 subtypes. Simultaneously, it was revealed that FV was also related to increased overall survival in patients with basal tumors. The findings may be valuable for determining

clinical prognosis and treatment of patients with aggressive breast cancer (Tinholt et al., 2018). A more recent study by Tinholt et al. (2020) found an association between higher expression of *F5* and lymphocyte infiltration in breast cancer patients. Overall, these findings may indicate that FV is involved in cancer as a possible tumor suppressor (Tinholt et al., 2018).

APC have multiple effects in coagulation, fibrinolysis and inflammation. APC is the key effector molecule in the protein C anticoagulant pathway. Still, the coagulation-independent cell signaling effects of APC seems to be the most important according to the therapeutic effect of infection and injury in animal models (Liang et al., 2015). In a study conducted by Liang et al. (2015), the effect of the coagulation-independent functions of APC was examined in a mouse model of *Staphylococcus aureus* sepsis. The study revealed that FV (cleaved by APC) and PS are essential for the APC-mediated inhibition of inflammatory TF signaling and thus inhibition of the PAR2 activation. In mouse models with the FV Leiden mutation, the anti-inflammatory and mortality-reducing effects of APC are abrogated (Liang et al., 2015). A suggestion for the mechanism of inhibition of the TF-mediated PAR2 activation is shown in Figure 12.

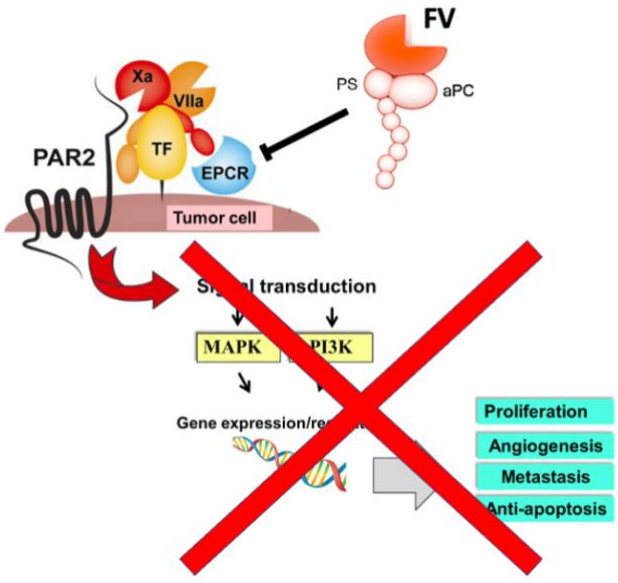

Figure 12: Suggested mechanism of inhibition of the TF-mediated PAR2 activation by FV, PS and APC. *Figure modified from Ruf (2014) and Sun (2015).*

1.7 Regulation of gene expression

The regulation of gene expression in eukaryotic cells is tightly controlled at several levels. This includes regulation of chromatin accessibility, transcriptional regulation, RNA processing, RNA stability, translation, and protein activity.

Transcriptional regulation is the key regulator for many genes and involves the binding of transcription factors. The regulation by transcription factors is considered as one of the most important mechanism for gene regulation (Mitsis et al., 2020; Pulverer, 2005).

In the promoter region, transcription of the gene is initiated. The promoter contains response elements where transcription factors can bind and enable the binding of polymerase. At least seven transcription factors are required to facilitate the binding of polymerase. Multiple regulatory sequences are involved in the regulation of the promoter. This includes enhancers, silencers, insulators, and boundary elements. The regulatory sequences can be located several kilobases away from the promoter, and are involved in increasing or decreasing the transcription rate of the gene (Phillips, 2008).

2. AIMS

Cancer patients are 5- to 6-fold more likely to develop venous thromboembolism compared to the general population (Fennerty, 2006). Thrombosis is one of the most common causes of death among cancer patients. By understanding the molecular mechanisms behind the link between cancer and coagulation, it may be possible to provide a more individualized treatment for both cancer and thrombosis in cancer patients. Moreover, it can contribute to attenuate cancer progression.

The purpose of this thesis was therefore to study the expression, regulation and functional effects of FV during treatment with chemotherapy.

The specific aims of the study:

I. Analysis of clinical data materials from breast cancer patients:
    i. Investigate if the expression of *F5* before chemotherapy treatment was associated with treatment response in breast cancer in different cohorts, subtypes, and hormone receptor status.
    ii. Investigate differences in the expression of *F5* in different cohorts, subtypes, and hormone receptor status.

II. *In vitro* studies in breast cancer cell lines:
    i. Investigate the viability of breast cancer cell lines during different chemotherapy treatment.
    ii. Investigate the effect of chemotherapy treatment on *F5* expression.
    iii. Investigate the effect of p53 in the doxorubicin induced expression of *F5*.
    iv. Investigate the functional effects of FV with and without doxorubicin treatment.

3. MATERIALS AND METHODS

Complete lists of instruments, kits, reagents, disposables, plasmids, siRNAs, drugs, coagulation factors, software and solution recipes used in this thesis are listed in Appendix A and C.

3.1 PLASMIDS

Previous findings have indicated that p53 may have a role in the regulation of the *F5* gene in breast cancer cells. Two potential p53 half-sites in the *F5* promoter (c.-300/-290 and c.-766/-760) were identified using the PROMO program with the TRANSFAC version 8.3 with cut-off for dissimilarity rate at 15%. To study the role of p53 in the regulation of *F5* further, plasmids containing either the wild type *F5* promoter or the *F5* promoter with mutated p53 half-sites were used.

Examination of the *F5* promoter was performed using luciferase reporter plasmids. A vector containing the *F5* promoter and firefly luciferase gene was previously made by the research group, and was generated by cloning a 1336 base pair (bp) fragment located from c.-1419 to -84 upstream of the *F5* gene from human genomic DNA (Appendix B, Table B 1) into the pGL3-Basic vector (Figure 13A) with the restrictions enzymes *KpnI* and *HindIII*. This construct, named pGL3-Basic-F5-prom wt, was thereafter used by the research group to generate two luciferase constructs with each p53 half-site mutated (Table 1) by site-directed mutagenesis using primers described in Table 2.

In transfection experiments, the pRL-SV40 vector (Figure 13B) which constitutively expresses renilla luciferase was used for normalization by correction of transfection efficiency, cell viability and starting and ending cell number. For checking transfection efficiency visually, the pMaxGFP plasmid encoding a green fluorescent protein was used. The plasmids used in the study of the *F5* promoter are listed and explained in Table 3.

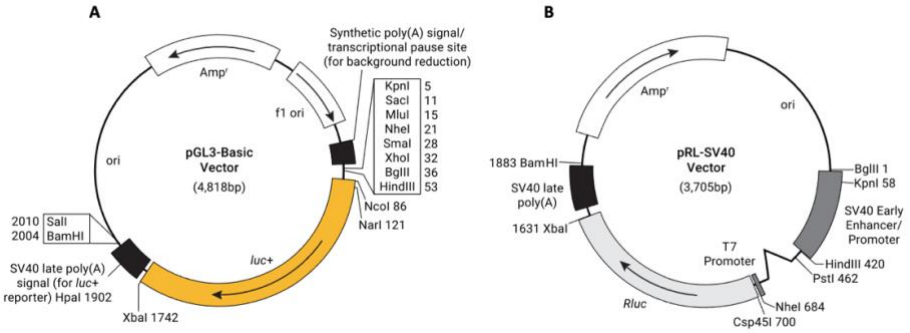

Figure 13: Schematic illustration of luciferase vectors. A) pGL3-Basic Vector with Firefly luciferase gene. B) pRL-SV40 Vector with Renilla luciferase gene (Promega; Promega)

Table 1: Wild type and mutated p53 bindings sites

Name:	Location:	WT sequence 5´-3´:	Mutated sequence 5´-3´:
p53 binding site 1	c.-300/-294	TCTGCCC	TCTTCCC
p53 binding site 2	c.-766/-760	CTTGCCC	CTTTCCT

Table 2: Primers used for mutagenesis of p53 binding sites

Primers for mutagenesis:	Direction:	Sequence 5´-3´:
p53 binding site 1	Forward	ACAGTAACTTTCCTAAGACAACAC
	Reverse	ACCTCTCTGTTCAGTTTTG
p53 binding site 2	Forward	TCTGATCTCTTCCCCTTCTTCACCTGC
	Reverse	GGCTCTAGCAGGCGGGAC

Table 3: Description of plasmids

Plasmid name:	Description:
pGL3-Basic-F5-prom wt	Wild type of *F5* promoter (c.-1419/-84)
pGL3-Basic-F5-prom p53_1	*F5* promoter with mutated p53 site 1 (c.-300/-290)
pGL3-Basic-F5-prom p53_2	*F5* promoter with mutated p53 site 2 (c.-766/-760)
pGL3-Basic-F5-prom p53_1+2	*F5* promoter with mutated p53 site 1 (c.-300/-290) and 2 (c.-766/-760)
pGL3-Prom	Positive control: Empty vector with firefly luciferase with promoter
pGL3-Basic	Negative control: Empty vector with firefly luciferase without promoter
Cignal Finder p53	Detects activation of the p53 pathway
pMax GFP	Control for transfection efficiency
pRL-SV40	Internal control: Renilla plasmid co-transfected with pGL3 vectors

3.2 Molecular techniques

3.2.1 In vitro mutagenesis

Mutagenesis is the generation of alterations in the genetic material, leading to a mutation. The method can be used to investigate genes, gene products and mechanisms in more detail.

Mutagenesis was used to generate a new version of the *F5* promoter construct with both *p53* half-sites mutated. This was done using the Q5® Site-Directed Mutagenesis Kit with the primers for mutation of *p53* half-site 1 (c.-300/-290) (Table 2) and pGL3-Basic-F5-prom p53_2 as a template. The reaction mix was made following manufacturer´s protocol with 10 ng template DNA and transferred to a Veriti™ 96 well Thermal Cycler with polymerase chain reaction (PCR) program as listed in Table 4.

The PCR-products undergo kinase, ligase and *DpnI* treatments at room temperature. The phosphorylation and ligation result in circulation of the DNA. The *DpnI* restriction enzyme, targets methylated DNA, and results in degradation of the template plasmids. Newly synthetized DNA is unmethylated and thereby not degraded by *DpnI*.

*Table 4: Thermocycling Conditions for routine PCR. *=NEBBaseChanger™ was used for finding annealing temperature. **=(20-30 seconds/kb) The vector is 4772 bp and the insert is 1336 bp which gives a construct at 6108 bp.*

Step:	Temperature:	Time:
Initial denaturation	98°C	30 seconds
25 Cycles	98°C	10 seconds
	57°C *	30 seconds
	72°C	185 seconds **
Final extension	72°C	2 minutes
Hold	4-10°C	

3.2.2 Sanger sequencing

Sanger sequencing determine DNA sequences using the DNA strand as a template in a chain-termination PCR process. In the process, a low ratio of the modified dideoxyribonucleotide triphosphate (ddNTP) is added in addition to deoxyribonucleotide triphosphate (dNTP). After hybridization, DNA polymerase extends the DNA strand by adding dNTPs and catalyzing the phosphodiester bond formation between the free 3´-OH group and the 5´-phosphate between nucleotides. The ddNTPs lacks the 3´-OH group, resulting in inability to form phosphodiester

bonds and causes extension to stop. ddNTPs is added randomly, which results in oligonucleotide fragments with different lengths. After separation of oligonucleotides by size in the capillary gel electrophoresis, the unique fluorescent label of each ddNTP is detected, and the sequence can be determined as peaks in a chromatogram. An overview of the process is described in Figure 14.

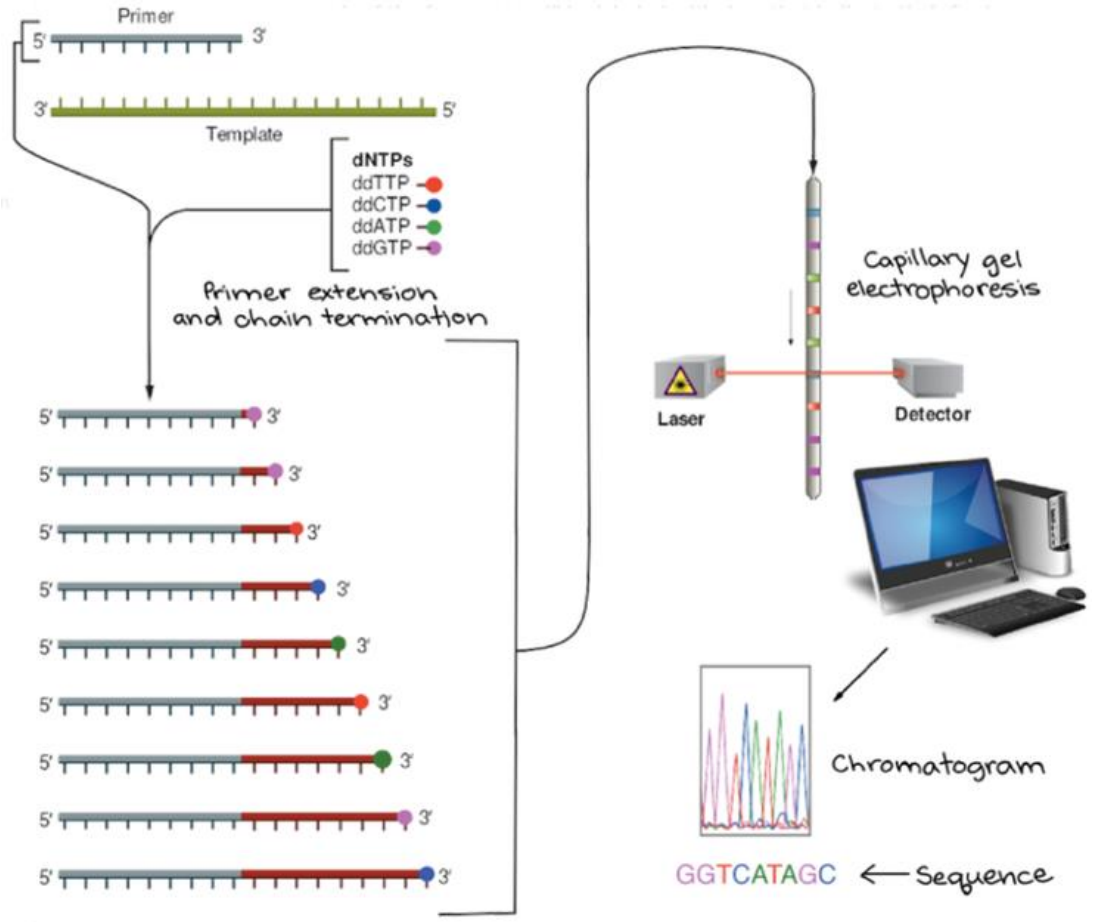

Figure 14: Overview of the Sanger sequencing process with hybridization, primer extension, chain termination, capillary gel electrophoresis, detection and data analyzation. *Figure modified from Estevezj (2012).*

Sanger sequencing was used to verify whether the pGL3-Basic-F5-prom p53_1+2 plasmid was properly made, that the desired mutations had been introduced in the *p53* half-sites, and that unwanted mutations had not been introduced during the *in vitro* mutagenesis process.

Eight different plasmids from the minipreparations (described in section *3.3.3*) were sequenced using the BigDye Terminator v3.1 Cycle Sequencing Kit on a Veriti™ 96 well Thermal Cycler. Reagents for one sequencing reaction are listed in Table 5, and the cycling program is

followed as described in the manufacturer´s protocol. For amplification of all parts of the *F5* promoter, five different sequencing primers described in Table 6 were used. After chain-termination PCR, Agencourt® CleanSEQ Dye-Terminator Removal Kit was used to purify the samples (described in section *3.2.2.1*). Sanger sequencing was performed on an ABI 3730 DNA Analyzer and the sequences were aligned with SeqScape™ v4.0 software using the wild type *F5* promoter (NM_000130.4) as a reference sequence.

Table 5: Reagents and amounts per reaction for Sanger sequencing in a 96-well plate.

Reagent:	Volume:
Nuclease free H_2O	x µl
Plasmid	88-150 ng
5x Sequencing buffer	2 µl
Primer	3.2 pmol
BigDye® Terminator v3.1 Ready Reaction Mix	0.25 µl
Total	10 µl

Table 6: Sequencing primers used in Sanger sequencing.

Primer name:	Sequence 5´-3´:
F5promotor_3F	TAAGCAGGTACCGGAGCCATGCAGATACAGGG
F5promotor_1R	TGCTTAAAGCTTCCCAGCTGCAATGAGCTCTA
FV_Ex1_R	CAGGAAACAGCTATGACCAGTTTGGTTGCTCTCCCTAATACCT
RVprimer3	CTAGCAAAATAGGCTGTCCC
GLprimer2	CTTTATGTTTTTGGCGTCTTCCA

3.2.2.1 Purification of sequencing extension products prior to sequencing

Purification of sequencing extension products was performed to remove residual PCR elements. CleanSEQ Dye-Terminator Removal Kit was used and manufacturer´s protocol was followed. The process was performed automatically with a BioMek FX robot.

The principle of purification is illustrated in Figure 15. The process includes the binding of the sequencing extension products to magnetic beads, separation from unwanted items using a magnet plate on the outside of the well, washing with ethanol for removal of nucleotides, salts,

unincorporated dyes and other contaminants, and finally elution of DNA from the beads with an aqueous buffer.

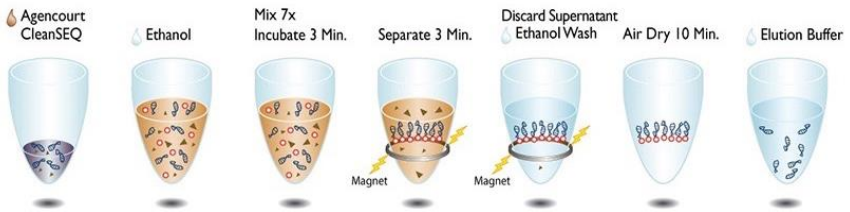

Figure 15: The principle of CleanSEQ illustrated in steps by DNA binding to magnetic beads, separation by magnet, washing and elution (Beckman Coulter, 2017).

3.2.3 Agarose gel electrophoresis

Agarose gel electrophoresis is effective for separation of DNA fragments by size. Agarose consists of L- and D-galactose, which forms non-covalent bounds resulting in generation of pores. During influence of an electric current, the uniform ratio between mass and charge separates DNA molecules by size during migration to the positive anode. By staining, the DNA molecules can eventually be visualized with UV light.

Agarose gel electrophoresis was used to verify that the plasmids were supercoiled. Plasmids made by bacterial hosts also contains linear and open circular isoforms of DNA due to conformational changes in the biomass processing. The transfection efficiency is considerably higher in the supercoiled isoform compared with the others.

Gel electrophoresis was performed in a 1% agarose gel containing GelRed in TAE buffer (recipe in Appendix C) at 80 Volts for 1 hour. The GeneRuler DNA Ladder Mix was used and 1 µg plasmid was loaded per well. Gel images were generated by ImageQuant™ LAS 4000 and the ImageQuant™ TL ID v8.1 software.

3.2.4 Real time qRT-PCR

Real time quantitative transcription polymerase chain reaction (RT-qPCR) is used for quantification of genetic material. Prior to RT-qPCR, RNA is converted to complementary DNA (cDNA) by reverse transcriptase. The cDNA is then amplified by RT-qPCR which enables a quantitative measurement of the genetic material in the samples. This is accomplished with a

fluorescent dye or DNA probe which can be detected and measured by a fluorometer for each PCR cycle.

3.2.4.1 Total RNA isolation

Total RNA was isolated from cell lysates using the Monarch® Total RNA Miniprep Kit which includes spin columns with an RNA binding filter for removal of genomic DNA (gDNA) and RNA purification. The manufacturer´s protocol was followed.

In brief, cell lysates were stored in 1X Monarch DNA/RNA Protection Reagent and the optional DNase I treatment was performed for removal of residual gDNA in the samples. The samples were eluted in 50-80 µl Nuclease-free Water and stored at -80°C prior to cDNA synthesis.

3.2.4.2 RNA and DNA quantification

Quantification of total RNA and plasmid DNA were performed with NanoDrop®ND-1000 at 260 nm. The 260/280 purity ratio was considered to be adequate at >2.0 for RNA and >1.8 for DNA.

3.2.4.3 cDNA synthesis

cDNA synthesis was performed using the High-Capacity cDNA Reverse Transcription Kit. Manufacturer´s protocol was followed. RNA samples were diluted in nuclease-free water to ensure equal amounts of RNA for each experiment (876-5056 ng). cDNA was made in 96-well plates as described in Table 7. The plates were run on a 2720 Thermal Cycler with the program described in the manufacturer´s protocol.

Table 7: Reagents and volumes for one cDNA reaction in a 96-well plate for cDNA synthesis.

Reagent:	Volume (µl):
10X RT Buffer	5.0
25X dNTP Mix	2.0
10XRT Random primers	5.0
Multiscribe™ Reverse transcriptase	2.5
Nuclease-free H_2O	10.5
RNA	25.0
Total	50

3.2.4.4 mRNA quantification using RT-qPCR

RT-qPCR allows real time measurements of fluorescence generated from the TaqMan probes during the amplification process. A sequence specific primer and probe bind to the target cDNA. The 5´-end of the probe is covalently bound to a reporter molecule and the 3´-end is covalently bound to a quencher. The quencher prevents excitation of the reporter when located in close proximality caused by the fluorescence resonance energy transfer phenomena, meaning that the energy is transferred from the reporter to the quencher molecule. This results in quenching of the emitted fluorescence. When Taq Polymerase encounters, the probe is cleaved, and the reporter and quencher molecule are separated. This allows the reporter to fluoresce. A rising fluorescent signal is generated as the amount of product increases (Figure 16).

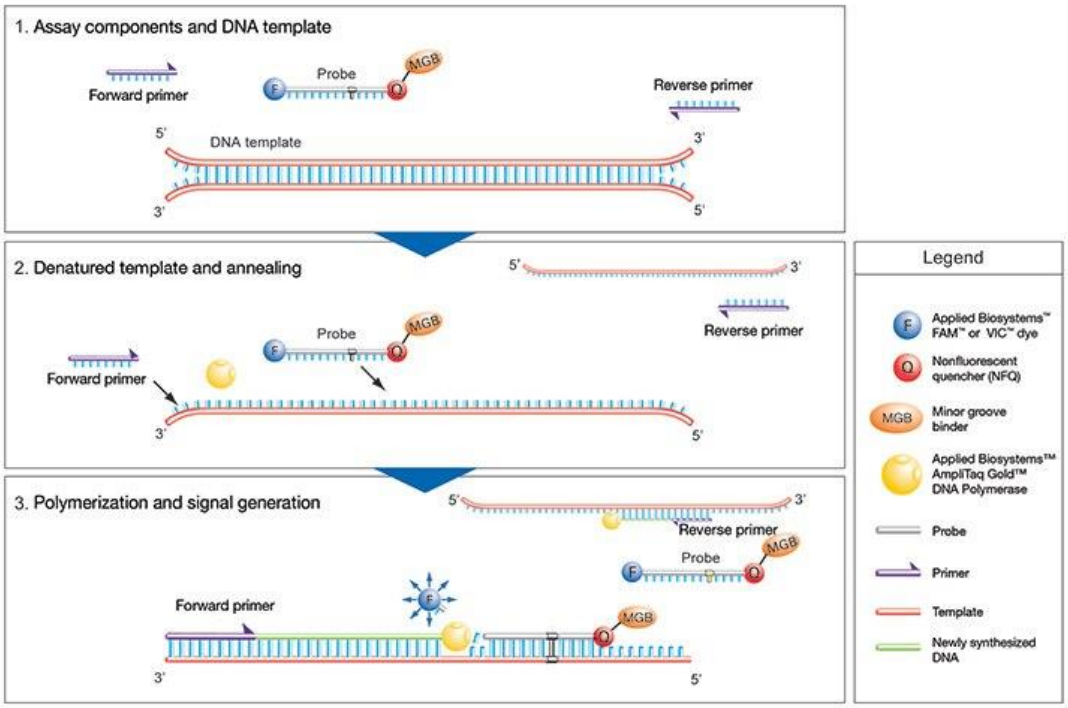

Figure 16: Principle of the TaqMan assay (Thermo Fisher Scientific).

Quantification is determined when the amplification curve is in the exponentially phase in the RT-qPCR process and the threshold and C_T value are calculated. The threshold is defined as the detection level where the fluorescence intensity is higher than the background level and the C_T value is the number of PCR cycle at which the threshold is reached.

The comparative C_T ($\Delta\Delta C_T$) method is used to analyze differences in gene expression relative to a reference sample. Relative quantity (RQ) is calculated to determine the expression level of mRNA using the following formulas:

$\Delta C_T = C_{T\,(Target)} - C_{T\,(Endogenous\ control)}$

$\Delta\Delta C_T = \Delta C_{T\,(Test)} - \Delta C_{T\,(Control)}$

$RQ = 2^{-\Delta\Delta CT}$

An RQ-value<1 is interpreted as downregulation of the gene whereas an RQ-value>1 is interpreted as upregulation of the gene.

TaqMan Assays and RT-qPCR were used for quantification of mRNA. *F5* and *p53* were the target sequences. Glyceraldehyde-3-Phosphate Dehydrogenase (GAPDH) was used as endogenous control for MCF-7 cells and Hypoxanthine Phosphoribosyltransferase (HPRT1) was used as endogenous control for MDA-MB-231 cells. The endogenous controls were used to normalize for variations in reverse transcription efficiency and cDNA template input and the regulation of these genes should not be affected by the chemotherapy treatments used in the samples. TaqMan™ Gene Expression Master Mix was used and the manufacturer´s protocol was followed. The RT-qPCR TaqMan reaction mix was prepared as described in the protocol for singleplex reactions in a 384-well plate. Each reaction was run in triplicates. For each assay a non-template control (NTC) sample was made using RNase-free water instead of cDNA. The samples were run and analyzed with QuantStudio 12k Flex Instrument according to the program described in the protocol.

Table 8: Primers used in TaqMan Assays

Name:	Location:
F5	Hs00914120_m1
p53	Hs01034249_m1
HPRT1	Hs02800695_m1
GAPDH	Hs99999905_m1

3.3 Microbiological techniques

3.3.1 Transformation

Transformation is the alteration of genetic material by absorption and incorporation of exogenous genetic material into a bacterial cell.

Plasmids generated by site-directed mutagenesis (described in section *3.2.1*) were transformed into chemically competent NEB 5-alpha Competent *Escherichia coli* following the Q5® Site-Directed Mutagenesis Kit Protocol. The competent state allows exogenous genetic material to pass through pores in the cell membrane and the uptake of the plasmids is triggered by exposing the cells to a heat shock.

After transformation, *E. coli* cells were spread onto selective Lysogeny Broth (LB) agar plates containing 100 µg/mL ampicillin and incubated at 37°C overnight for selective growth of transformed cells.

3.3.2 Cultivation of transformed E. coli

Amplification of plasmids for minipreparation for was performed by picking single colonies from the LB agar plates into separate tubes with 5 ml LB-medium containing 100 µg/mL ampicillin. The tubes were incubated at 37°C and 200 rpm shaking. Amplification of plasmids for maxipreparation was performed by transferring 1 ml of isolated bacterial culture to 120 ml LB-medium containing 100 µg/mL ampicillin followed by incubation at 37°C and 200 rpm shaking.

3.3.3 Plasmid DNA isolation from transformed E. coli

Extraction and purification of plasmid DNA can be performed in various ways depending on the desired plasmid yield. The method is accomplished by lysing cells under alkaline conditions which leads to denaturation of linearly chromosomal DNA and proteins whereas small circular plasmids remain stable. A neutralizing buffer enables the proteins, RNA and larger and less supercoiled chromosomal DNA to precipitate while the smaller DNA plasmids remain in solution. Plasmids are separated from the supernatant using a spin column with a DNA binding filter. Several washing steps purifies the plasmid DNA before elution into a collection tube.

Minipreparation was used for preparations for initial sequencing. The Zyppy™ Plasmid Miniprep Kit was used and the manufacturer´s protocol was followed. 3 ml of each isolated bacterial culture was used.

Maxipreparation was used to gain sufficient amounts of plasmid for transfection into cancer cells. The ZymoPURE™ II Plasmid Maxiprep Kit was used as described in the manufacturer´s protocol using the centrifugation alternative. The last optional step was performed for removal of endotoxins which may have a negative effect on living cells. 120 ml of isolated bacterial culture was used.

DNA was quantified as described in section *3.2.4.2*.

3.4 PROTEIN TECHNIQUES

3.4.1 TOTAL PROTEIN QUANTIFICATION

Determination of total protein concentration in cell lysates were performed using the Pierce™ BCA Protein Assay Kit. The method involves both the reduction of Cu^{2+} to Cu^{1+} by proteins solved in alkaline medium, and the selective colorimetric detection of Cu^{1+} by bicinchoninic acid (BCA). The reduction of Cu^{2+} to Cu^{1+} (called the biuret reaction) generates a light blue complex in alkaline environment. Next, two BCA-molecules reacts with one Cu^{1+}-molecule resulting in an intense, purple-colored reaction product. The complex of BCA and Cu^{1+} shows a strong linear absorbance at 562 nm with increasing concentrations of proteins.

The kit was used for total protein quantification in MDA-MB-231 and MCF-7 cell lysates from stimulation experiments. A modified version of the manufacturer´s protocol was followed. For generation of a standard curve, albumin (BSA) was diluted in radioimmunoprecipitation assay (RIPA) buffer with 1xHalt™ Protease and Phosphatase Inhibitor Cocktail to concentrations of 2 mg/ml, 1 mg/ml, 0.5 mg/ml, 0,25 mg/ml and 0,125 mg/ml. RIPA with inhibitor was also used as a blank sample. 5 µl of standards, samples or blank were added in duplicates in a 96-well plate with flat bottoms. 200 µl WR reagent was added to each well and mixed on a plate shaker. The plate was incubated at 37°C for 30 minutes before absorbance was measured at 562 nm with a VersaMax microplate reader. Protein concentrations in the samples were calculated

with the SoftMax Pro 6.4 software using a quadratic fit standard curve (shown in Appendix D, Figure D1).

3.4.2 FV ELISA

Enzyme-Linked Immunosorbent Assay (ELISA) is a method to quantify even small amounts of specific proteins, peptides, antibodies or biomolecules in a sample.

ELISA capture assay (also called ELISA "sandwich" assay) is performed in several steps. The polystyrene microplate wells are coated by binding and immobilization of antigen specific high-affinity antibodies. Plate blocking ensures covering of unsaturated sites by adding irrelevant molecules or proteins. Antigen containing samples are added, resulting in the binding of antigens to antibodies which allows them to easily be separated from unbound proteins. Then, a specific primary antibody is added, resulting in sandwiching of the antigen. A secondary enzyme linked antibody is added which binds to the primary antibody. By adding a substrate for the enzyme, a dye is generated which allows quantification of the antigens. The principle is illustrated in Figure 17.

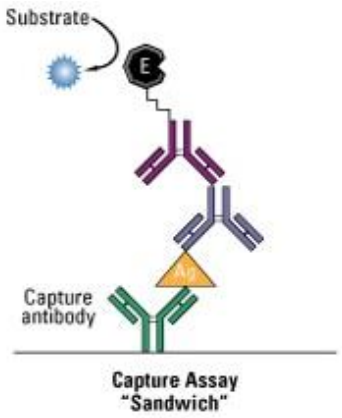

Figure 17: ELISA capture assay
(Thermo Fisher Scientific)

Human Factor V ELISA Kit was used to detect FV in cell media and lysates from MDA-MB-231 and MCF-7 cells, treated and not treated with doxorubicin, to study the effect of doxorubicin on the FV protein level. The method was also used to confirm that overexpression of FV with the pMT2-FV plasmid was successful. The manufacturer's protocol was followed. For preparation, all samples were diluted 1:5 in 1x Diluent M. Samples and standards were assayed in duplicates. Quantification was performed by measuring the absorbance of the generated dye using the VersaMax™ microplate reader. The standard solutions, with concentrations from 0-120 ng/mL, were used to generate a standard curve with the SoftMax Pro 6.4 software. The concentrations of FV in the samples were calculated using the standard curve (Appendix D, Figure D2).

3.5 FUNCTIONAL ASSAYS

3.5.1 CELL PROLIFERATION MEASUREMENTS

Cell proliferation measurements were performed using the Cell Proliferation Reagent WST-1. WST-1 is a water-soluble tetrazolium salt which can be cleaved by mitochondrial dehydrogenase enzymes in living cells. The cleaving results in generation of WST-1 formazan dye with a dark yellow color which can be quantified by measuring absorbance at 420-480 nm using a microplate reader. The amount of WST-1 formazan dye is strongly corelated to the number of living and metabolically active cells. The process of WST-1 is illustrated in Figure 18.

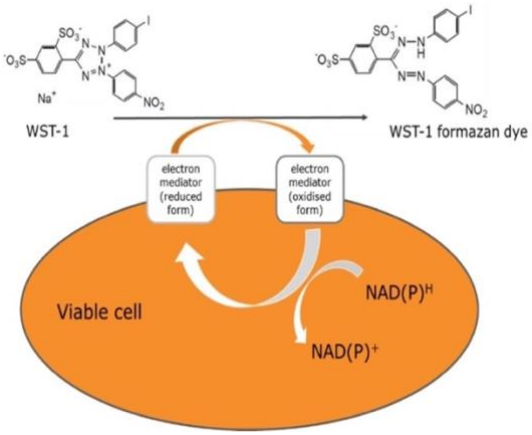

Figure 18: Cleavage of WST-1 to WST-1 formazan dye by viable cells (GmbH, 2015).

WST-1 was added in a ratio of 1:10 of the original volumes of media in the wells and incubated at 37°C in 30 minutes. Measurement of WST-1 was performed using the VersaMax™ microplate reader at 450 nm with 745 nm as reference. The SoftMax Pro 6.4 software was used. Measurements of wells containing only media and WST-1 were used to determine background absorbance.

3.5.2 LUCIFERASE REPORTER ASSAY

Luciferase reporter assay was used to examine the activity of the FV promoter by using luciferase as a reporter gene. The energetically efficiency of the bioluminescence reaction makes it highly sensitive and thus very suitable for reporter assays because it can detect even small transcriptional changes.

Dual luciferase assays were performed after transfection of luciferase plasmids in MDA-MB-231 and MCF-7 cells. In the assay, the cells were lysed resulting in the release of intracellular proteins including the luciferases. Luciferin and the necessary cofactors were added and the Luciferin/Luciferase process, which occurs when luciferin is catalyzed and converted to oxyluciferin by the luciferase enzyme, lead to emission of light. The enzymatic activity of luciferase in cell lysates, which is directly correlated with the activity of the gene of interest,

was measured using a luminometer. The results were normalized by calculating the firefly/renilla-ratio and thus improve the accuracy. An overview of the principle of the luciferase reporter assay is illustrated in Figure 19.

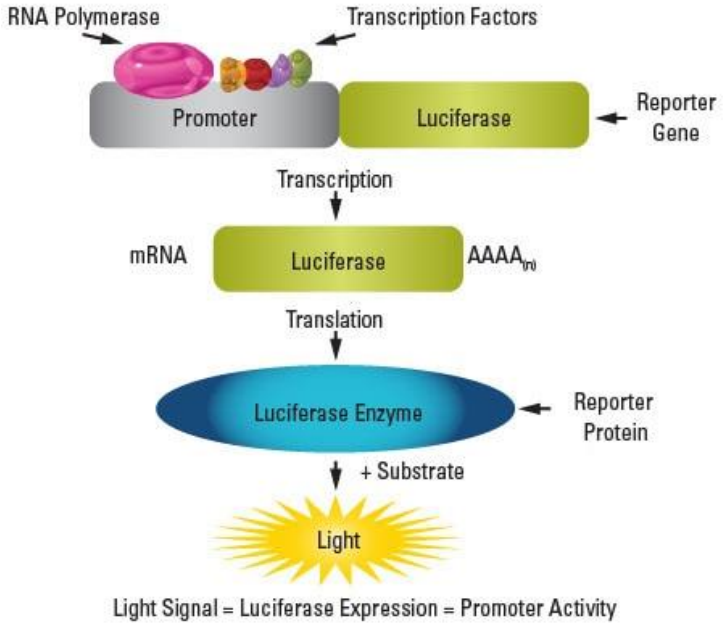

Figure 19: The principle of luciferase reporter assay (Thermo Fisher Scientific).

In this thesis, the Dual-Luciferase® Reporter Assay System was used and a modified version of the manufacturer´s protocol was followed. Half-area 96-well microplates were used which allowed a halving of volumes with cell lysate, luciferase assay reagent II (LAR II) and Stop & Glow reagent. Cells were harvested as described in section *3.6.3.3*. Measurements were conducted on a GloMax 96 Microplate Luminometer with automatic injection of LAR II and Stop & Glo® reagent.

3.5.3 Detection of apoptosis

Cell Death Detection ELISA^{PLUS} Kit was used for detection of apoptosis in functional experiments in MDA-MB-231 cells following the manufacturers protocol.

When the cells are exposed to an apoptosis-inducing agent, DNA and histone complexes (nucleosomes) are released into the cytoplasm of apoptotic cells. Lysis of the cells will release the nucleosomes and make them detectable. Cell Death Detection ELISA^{PLUS} Kit is used for

quantification of nucleosomes using monoclonal antibodies against DNA and histones with a sandwich-enzyme-immunoassay-based method. The wells in the microwell plate are coated with streptavidin. Nucleosomes in the sample are detected with the antibodies Anti-histone-biotin and Anti-DNA-peroxidase forming an immunocomplex. The immunocomplex attaches to the streptavidin coated microwell plate via biotinylation. After removal of unbound components, the amount of nucleosomes is determined quantitatively by the color reaction generated by peroxidase with the ABTS Substrate. The process is illustrated in Figure 20.

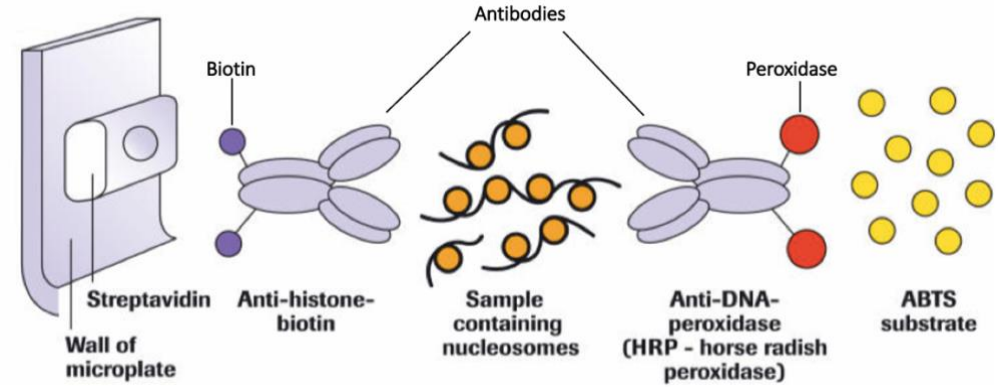

Figure 20: The principle of Cell Death Detection ELISA^{PLUS}. Figure modified from Roche (2016).

3.6 Cell techniques

3.6.1 Breast cancer cell lines

Breast cancer cell lines are a highly valuable resource for the ability to study the biology of breast cancer as well as effects of various treatments. Cancer cell lines consists of cells that have infinite cell division potential under certain conditions in a laboratory.

MCF-7 cells (Figure 21) are a human epithelial luminal adenocarcinoma cancer cell line, well suitable as a transfection host. It is a metastatic cell line with adherent properties. MCF-7 cells has the wild-type p53 gene (*TP53*), are estrogen receptor (ER) positive, progesterone receptor (PR) positive, human epidermal growth receptor 2 (HER2) negative and are known to be sensitive to doxorubicin (ECACC, 2017a).

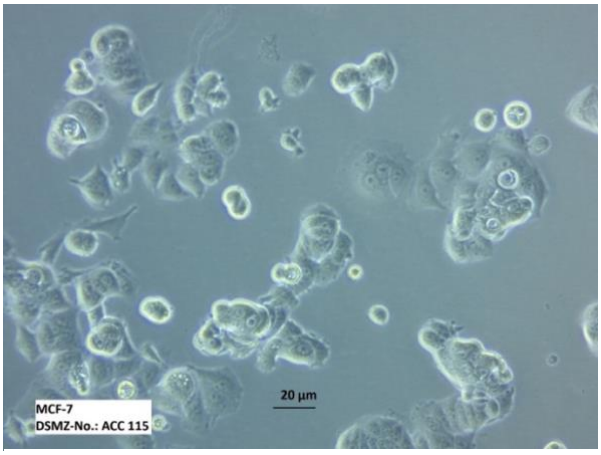

Figure 21: MCF-7 cells in culture (Leibniz Institute).

MDA-MB-231 cells (Figure 22) are a human epithelial adenocarcinoma cancer cell line and are one of the most common cancer cell lines used in medical research. MDA-MB-231 cells are ER-negative, PR-negative and HER2-negative and are therefore referred to as a triple negative breast cancer cell line. The triple negative type is the most aggressive form of breast cancer due to limited treatment possibilities (ECACC, 2017b). MDA-MB-231 cells are *TP53* mutant, but the p53 protein still has a partial function.

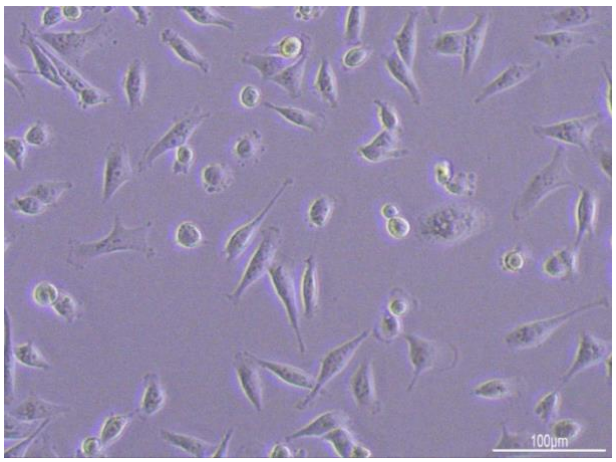

Figure 22: MDA-MB-231 cells in culture.

Both cell lines were cultured in Thermo Fisher™ Nunc™ Cell Culture treated bottles with 10 % Fetal bovine serum (FBS) in Dulbecco´s Modified Eagle Medium (DMEM) with 4.5 g/l Glucose and L-Glutamine. Cells were maintained at 37°C in a humidified atmosphere with 5% CO_2. The cells were regularly tested for mycoplasma using MycoAlert® Mycoplasma Detection Kit and only mycoplasma negative cells were used in experiments.

3.6.2 TRANSFECTION

Transfection is a process in which foreign DNA or RNA are artificially introduced into host cells, making it possible to examine e.g., protein expression, regulatory elements and gene functions, and enables mutation analysis and biochemical characterization. In transient transfection, the

nucleic acid is not integrated in the host genome and will not replicate during cell division. Stable transfection results in integration of the nucleic acid at the host genome, which leads to long-term expression and the inheritance to progenies.

In this thesis, liposome-based transient transfection was used. In this process, cationic lipids, dissolved in an aqueous solution, forms positive charged micelles called liposomes. The liposomes and negative charged DNA forms a lipoplex by self-assembly. The lipoplex is internalized by endocytosis, fusion with the cell membrane or phagocytosis. Inside the cell, the cationic lipids from the lipoplex and anionic liposomes of the endosome are mixed which results in endosomal rupture and release of DNA. Thereafter, DNA can be imported to the nucleus where it potentially can be expressed. Alternatively, the endosome matures and fuse with a lysosome which leads to degradation of DNA. The principle of transfection is illustrated in Figure 23.

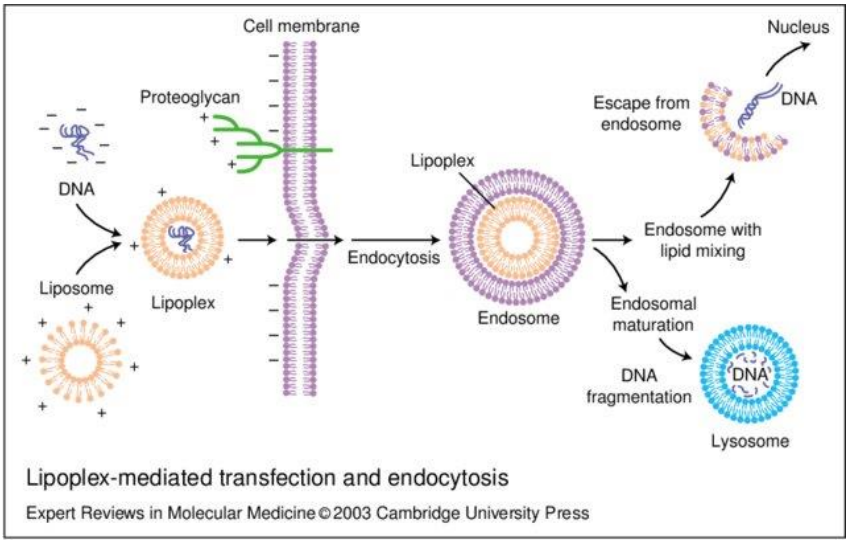

Figure 23: The principle of liposome-based transfection with lipoplex generation, endocytosis and endosome generation and either escape or fragmentation of DNA (Parker et al., 2003).

Forward and reverse transfection were both used in this thesis. Forward transfection is accomplished when cells are seeded and cultured for 24 hours prior to transfection. In reverse transfection the transfection reagents are added to wells simultaneously with the cell suspension.

3.6.2.1 Transfection of plasmids

Transfection of plasmids was used to examine the *p53* half-sites in the *F5* promoter and to study the functional effect of overexpression of FV.

The transfection of plasmids was accomplished using the Lipofectamine™ 3000 Transfection Reagent kit and Reduced Serum Medium Opti-MEM®. The P3000 reagent is wrapping the DNA into a micelle and Lipofectamine 3000 is increasing the positive charge of the micelle to promote endocytosis into the cell. Detailed descriptions of the transfection of plasmids are described in section *3.6.7* and *3.6.8*.

3.6.2.2 Transfection of siRNA for gene knockdown

In vitro gene knockdown, also called gene silencing, can be achieved with the RNA interference (RNAi) process. The RNAi process consist of multiple steps, initiated with the introduction of double stranded RNA (dsRNA) from an exogenous source. The Dicer enzyme cleaves dsRNA into smaller fragment at approximately 20 bp called small interfering RNA (siRNA). The antisense strand of siRNA can bind to the Argonaute protein, which is a part of the RNA-Induced Silencing Complex (RISC) while the sense strand is cleaved and degraded. The antisense strand in the RISC complex works as a guide to the complementary strand on a mRNA-strand resulting in binding and regulation of expression of the target by mRNA cleavage, translation inhibition or DNA methylation. The siRNA process is illustrated in Figure 24.

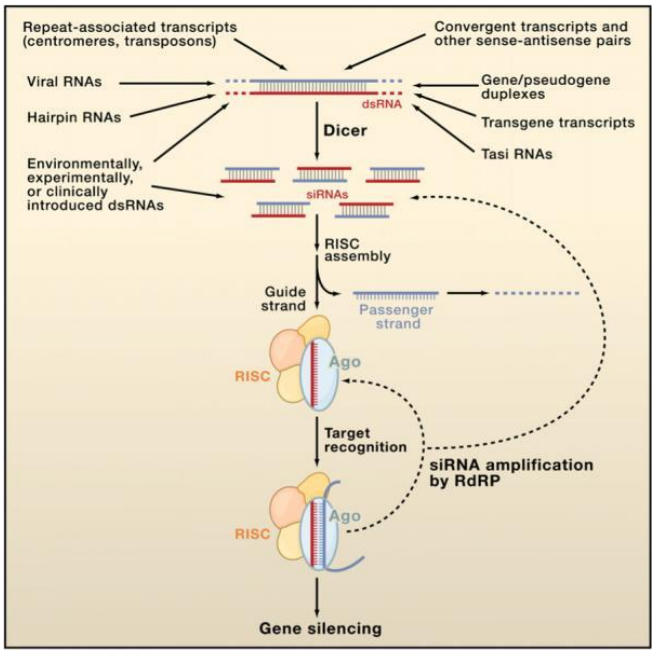

Figure 24: Overview of the mechanism of siRNA gene knockdown (Carthew & Sontheimer, 2009).

Transfection of siRNA was used to examine the effect of *p53* in doxorubicin-mediated upregulation of *F5*. Transfection of siRNA was accomplished using Lipofectamine™RNAiMax and Reduced Serum Medium Opti-MEM®.

3.6.3 HARVEST OF CELLS AND CELL MEDIA

3.6.3.1 Harvesting of cells for RNA examination

For harvesting of cells for RNA examination, cell media was removed, and the cells were carefully washed 1x in cold DPBS before addition of DNA/RNA Protection Reagent from Monarch® Total RNA Miniprep Kit. The cells were scraped, transferred to fresh tubes, and stored at -80°C prior to RNA isolation.

3.6.3.2 Harvesting of cells and cell media for protein or apoptosis examination

Cell media from the samples was transferred to fresh tubes and centrifuged at 3000 rpm for 10 minutes at 4°C. The supernatant was transferred to fresh tubes and stored at -80°C prior to total protein quantification.

To prepare protein lysates, the cells were carefully washed 3x in cold DPBS. RIPA with 1x Halt™ Protease and Phosphatase Inhibitor Cocktail was added to each well, 150 µl for 12-well plates and 100 µl for 24-well plates. The cells were scraped and transferred to fresh tubes.

For protein examination, the protein lysates were incubated for 30 minutes at 4°C and centrifuged at 3500 rpm for 10 minutes at 4°C. The supernatant was transferred to fresh tubes and stored at -80°C prior to total protein quantification.

For apoptosis examination, the protein lysates were centrifuged at 200G for 10 minutes at 4°C. The supernatant was transferred to fresh tubes. Fresh lysates were examined as described in section *3.5.3*.

3.6.3.3 Harvesting of cells for luciferase assays

For harvesting of cell lysates for luciferase assays, Dual-Luciferase® Reporter Assay System was used following manufacturer´s protocol for passive lysis of cells cultured in 96-well plates. The Passive Lysis Buffer (PLB) decreases background autoluminescence and is thus well suited for luciferase assays. Samples were stored at -80°C prior to luciferase assays.

3.6.4 CELL VIABILITY AND IC_{50} VALUES DURING CHEMOTHERAPY TREATMENT

Drug sensitivity was studied by examination of cell viability during treatment with different chemotherapy drugs at several concentrations. The sensitivity was measured by calculating the IC_{50} value, which is the drug concentration resulting in 50% growth inhibition. The IC_{50} value was used to determine drug concentrations for the experiments conducted to study the mRNA expression of *F5* and protein levels of FV during drug treatment of breast cancer cell lines.

Cell viability was studied in MDA-MB-231 and MCF-7 cells with drugs used for the patients in the Osaka and NeoAva study which constituted 5-fluorouracil, epirubicin, cyclophosphamide and bevacizumab. In addition, doxorubicin was tested. The cells were seeded out in 96-wells plates and cultured for 24 hours. The cells were then treated with drugs in concentrations listed in Table 9 or with PBS for 24 and 48 hours in six replicates for each concentration. To correct for disturbances from the red dye in doxorubicin and epirubicin, all concentrations of these drugs were also added to cell-free wells containing DMEM with 10% FBS and added WST-1 like the other samples (Appendix D, Figure D3). After drug incubation, cell viability was measured as described in section *3.5.1*.

Table 9: Total cell number and drug concentrations per well in 96-well plates for viability experiments with MDA-MB-231 and MCF-7 cells.

	Concentrations (µM):	
	MCF-7	MDA-MB-231
Multiwell plate	96-well	96-well
Total cell number/well	$6*10^3$	$6*10^3$
5-fluorouracil (µM)	Not tested	5-1000.5-100 µM
Epirubicin (µM)	Not tested	0.5-100 µM
Doxorubicin (µM)	Not tested	0.5-100 µM
Bevacizumab (µM)	0.16-160 µM	0.16-160 µM
Cyclophosphamide (µM)	0.5-25 mM	0.5-25 mM

3.6.5 CHEMOTHERAPY TREATMENT OF BREAST CANCER CELLS

Stimulation experiments in MDA-MB-231 and MCF-7 cells were performed with treatment of each chemotherapy drug and drug combinations to investigate the effect on the expression of *F5*.

The drug concentrations used in the stimulation experiments were based on the IC_{50} values found in this thesis and concentrations used in similar experiments found in the literature. A combination of 5-flourouacil, epirubicin and cyclophosphamide (FEC) and eventually bevacizumab was prepared at a molar ratio of 26:1:12:4, similar to the clinical dosage in the NeoAva cohort. All references on FEC/FEC-BEV in this thesis are based on the concentration of 5-fluorouracil.

MDA-MB-231 and MCF-7 cells were seeded out in 12-well plates. The cells were then treated with drugs or PBS with the concentrations listed in Table 10 for 24 hours in three replicates. Cell lysates were harvested and *F5* expression was analyzed as described in section *3.6.3.1* and *3.2.4.4* respectively.

Table 10: Drug concentrations and total cell number per well in 12-well plates for stimulation experiments with MDA-MB-231 and MCF-7 cells.

	MDA-MB-231 / MCF-7
Multiwell plate	12-well
Total cell number/well	$1.7*10^5$
5-fluorouracil (µM)	20 µM and 100 µM
Epirubicin (µM)	0.1 µM and 1 µM
Cyclophosphamide (µM)	1.5 µM and 15 µM
Bevacizumab (µM)	5 µM and 50 µM
FEC	2.5 µM and 12.5 µM
FEC-BEV	2.5 µM and 12.5 µM

3.6.6 Inhibition of p53

3.6.6.1 Inhibition of p53 with Pifithrin-α

p53 inhibition with Pifithrin-α (PFT-α) was performed in MDA-MB-231 cells to examine whether p53 inhibition affected doxorubicin induced *F5* expression.

MDA-MB-231 cells were seeded out in 12-well plates. Three replicates were used. Pifithrin-α (PFT-α) and DMSO were diluted in DMEM with 10% FBS in concentrations as described in Table 11. Media was carefully removed from the wells, and fresh PFT-α- or DMSO-media were added to the wells. The cells were incubated for 2 hours, before treatment with 1 µM doxorubicin or

PBS. After 24 hours of treatment, cell lysates were harvested as described in section *3.6.3.1* and *F5* expression was analyzed as described in section *3.2.4.4*. Cell media was also harvested after 48 hours treatment as described in section *3.6.3.2* and FV protein levels were analyzed as described in section *3.4.2*.

Table 11: Concentrations and amounts per well in 12-well plates for p53 inhibition experiments with MDA-MB-231 cells.

	Concentration and amounts per well
Multiwell plate	12-well
MDA-MB-231	$1.7*10^5$
DMSO	0.5%
PFT-α	20 µM
Doxorubicin	1 µM

3.6.6.2 Inhibition of p53 with siRNA

Knockdown of *TP53* was performed in MCF-7 and MDA-MB-231 cells to investigate whether *TP53* knockdown affected doxorubicin induced *F5* expression.

The cells were seeded out in 12-well plates. Three replicates were used. Cells were transfected with siRNA-p53 or siRNA negative control using Lipofectamine RNAiMax with reagents and cell numbers as described in Table 12. 24 hours after transfection the cells were treated with either 1 µM doxorubicin or PBS. The cells were incubated for another 24 and 48 hours before harvesting of cell lysates and media as described in section *3.6.3.1* and *3.6.3.2* respectively. *F5* expression and FV protein levels were analyzed as described in section *3.2.4.4* and *3.4.2* respectively.

Table 12: Transfection reagents, total cell number and amounts per well in 12-well plates for siRNA transfection experiments with MCF-7 and MDA-MB-231 cells.

	Amount per well:
Multiwell plate	12-well
Total cell number (MCF-7/MDA-MB-231)	$1.7x10^5$
siRNA	10 pmol
Lipofectamine®RNAiMax	3 µl
OptiMEM	100 µl
DMEM with 10% FBS	900 µl
Total	1000 µl

3.6.7 The role of p53 in the FV promoter

Plasmids used in experiments with mutated p53 half-sites in the *F5* promoter were previously described in Table 3. Amounts of transfection reagents and total cell number are listed in Table 13. Five replicates were used. Cells were reverse transfected in 96-well plates and incubated for 24 hours. Cells were treated with 1 µM doxorubicin or DMEM with 10 % FBS for 24 hours before harvesting as described in section *3.6.3.3*.

Table 13: Transfection reagents, total cell number and amounts per well in 96-well plates for experiments with transfection of F5 promoters with different status in the p53 half-sites in MCF-7 and MDA-MB-231 cells.

	Amount per well:
Multiwell plate	96-well
Total cell number (MCF-7/MDA-MB-231)	$3x10^4$ / $2.8x10^4$
Plasmid	150 ng
pRL-SV40	10 ng
P3000 reagent	0.3 µl
Lipofectamine 3000	0.3 µl
OptiMEM	20 µl
DMEM with 10% FBS	100 µl
Total	120 µl

3.6.8 Overexpression of FV with and without doxorubicin treatment

Functional experiments were performed to study the effect of FV on apoptosis and proliferation in MDA-MB-231 cells. The number of replicates, amounts, and cell number per well are described in Table 14.

Table 14: Amounts per well in 24- and 96 well plates for experiments on the functional effect of FV on apoptosis and proliferation in MDA-MB-231 cells.

	Apoptosis	Proliferation
Multiwell plate	24-well	96-well
Total cell number/well	$8.5*10^4$	$2*10^4$
pMT2-FV	1.25 µg	0.125 µg
pMT2-negative control	1.25 µg	0.125 µg
P3000 reagent	2.5 µl	0.25 µl
OptiMem	50 µl	5 µl
Lipofectamine 3000	3.75 µl	0.375 µl

3.6.8.1 Effect of FV overexpression on apoptosis

MDA-MB-231 cells were seeded out in 24-well plates. Three replicates were used. Cells were transfected with the FV overexpression plasmid, pMT2-FV, or pMT2-negative control according to Table 14. After 24 hours, cells were treated with 1 µM doxorubicin or PBS. After 48 hours with treatment, cell lysates and media were harvested as described in section *3.6.3.2* and apoptosis was examined as described in section *3.5.3*.

3.6.8.2 Effect of FV overexpression on cell proliferation

MDA-MB-231 cells were seeded out in 96-well plates and reverse transfected with overexpression FV plasmids according to Table 14. Six replicates were used. After 24 hours the cells were treated with 1 µM doxorubicin or PBS. After 48 hours with treatment, proliferation was examined as described in section *3.5.1*.

3.6.9 Coagulation factors with and without doxorubicin treatment

Functional experiments were performed to study the effect of coagulation factors on apoptosis and proliferation in MDA-MB-231 cells with and without doxorubicin treatment. Coagulation factor combinations are described in Table 15 and cell numbers and concentrations are described in Table 16.

*Table 15: Coagulation factor, plasma, media and treatment combinations for apoptosis and proliferation experiments with factors and cofactors. *=only for proliferation experiments.*

Media / Treatment:	Coagulation factor/reagent combination:
DMEM with 10% FBS + 10% FV def plasma + 2 U/mL Hirudin	Glycerol/H_2O control
	Glycerol/H_2O + APC
	FV *
	FV + APC
	FVa *
	FVa + APC
DMEM with 10% FBS	Glycerol/H_2O control
	Glycerol/H_2O + APC + PS + FVIIa + FXa
	FV + APC + PS + FVIIa + FXa
	FVa + APC + PS + FVIIa + FXa
	DMSO control
	PAR2 agonist

Table 16: Amounts and concentrations per well for 24- and 96 well plates for apoptosis and proliferation experiments with factors and cofactors.

	Apoptosis	Proliferation
Multiwell plate	24-well	96-well
Total cell number/well	$8.5*10^4$	$2*10^4$
Factor concentration	100 ng/ml	100 ng/ml
PAR2 concentration	20 µM	20 µM
DMSO concentration	0.01%	0.01%

3.6.9.1 Effect of coagulation factors on apoptosis

MDA-MB-231 cells were seeded out in 24-well plates and incubated for 24 hours. Three replicates were used. The cells were incubated in either DMEM with 10% FBS or DMEM with 10% FBS, 10% FV deficient plasma and hirudin. Thereafter, reagent combinations and concentrations as described in Table 15 and Table 16 were added. The cells were treated with 1 µM doxorubicin or PBS. After 48 hours of treatment, cell lysates and media were harvested as described in section *3.6.3.2*. Apoptosis was examined as described in section *3.5.3*.

3.6.9.2 Effect of coagulation factors on cell proliferation

MDA-MB-231 cells were seeded out in 96-well plates and incubated for 24 hours. Four replicates were used. Cells were treated with the reagent combinations and concentrations as described in Table 15 and Table 16 and were treated with 1 µM doxorubicin or PBS. After 24 and 48 hours with doxorubicin treatment, proliferation was examined as described in section *3.5.1*.

3.7 Tumor expression of *F5* and response to neoadjuvant chemotherapy in breast cancer

Data analysis of gene expression and treatment response for various treatments in distinct cancer subtypes can lead to new valuable insight in cancer treatment. Identification of markers for treatment response can facilitate specific treatment of patients based on cancer type. In this thesis, expression of *F5* was examined as a candidate gene marker for treatment response.

3.7.1 Patient cohorts

Nine publicly available breast cancer cohorts with gene expression data were kindly provided by Scientist Xavier Tekpli, Department of Medical Genetics, OUS. Patients' consents and ethical approval are accessible in the original studies. The nine data materials used in this thesis and the treatments of the patients in the separate cohorts are listed in Table 17. Gene expression was measured before treatment. Pathologic complete response (pCR) was used as endpoint measurement. pCR is defined as the absent of invasive in tissue samples from patients which have received radiation or chemotherapy treatment.

Table 17: Name, treatment, additional information, source, accession number and PMID for the nine cohorts collected for analyses of F5 expression. *FEC=5-fluorouracil, epirubicin and cyclophosphamide. FAC=5-fluorouacil, doxorubicin and cyclophosphamide. P-FAC=Paclitaxel followed by FAC. AE=Array Express Archive of Functional Genomics Data. GEO=Gene Expression Omnibus. *=Halves of the patients in the cohort was treated with the specific drug in addition.*

Name:	Patients:	Treatment:	Additional information:	Source:	Accession no:	PMID:
NeoAva	106	Bevacizumab* FEC Docetaxel/Paclitaxel	ER PAM50	AE	E-MTAB-4439	28487444
MDACC	508	Anthracyclines Taxanes	ER PR HER2 PAM50	GEO	GSE25066	21558518
MDACC MAQC	278	P-FAC		GEO	GSE20194	20064235
MDACC TFAC	178	P-FAC	ER	GEO	GSE20271	20829329
MDACC IGR	103	FAC	ER *p53*	GEO	GSE22093	21191116
Osaka	115	P-FEC	ER PR HER2	GEO	GSE32646	22320227
USO	61	P-FEC Docetaxel Capecitabine	ER	GEO	GSE23988	21191116
VAN	28	Paclitaxel Radiation		GEO	GSE22513	20068102
WASH2	24	Unknown	ER HER2	Unknown	Unknown	Unknown

3.8 STATISTICS

3.8.1 STATISTICAL ANALYSES FOR CLINICAL DATA MATERIALS

All analyses were performed in the R version 4.0.3. The R packages ggpubr and dplyr were used for examination of distribution of *F5* and to perform Wilcoxon rank sum test or Kruskal Wallis test. The ggplot2 package was used to draw boxplots to visualize the data. *P*-values <0.05 were considered statistically significant.

The tumor gene expression levels of *F5*, measured before treatment, were compared between the patients with responding tumors and nonresponding tumors using Wilcoxon rank sum test. Analyses were performed in all cohorts merged together, and in each cohort separately. The cohorts were also divided into subtype groups according to ER/PR/HER2 status, *TP53* status, and PAM50-subtypes. Moreover, differences in *F5* tumor expression across the different tumor subtypes were investigated using Kruskal Wallis test.

3.8.2 STATISTICAL ANALYSES FOR CELL EXPERIMENTS

Statistics for the results of cell experiments were performed by un-paired t-test. *P*-values≤0.05 were considered statistically significant. In figures statistically significant results are marked with * for p≤0.05 and ** for p≤0.001.

4. RESULTS

4.1 ANALYSIS OF *F5* EXPRESSION IN CLINICAL DATA MATERIALS

4.1.1 TUMOR EXPRESSION OF F5 AND TREATMENT RESPONSE TO NEOADJUVANT CHEMOTHERAPY

To study if there was an association between the expression of *F5* and treatment response in breast cancer tumors, nine publicly available breast cancer cohorts with gene expression data were examined.

In the NeoAva cohort, a higher expression of *F5* in responders (Wilcoxon, *P*=0.03) compared with non-responders to neoadjuvant chemotherapy was observed (Figure 25A). By separating the patients treated with bevacizumab from patients not treated with bevacizumab, it was found that the elevated level in *F5* expression in tumors were located in the patient group receiving bevacizumab (Wilcoxon, *P*=0.02) (Figure 25B). It was no significance difference in *F5* expression in the group which had not received bevacizumab (Figure 25C). The results may indicate an association with sensitivity to the combinatory treatment with FEC (5-fluorouacil, epirubicin and cyclophosphamide) and bevacizumab and elevated expression of *F5* in breast cancer tumors.

In the Osaka cohort, a higher expression of *F5* in responders (Wilcoxon, *P*=0.03) compared with non-responders to neoadjuvant chemotherapy was shown (Figure 26). The result may indicate an association with sensitivity to paclitaxel and FEC treatment and elevated expression of *F5* in breast cancer tumors. No significant differences in tumor *F5* expression in responders compared with non-responders to neoadjuvant chemotherapy were found in the other cohorts (results not shown).

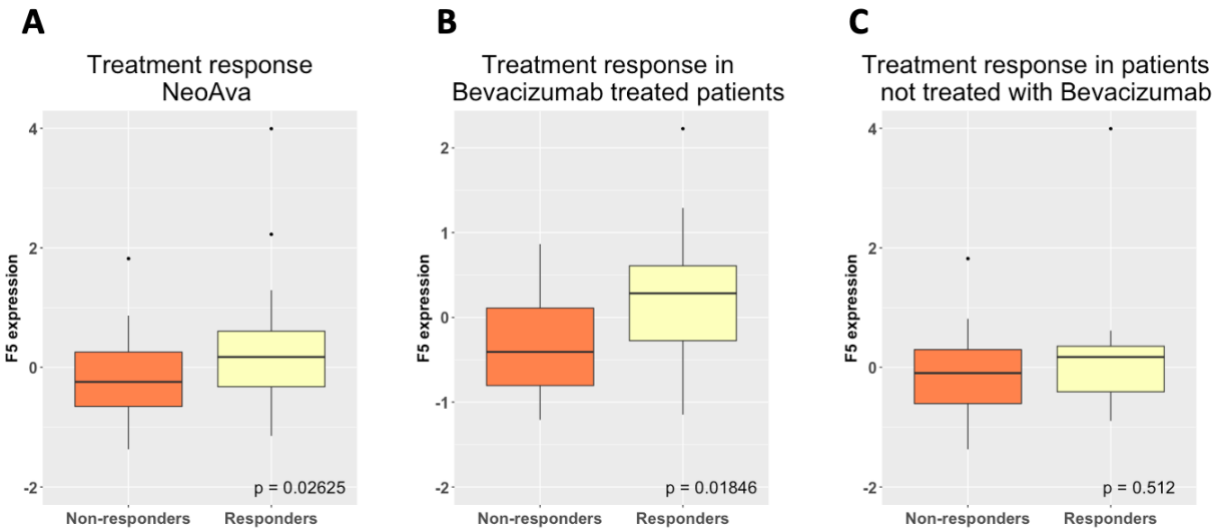

Figure 25: A) F5 expression in non-responders and responders in the NeoAva cohort (n=106). B) F5 expression in non-responders and responders in the bevacizumab-patient group in the NeoAva cohort (n=53). C) F5 expression in non-responders and responders in the patient group not received bevacizumab in the NeoAva cohort (n=53). *P-values were generated from Wilcoxon rank sum test. Boxplots show the distribution of expression of F5, where the midline within each box represent the median, upper and lower edges of the boxes represent 75th and 25th percentiles respectively, whiskers under the box represent the lowest value within [1.5x(75th-25th percentile)] of the lower quartile and whiskers over the box represent the highest value within [1.5x(75th-25th percentile)] of the upper quartile, and dots represent outliers.*

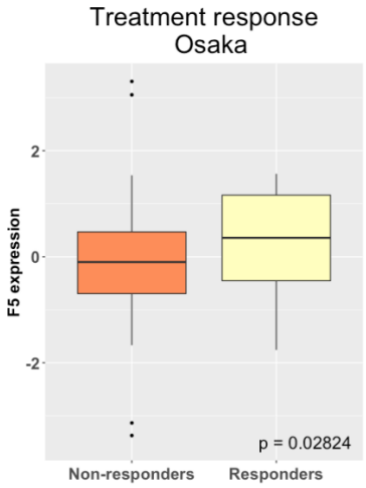

Figure 26: F5 expression in non-responders and responders in the Osaka cohort (n=115). *P-value was generated from Wilcoxon rank sum test. Boxplots show the distribution of expression of F5, where the midline within each box represent the median, upper and lower edges of the boxes represent 75th and 25th percentiles respectively, whiskers under the box represent the lowest value within [1.5x(75th-25th percentile)] of the lower quartile and whiskers over the box represent the highest value within [1.5x(75th-25th percentile)] of the upper quartile, and dots represent outliers.*

4.1.1.1 Distribution of breast cancer subtypes and hormone receptor status in the NeoAva and Osaka cohort

In patients with tumors responding to neoadjuvant chemotherapy in the NeoAva cohort, it was found that 53% was ER negative and in non-responding tumors 85% was ER positive (Figure 27).

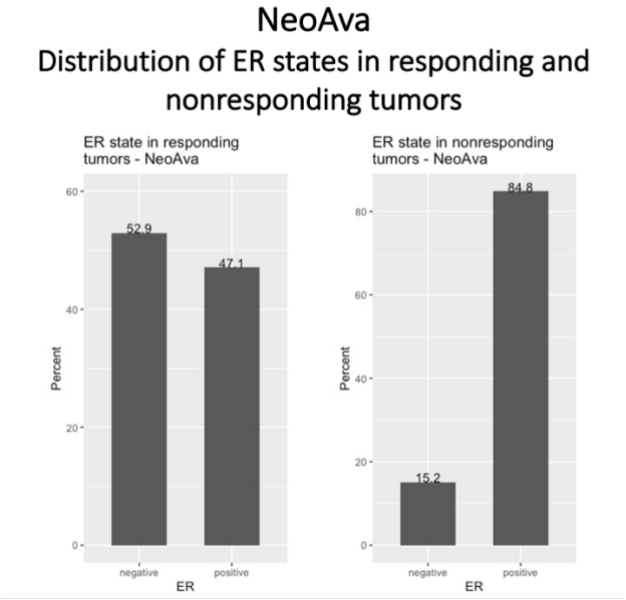

Figure 27: Distribution of ER status in responding (n=17) and non-responding tumors in the NeoAva cohort (n=33).

In patients with tumors responding to neoadjuvant chemotherapy in the Osaka cohort, it was found that 70% was ER negative and 82% was PR negative. The distribution of HER2 statuses were less distinct with 57% HER2 negative (Figure 28). In patients with non-responding tumors in the Osaka cohort, it was found that 72% was ER positive, and 75% was HER2 negative. PR status was less distinct with 55% PR negative (Figure 29).

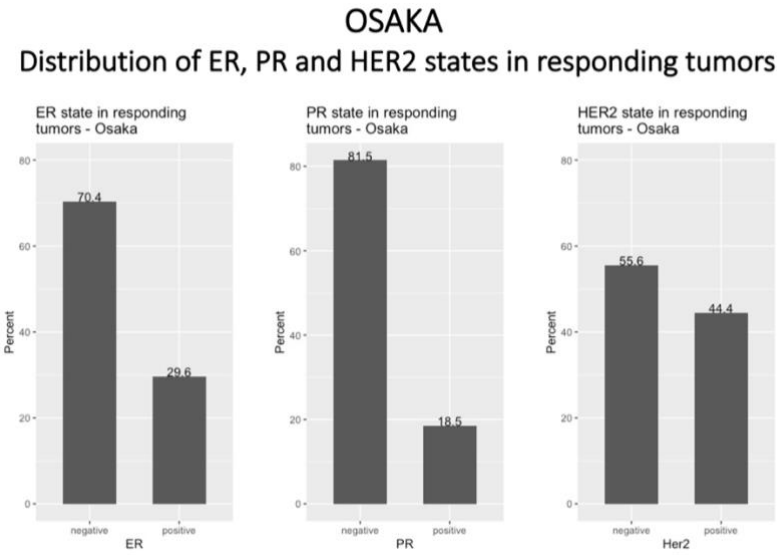

Figure 28: Distribution of ER, PR and HER2 status in responding tumors in the Osaka cohort (n=27).

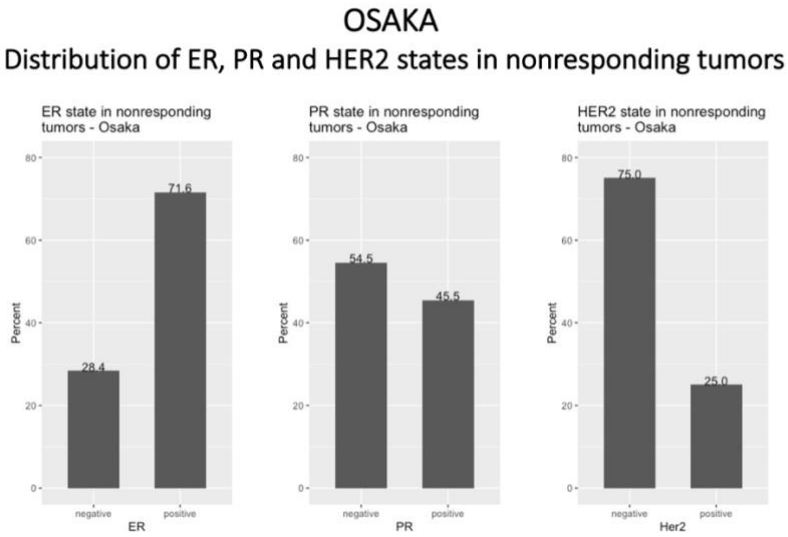

Figure 29: Distribution of ER, PR and HER2 status in non-responding tumors in the Osaka cohort (n=88).

The distribution of responders and non-responders to neoadjuvant chemotherapy in each PAM50 subgroup in the NeoAva cohort were showed in Figure 30. Within the basal subtype, 78% of the tumors were responders. Within the luminal A subtype, 16% of the tumors were responders and within the luminal B subtype, 35% of the tumors were responders. Due to low numbers of patients with HER2 (n=2) and normal-like (n=3) tumors in the NeoAva-Bevacizumab cohort, calculations for these subtypes were not performed due to low accuracy.

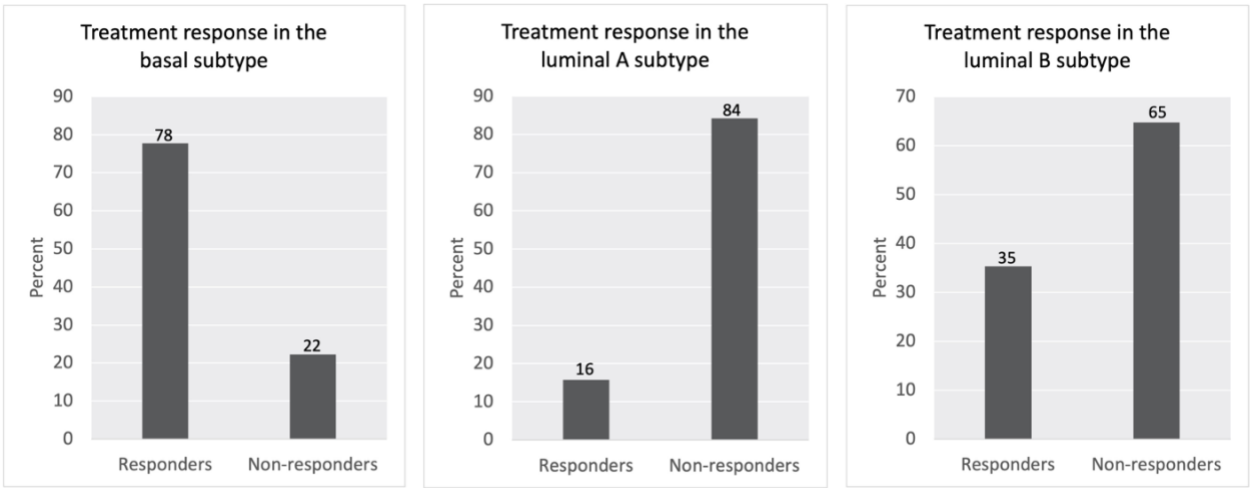

Figure 30: Treatment response within the basal (n=9), luminal A (n=19) and luminal B (n=17) PAM50 subtypes in the NeoAva-Bevacizumab cohorts.

These results indicated an association between ER negative and PR negative hormone receptor status and patients with tumors responding to neoadjuvant chemotherapy. Within the patients with basal tumors, the large majority of them were responding to neoadjuvant chemotherapy which indicated an association between the basal subtype and responding tumors. Within the patients with luminal A or luminal B tumors, the large majority of them were non-responding to neoadjuvant chemotherapy which indicated an association between the luminal A and luminal B subtype and non-responding tumors.

4.1.2 F5 EXPRESSION IN BREAST CANCER SUBTYPES

Investigation of *F5* expression according to cancer subgroups was performed in cohorts with the necessary information provided. The *F5* expression in negative and positive status of ER/PR/HER2 were compared.

In the MDACC cohort a difference in expression of *F5* according to both PR status (Wilcoxon, *P*=0.04) (Figure 31A) and ER status (Wilcoxon, *P*=0.04) (Figure 31B) were shown, with a higher expression of *F5* in the negative status. The MDACC TFAC cohort showed a higher expression of *F5* in ER negative (Wilcoxon, *P*=0.01) compared with ER positive status (Figure 31C). The results may indicate that the expression of *F5* is higher in certain PR-negative and ER-negative cancer types. No differences in *F5* expression in the other cohorts were found (result not shown).

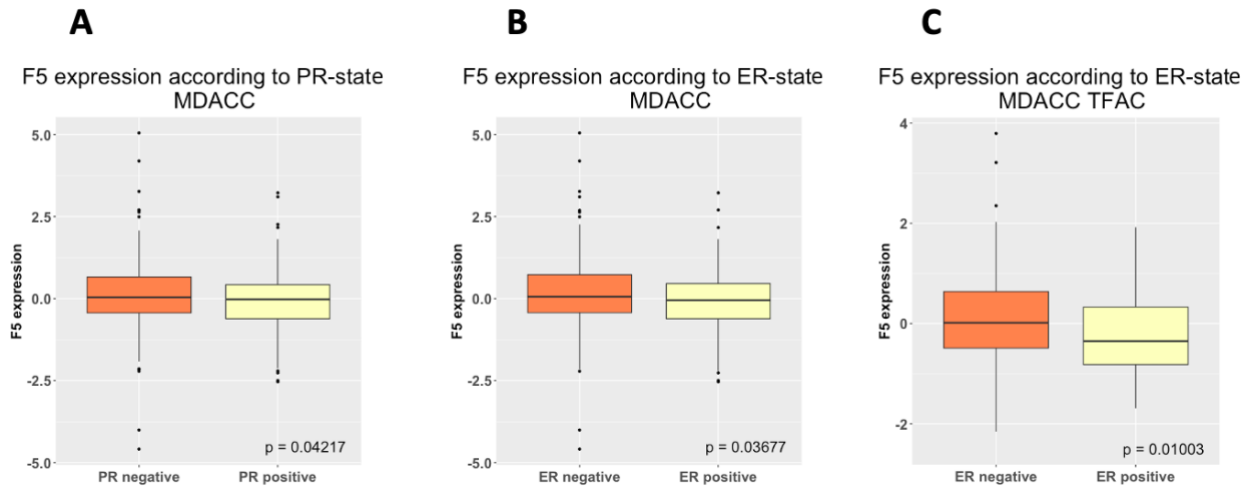

Figure 31: A) F5 expression in cancers with different PR status in the MDACC cohort (n=503). B) F5 expression in cancers with different ER status in the MDACC cohort (n=508). C) F5 expression in cancers with different ER status in the MDACC TFAC cohort (n=178). *All p-values were generated from Wilcoxon rank sum test. Boxplots show the distribution of expression of F5, where the midline within each box represent the median, upper and lower edges of the boxes represent 75th and 25th percentiles respectively, whiskers under the box represent the lowest value within [1.5x(75th-25th percentile)] of the lower quartile and whiskers over the box represent the highest value within [1.5x(75th-25th percentile)] of the upper quartile, and dots represent outliers.*

The datasets were merged to examine if it was a significant difference in *F5* expression in different cancers with distinct characteristics. ER, PR and HER2 status were examined. ER status was available in the MDACC, MDACC IGR, MDACC TFAC, NeoAva, Osaka, USO and WASH2 study and provided a merged dataset with 1095 patients. In the merged dataset it was found a higher expression of *F5* in ER negative (Wilcoxon, *P*=0.0002) compared to ER positive (Figure 32A). PR status was available in the MDACC and Osaka study and provided a merged dataset with 618 patients. In this merged dataset it was found a higher expression of *F5* in PR negative (Wilcoxon, *P*=0.017) compared to PR positive (Figure 32B). HER2 status was available in Osaka, MDACC and WASH2 and provided a merged dataset with 643 patients. In the merged dataset the difference in *F5* expression according to HER2 status was not significant (Figure 32C). Together with the results for the separate cohorts shown above, these results strengthen the indication of an association between ER-negative and PR-negative breast cancer tumors and higher expression of *F5* even further.

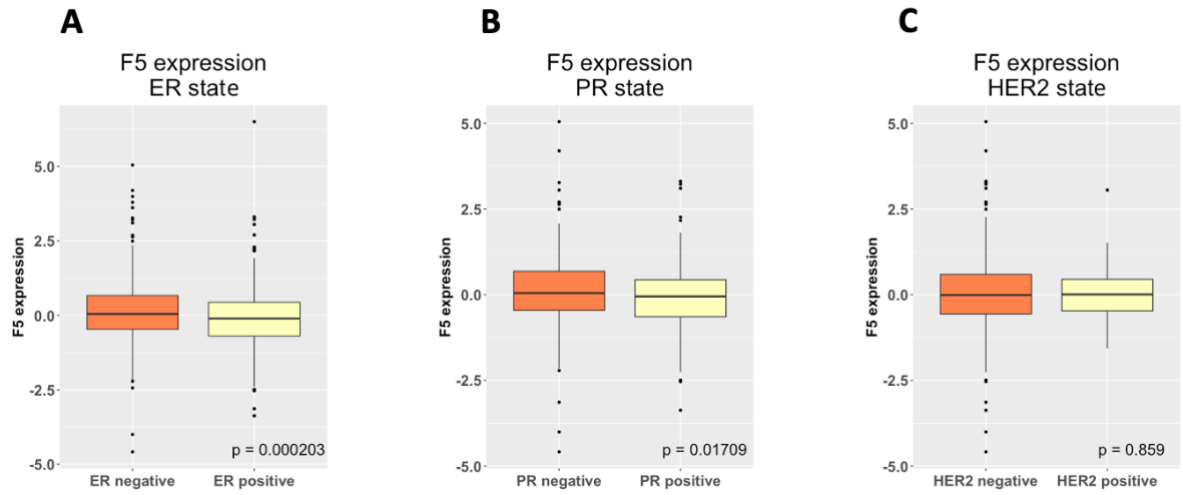

Figure 32: A) F5 expression in tumors with different ER status. The NeoAva, MDACC, MDACC TFAC, MDACC IGR, Osaka, USO and WASH2 cohort reported the ER status and were merged to a dataset with n=1095 patients (P=0.0002). B) F5 expression in cancers with different PR status. The MDACC and Osaka cohort reported the PR status and were merged to a dataset with n=618 patients (P=0.02). C) F5 expression in cancers with different HER2 status. The MDACC, Osaka and WASH2 cohort reported the HER2 status and were merged to a dataset with n=643 patients (P=0.859). *All p-values were generated by Wilcoxon rank sum test. Boxplots show the distribution of expression of F5, where the midline within each box represent the median, upper and lower edges of the boxes represent 75th and 25th percentiles respectively, whiskers under the box represent the lowest value within [1.5x(75th-25th percentile)] of the lower quartile and whiskers over the box represent the highest value within [1.5x(75th-25th percentile)] of the upper quartile, and dots represent outliers.*

PAM50 cancer subtypes were available in the NeoAva and MDACC cohort. The result for the merged dataset was shown in Figure 33. The result showed highest expression of *F5* in Basal and Normal-like subtypes, lower in Luminal A and Luminal B subtypes and lowest in HER2 subtype (Kruskal Wallis test *P*=0.05).

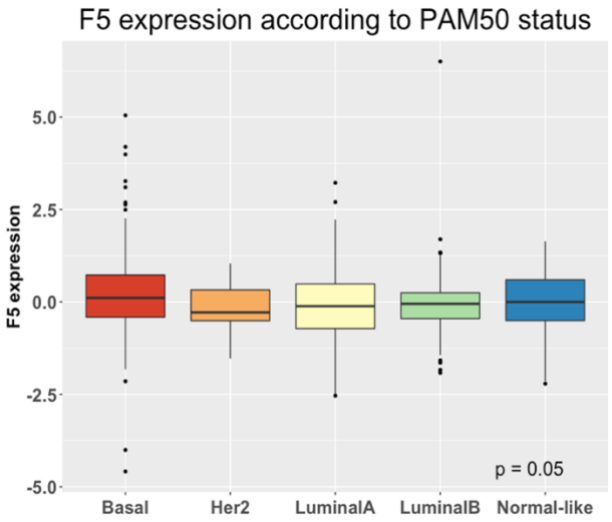

Figure 33: F5 expression in the Basal, Her2, Luminal A, Luminal B and Normal-like PAM50 cancer subtypes in the NeoAva and MDACC cohort merged to a dataset with n=614 patients (P=0.05). *The p-value was generated from Kruskal Wallis test. Boxplots show the distribution of expression of F5, where the midline within each box represent the median, upper and lower edges of the boxes represent 75th and 25th percentiles respectively, whiskers under the box represent the lowest value within [1.5x(75th-25th percentile)] of the lower quartile and whiskers over the box represent the highest value within [1.5x(75th-25th percentile)] of the upper quartile, and dots represent outliers.*

4.1.3 FV AND TREATMENT RESPONSE IN BREAST CANCER SUBTYPES

ER, PR, HER2 and PAM50 groups within in each cohort were studied to examine if there was a difference in expression of *F5* in responders compared with non-responders. No significant differences in *F5* expression in responders compared with responders in either of these groups were found (results not shown).

4.2 THE EFFECT OF CHEMOTHERAPY IN BREAST CANCER CELL LINES

Based on the result in the clinical data material which showed an association between *F5* expression and treatment response in the NeoAva and Osaka cohort, it was interesting to test whether the drugs used in theses cohorts had an effect on *F5* expression.

4.2.1 DETERMINATION OF IC_{50} VALUES DURING CHEMOTHERAPY TREATMENT

To calculate drug concentrations for stimulation experiments with the drugs from the NeoAva and Osaka cohorts, the IC_{50} values for doxorubicin, epirubicin, 5-fluorouracil, cyclophosphamide and bevacizumab were found in MCF-7 and/or MDA-MB-231 cell lines.

IC_{50} values for MDA-MB-231 and MCF-7 cells after 24- and 48-hours treatment with doxorubicin, epirubicin, 5-fluorouracil, cyclophosphamide and bevacizumab were shown in Figure 34.

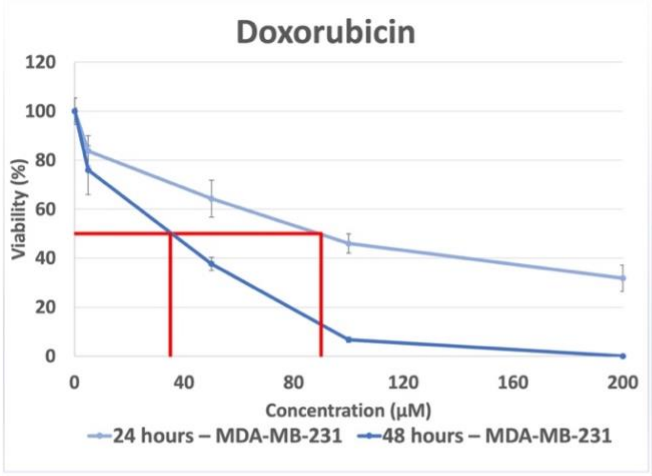

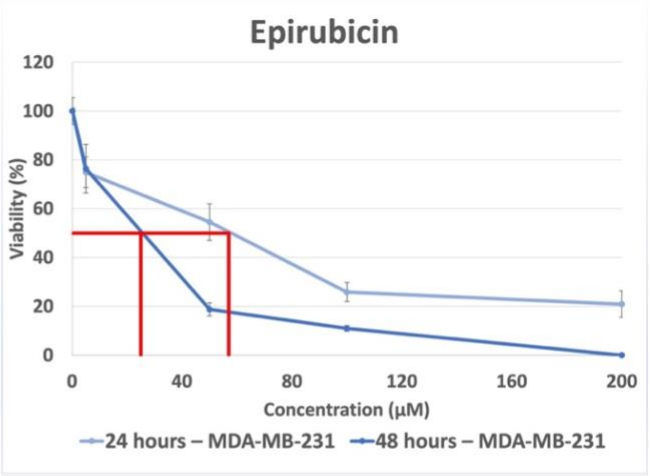

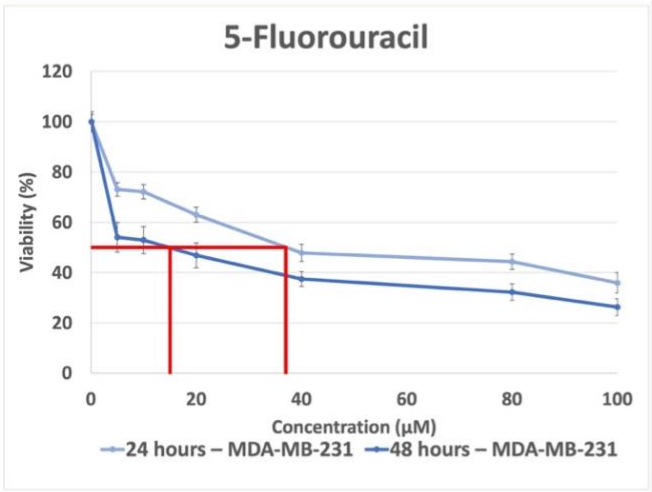

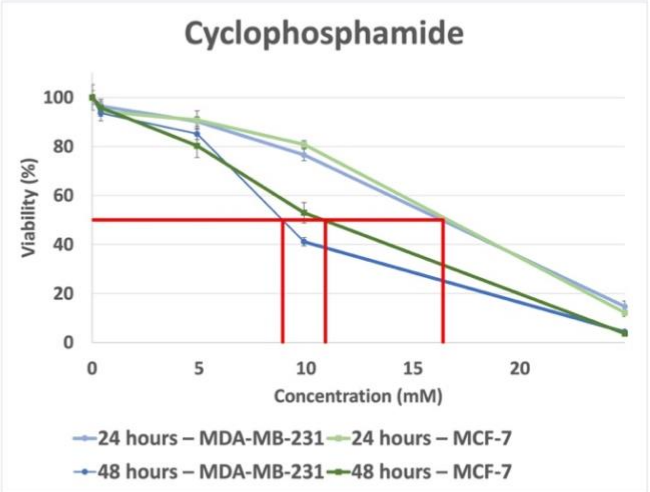

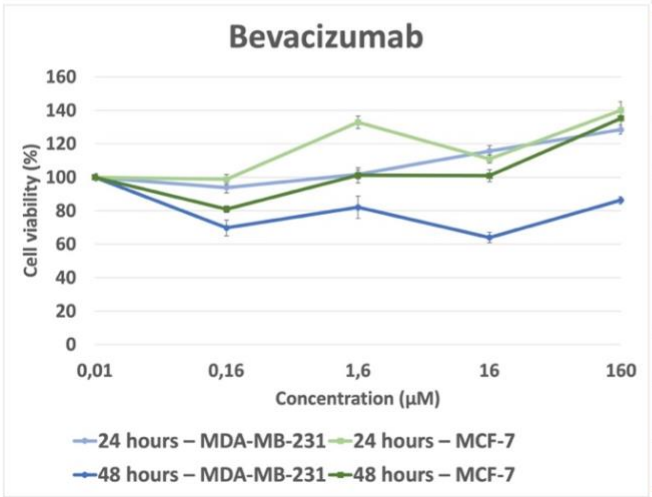

Cell type	Cytostatica	IC_{50}	
		24 hours	48 hours
MDA-MB-231	Doxorubicin	90 µM	35 µM
MDA-MB-231	Epirubicin	57 µM	25 µM
MDA-MB-231	5-Fluorouracil	37 µM	15 µM
MDA-MB-231	Cyclophosphamide	16.5 mM	9 mM
MCF-7	Cyclophosphamide	16.5 mM	11 mM
MDA-MB-231	Bevacizumab	Not found	Not found
MCF-7	Bevacizumab	Not found	Not found

Figure 34: Cell viability and IC50 values for MDA-MB-231 and/or MCF-7 after 24 and 48 hours with treatment with doxorubicin (1-200 µM), epirubicin (1-200 µM), 5-fluorouracil (10-200 µM), cyclophosphamide (0.5-25 mM) or bevacizumab (0.16-160 µM) measured by WST-1. Mean values (n=12) and SEM from minimum two separate experiments were shown.

4.2.2 The effect of chemotherapy treatment on F5 expression

The IC_{50} values were used to determine the drug concentrations in the stimulation experiments. These stimulation experiments were conducted to examine if the drugs used in the NeoAva and Osaka cohorts have an effect on *F5* expression.

In MDA-MB-231 cells, an increase in *F5* expression after 1 µM epirubicin treatment of approximately 41-fold (P=3.3*10^{-8}) was shown. It was also a small increase in *F5* expression after 12.5 µM FEC treatment (P=0.04) and FEC-Bevacizumab treatment (P=0.04) of approximately 13- and 9-fold respectively (Figure 35).

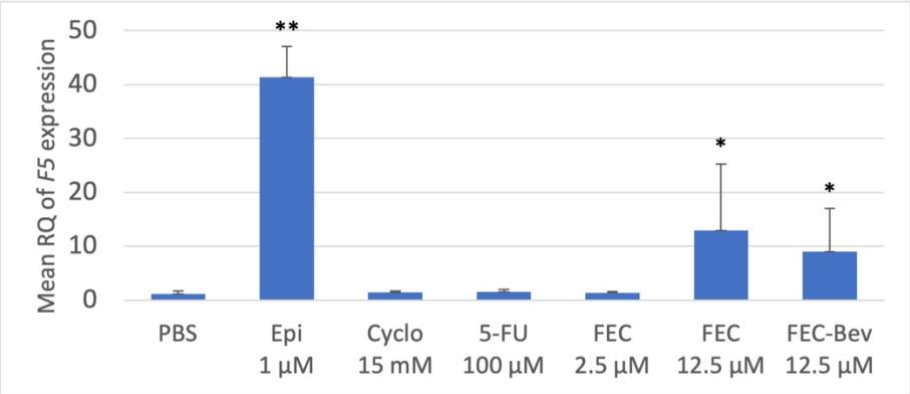

Figure 35: Expression of F5 in MDA-MB-231 cells with 24 hours with treatment of epirubicin (1 µM), cyclophosphamide (15 mM) 5-fluorouracil (100 µM), FEC (12.5 µM) and FEC-Bevacizumab (12.5 µM). *mRNA expression was measured using qRT-PCR and normalized against the endogenous control HPRT1. The RQ values were calculated relative to untreated control cells. Mean values (n=6) and SD from two separate experiments were shown. Significant differences in comparison to negative control were marked with *(p≤0.05) or **(p≤0.001).*

In MCF-7 cells, the results showed a slightly decrease in *F5* expression after 15 mM cyclophosphamide treatment (P=5.2*10^{-6}). An increase in *F5* expression of approximately 15-fold was shown after 100 µM 5-fluorouracil treatment (P=1.1*10^{-5}). There was also an increase of approximately 7-fold in *F5* expression after treatment with 2.5 µM FEC treatment (P=0.0004), 12.5 µM FEC treatment (P=8.9*10^{-8}) and 12.5 µM FEC-Bevacizumab treatment (P=8.3*10^{-7}) of approximately 7-, 10- and 10-fold respectively (Figure 36).

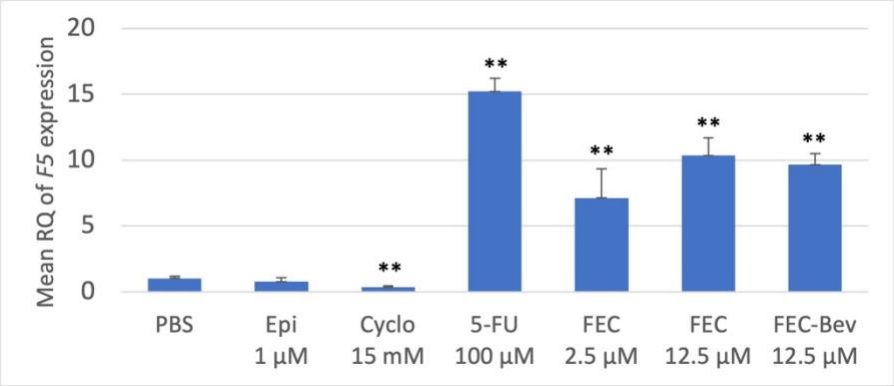

Figure 36: Expression of F5 in MCF-7 cells with 24 hours with treatment of epirubicin (1 µM), cyclophosphamide (15 mM) 5-fluorouracil (100 µM), FEC (12.5 µM) and FEC-Bevacizumab (12.5 µM). *mRNA expression was measured using qRT-PCR and normalized against the endogenous control GAPDH. The RQ values were calculated relative to untreated control cells. Mean values (n=6) and SD from two separate experiments were shown. Significant differences in comparison to negative control were marked with **(p≤0.001).*

4.2.3 Effect of doxorubicin on FV protein level

In the studies of the effects on chemotherapy on the FV protein level, doxorubicin was chosen because of its similarity to epirubicin, and because experiments with doxorubicin were already started. FV protein levels were examined in cell media and lysates in MCF-7 and MDA-MB-231 cells treated with doxorubicin to examine the effect of doxorubicin on FV protein production.

In MDA-MB-231 cell lysates an 1.5-1.8-fold increase in FV protein levels were observed after 48 hours of doxorubicin treatment compared to untreated control cells (P=0.01) (Figure 37A). No significant differences in FV protein levels were observed after 24 hours. In cell media, no significant differences in FV protein levels were observed (Figure 37B).

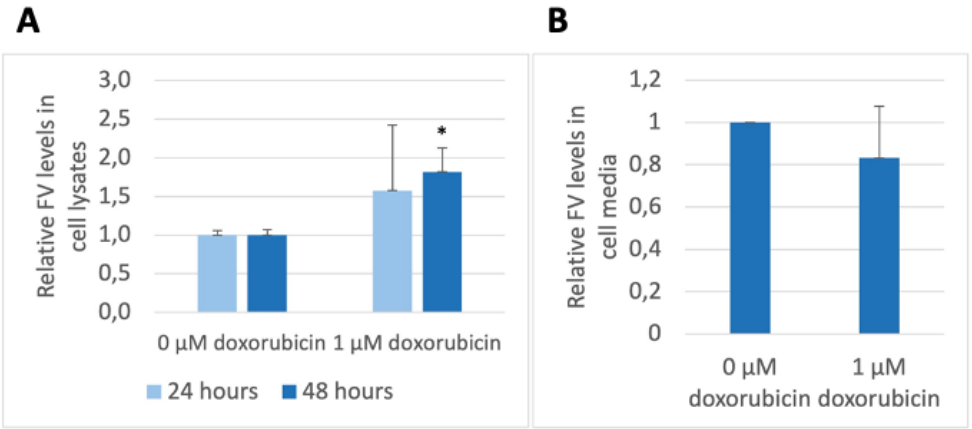

Figure 37: Relative protein levels of FV in MDA-MB-231 cells *measured by FV ELISA. A) FV protein levels in cell lysates. Cells were treated with 0 or 1 µM doxorubicin for 24 and 48 hours. The FV protein levels were corrected for total protein in cell lysates and calculated relative to untreated cells. Mean values (n>2) and SD from two separate experiments were shown.*

*Significant differences in comparison to negative control were marked with *(p≤0.05). B) FV protein levels in cell media. Cells were treated with 0 or 1 µM doxorubicin for 48 hours. The FV protein levels were calculated relative to the untreated cells. Mean values (n>4) and SD from at least two separate experiments were shown.*

In MCF-7 cell lysates the increase in FV protein level after 24 hours were not significant. A 4-fold increase in FV protein level was observed after 48 hours of doxorubicin treatment compared to untreated control cells (*P*=0.004) (Figure 38A). In cell media no significant differences in FV protein levels were observed (Figure 38B).

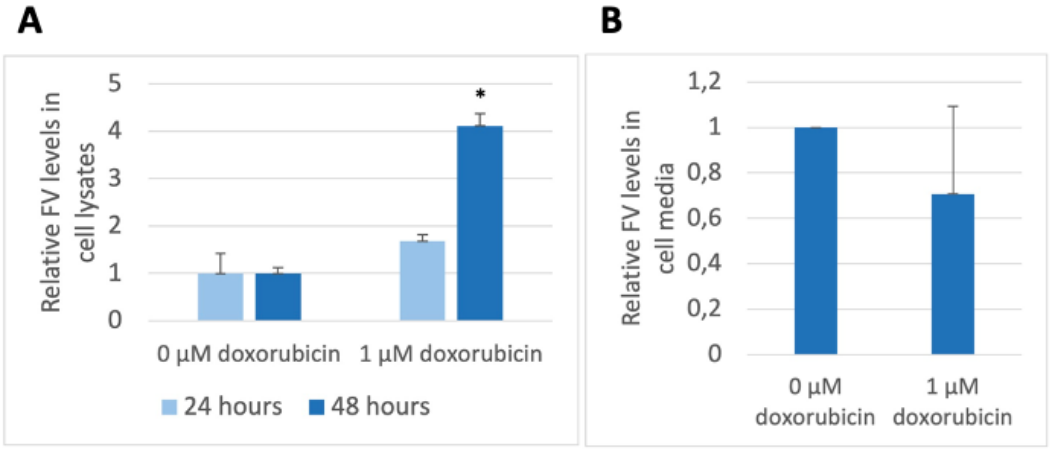

Figure 38: Relative protein levels of FV in MCF-7 cells *measured by FV ELISA. A) FV protein levels in cell lysates. Cells were treated with 0 or 1 µM doxorubicin for 24 and 48 hours. The FV protein levels were corrected for total protein lysates and calculated relative to untreated cells. Mean values (n=2) and SD from one representative experiment (of two) were shown. Significant differences in comparison to negative control were marked with *(p≤0.05). B) FV protein levels in cell media. Cells were treated with 0 or 1 µM doxorubicin for 48 hours. The FV protein levels were calculated relative to untreated cells. Mean values (n>4) and SD from at least two separate experiments were shown.*

4.3 THE EFFECT OF P53 ON *F5* EXPRESSION WITH AND WITHOUT DOXORUBICIN TREATMENT

Due to the findings in MDA-MB-231 cells which showed an induction of *F5* by epirubicin, it was interesting to study the mechanism behind this further. Epirubicin (and the highly similar doxorubicin) works, among other things, through the induction of p53 and it was therefore interesting to study if p53 had an effect on epirubicin/doxorubicin induced *F5* expression.

Initially, the role of p53 was studied in experiments with inhibition of p53 or knockdown of *TP53* with and without doxorubicin treatment.

4.3.1 P53 INHIBITION BY PIFITHRIN-ALPHA

Inhibition of p53 was performed using pifithrin-alpha (PFT-α) in MDA-MB-231 cells. An increase of approximately 20-fold in doxorubicin treated control cells compared with untreated control cells was shown. In PFT-α treated cells, the doxorubicin induced expression of *F5* was reduced by approximately 46% compared with the doxorubicin induced expression of *F5* in control cells (*P*=0.001) (Figure 39).

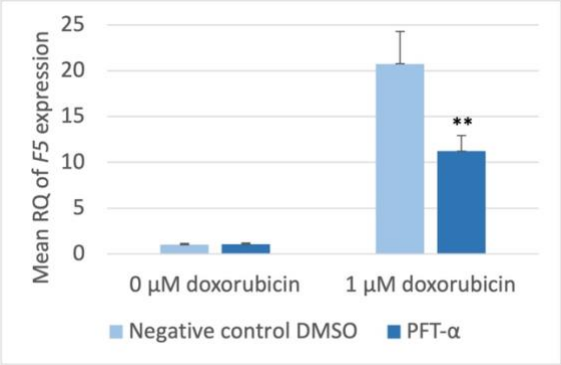

Figure 39: Expression of F5 in MDA-MB-231 cells treated with PFT-α in 2 hours followed by 24 hours with 1 µM doxorubicin treatment. *mRNA expression was measured using qRT-PCR and normalized against the endogenous control HPRT1. RQ values were calculated relative to untreated control cells. Mean values (n=6) and SD from two separate experiments were shown. Significant differences in comparison to negative control were marked with **(p≤0.001).*

4.3.2 TP53 KNOCKDOWN BY SIRNA

Due to the reduction in *F5* expression in cells treated with PFT-α, it was interesting to examine if similar results could be generated with knockdown of *TP53*. Knockdown of *TP53* was performed using siRNA-p53 in MDA-MB-231 and MCF-7 cells. Knockdown of *TP53* in siRNA-p53 transfected cells were verified by examine the *TP53* expression in all knockdown experiments.

In MDA-MB-231 cells, a 2.2-fold increase of *TP53* after doxorubicin treatment was shown. In doxorubicin treated cells *TP53* expression were reduced by approximately 57% in siRNA-p53 transfected cells compared to control cells (*P*=0.000003). In untreated cells, *TP53* expression were reduced by approximately 56% in siRNA-p53 transfected cells compared to control cells (*P*=0.000007) (Figure 40A).

The expression of *F5* was increased of approximately 17-fold in doxorubicin treated control cells compared with untreated control cells. In untreated cells, the expression of *F5* was

slightly reduced in siRNA-p53 transfected cells (*P*=0.0009). In doxorubicin treated cells, the induced expression of *F5* was reduced by approximately 36% compared with the doxorubicin induced expression of *F5* in control cells (*P*=0.003) (Figure 40B).

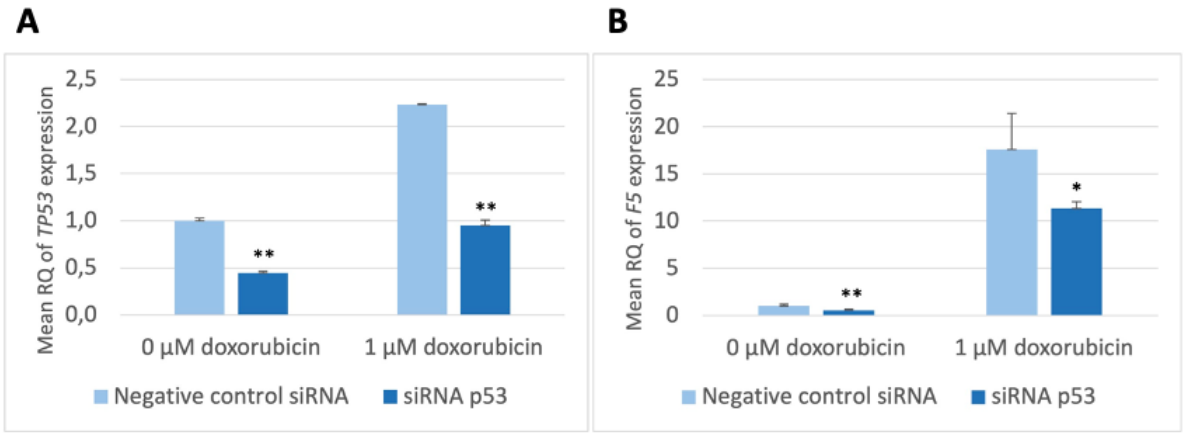

Figure 40: Expression of TP53 and F5 in MDA-MB-231 cells transfected with siRNA-53 or control siRNA. Cells were treated with 0 or 1 µM doxorubicin for 24 hours. *mRNA expression was measured using qRT-PCR and normalized against the endogenous control HPRT1. RQ values werre calculated relative to untreated negative control siRNA cells. Significant differences in comparison to negative control were marked with *(p≤0.05) or **(p≤0.001). A) Expression of TP53. Mean values (n=3) and SD from one experiment was shown. B) Expression of F5. Mean values (n=6) and SD from two separate experiments were shown.*

In MCF-7 cells, a 1.2-fold increase of *TP53* was observed after 24 hours. In untreated cells transfected with siRNA-p53, the level of *TP53* was reduced with 86% ($P=1.8*10^{-8}$) and 88% ($P=5.1*10^{-11}$) in comparison to control cells after 24 and 48 hours respectively. In doxorubicin treated cells transfected with siRNA-p53 the level of *TP53* was reduced with 86% ($P=1.9*10^{-7}$) and 90% ($P=1.1*10^{-5}$) in comparison to control cells after 24 and 48 hours respectively (Figure 41A).

The expression of *F5* showed no significant increase in doxorubicin treated control cells compared with untreated control cells after 24 hours. The expression of *F5* was still reduced by 45% in siRNA-p53 transfected cells compared with control cells (*P*=0.006). The expression of *F5* was increased by approximately 3.5-fold in doxorubicin treated control cells compared with untreated control cells after 48 hours. This increase was reduced by 35% in siRNA-p53 transfected cells compared with control cells (*P*=0.04). The expression of *F5* was also reduced in untreated cells transfected with siRNA-p53 by 69% (*P*=0.03) and 43% (*P*=0.006) compared with control cells after 24 and 48 hours respectively (Figure 41B).

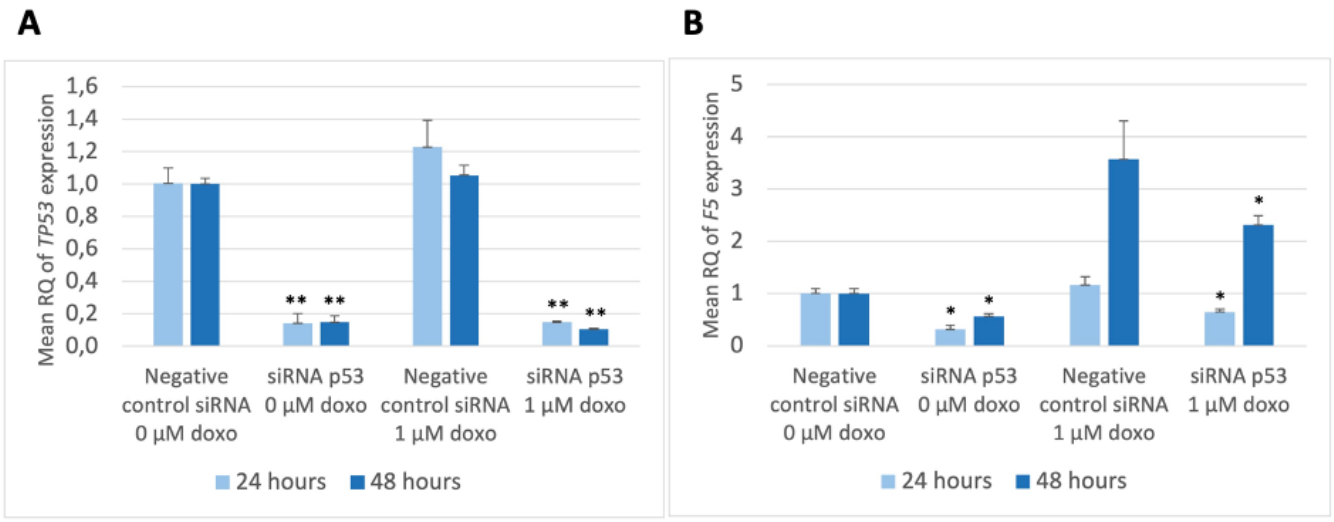

Figure 41: Expression of TP53 and F5 in MCF-7 cells transfected with siRNA-53 or control siRNA. Cells were treated with 0 or 1 µM doxorubicin for 24 and 48 hours. *mRNA expression was measured using qRT-PCR and normalized against the endogenous control GAPDH. RQ values were calculated relative to untreated negative control siRNA cells. Significant differences in comparison to negative control were marked with *(p≤0.05) or **(p≤0.001). A) Expression of TP53. Mean values (n=9) and SD from three separate experiments were shown. B) Expression of F5. Mean values (n=3) and SD from one representative experiment (of three) were shown.*

4.4 The role of p53 in the *F5* promoter

4.4.1 Mutagenesis

Due to the result which showed a decreased level in expression of *F5* in cells with inhibition or knockdown of p53/*TP53*, it was interesting to study the role of p53 even further. Two putative p53 half-sites in the *F5* promoter was previously found by the research group. The role of these binding sites in the regulation of *F5* was therefore interesting to study.

To examine the role of the p53 half-sites in doxorubicin induced expression of *F5* in breast cancer cell lines, it was made a plasmid with mutations in both half-sites by mutagenesis. The plasmid, named pGL3-Basic-F5-prom p53_1+2, was illustrated in Figure 42. Sanger sequencing revealed that in p53 half-site 1 (c.-300/-294) position c.-297 was mutated from G to T. In p53 half-site 2 (c.766/-760), position c.-760 was mutated from C to T and position c.-763 was mutated from G to T (Figure 43). No unwanted mutations were generated.

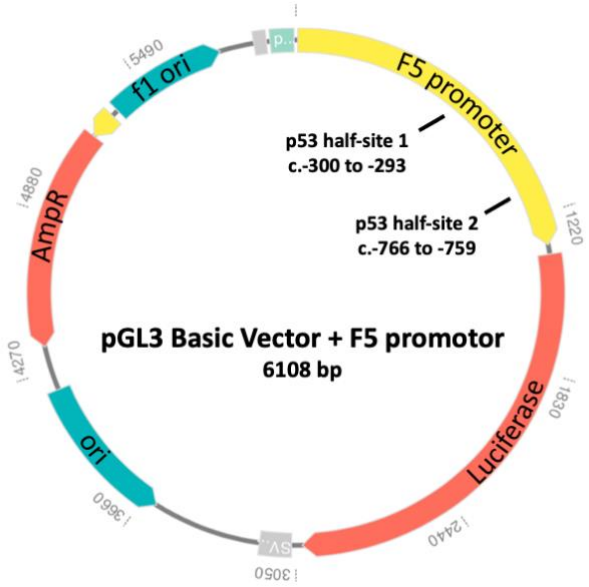

Figure 42: pGL3 vector with the F5 promoter showing the two putative p53 half-sites. *Modified illustration originally created with GenSmart Design, GenScript.*

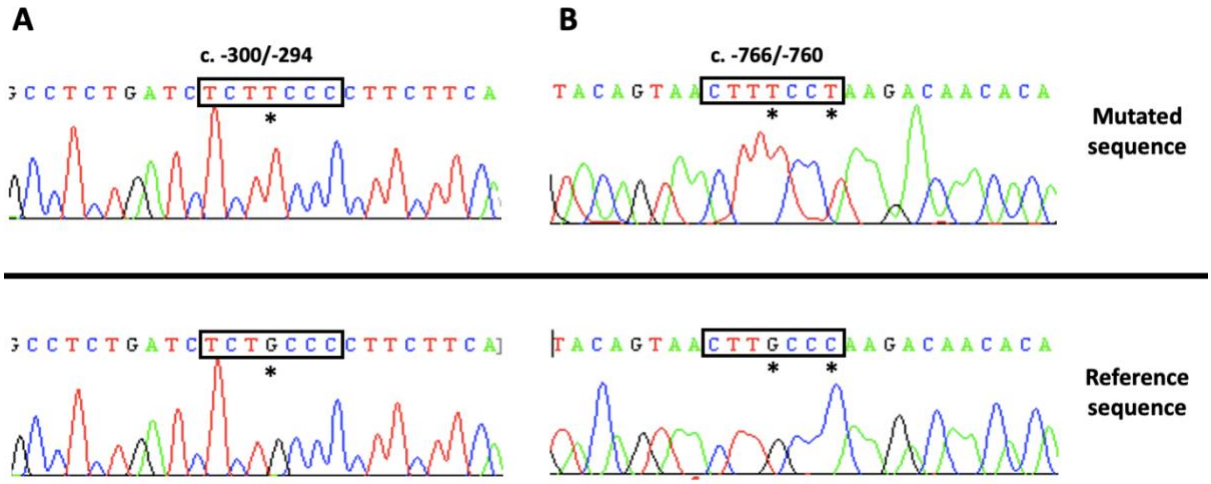

Figure 43: Sanger sequencing of the F5 promoter with both p53 sites mutated. *A) In p53 half-site 1 (c.-300/-294), position c.-297 was mutated from G to T. B) In p53 half-site 2 (c-766/-760), position c.-760 was mutated from C to T and position c.-763 was mutated from G to T. The figure showed a section of the analysis from the SeqScape™ software.*

4.4.2 Transfection of plasmids

Prior to transfection, agarose gel electrophoresis was run to ensure that the luciferase plasmids pGL3-prom, pRL-SV40, pGL3-Basic-F5-prom-wt, pGL3-Basic-F5-prom-p53_1+2 and pGL3-Basic were in the proper supercoiled state. The results revealed bands which verified that the plasmids supercoiled state were present (Figure 44).

Cells transfected with pMax GFP plasmid were used to verify that the transfection was successful and for checking transfection efficiency visually. Transfection efficiency was assessed by comparing all cells with GFP-expressing cells. The transfection was successful in both MDA-MB-231 and MCF-7 cell lines, with slightly greater transfection efficiency in MCF-7 cells compared with MDA-MB-231 cells (Figure 45).

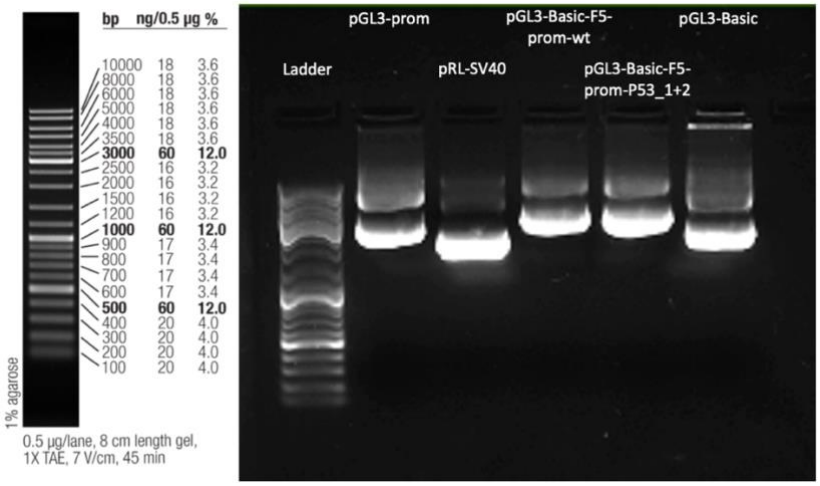

Figure 44: Agarose gel picture of plasmids and the Thermo Scientific GeneRuler DNA Ladder Mix (Scientific, 2018). From the left, the wells contain the DNA ladder followed by pGL3-prom, pRL-SV40, pGL3-Basic-F5-prom-wt, pGL3-Basic-F5-prom-p53_1+2 and pGL3-Basic plasmids.

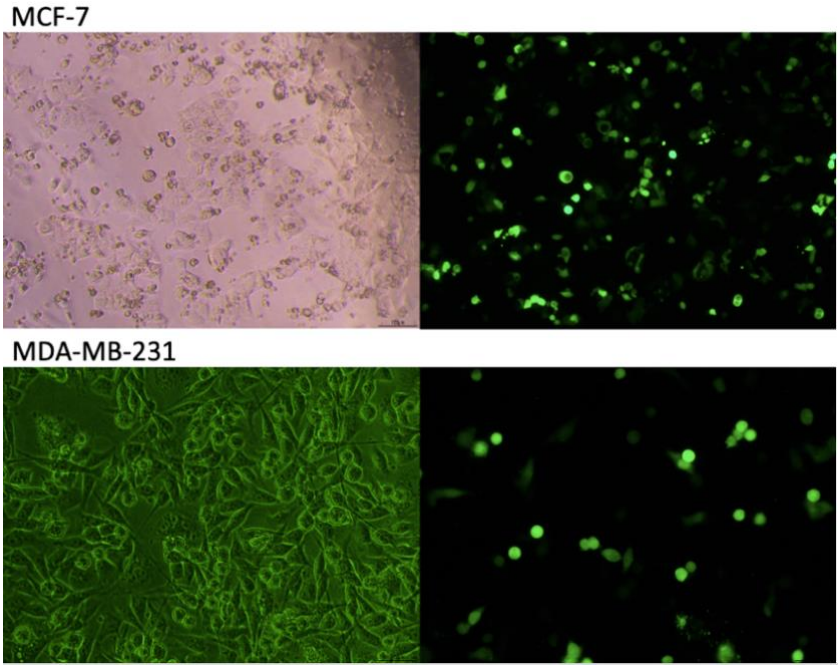

Figure 45: Illustration of all cells (left) compared with cells successfully transfected with the pMax GFP-plasmid (right). MDA-MB-231 and MCF-7 cells were shown.

4.4.3 *The role of the p53 sites in the F5 promoter*

To study the role of the p53 half-sites in the *F5* promoter in doxorubicin induced expression of *F5*, reporter plasmids with different status in the two p53 half-sites were transfected into MDA-MB-231 and MCF-7 cell lines. The cells were treated with doxorubicin to induce p53 activity, and the luciferase activity in the cells could be directly associated with the regulation in the *FV* promoter. The luciferase plasmids used in the experiments were schematically illustrated in Figure 46.

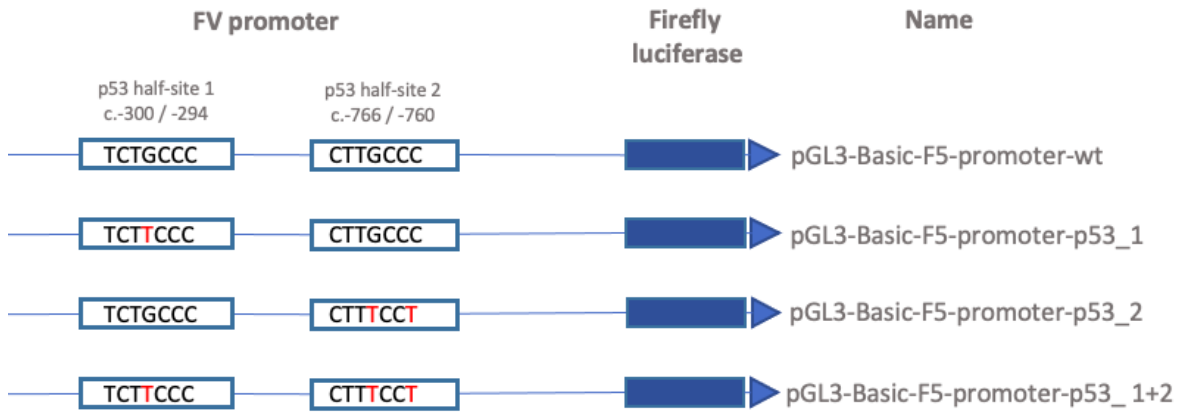

Figure 46: Schematic illustration of the pGL3-Basic-F5-prom wt, pGL3-Basic-F5-prom-p53_1, pGL3-Basic-F5-prom-p53_2 and pGL3-Basic-F5-prom-p53_1+2 luciferase constructs used in promoter experiments.

In MCF-7 cells, the induction of p53 was verified by Cignal Finder p53 reporter which showed an increase in luciferase activity with approximately 3-fold with doxorubicin treatment compared to untreated cells (result not shown). In doxorubicin treated cells a 13% reduction in relative luciferase activity with mutated p53 site 1 (P=0.01), and a further reduction of 18% with mutated p53 site 2 (P=0.0008) and 20% with both p53 sites mutated (P=0.00004) compared to wild type were shown (Figure 47).

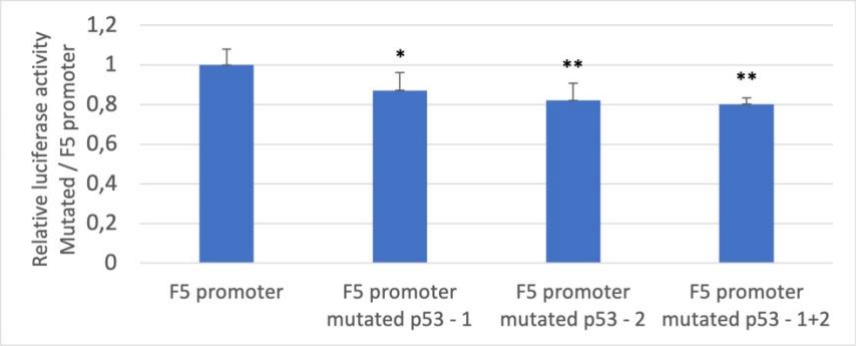

Figure 47: Luciferase activity for doxorubicin treated MCF-7 cells transfected with plasmids with different mutation status in the two p53 half-sites in the F5 promoter. Cells were treated with 1 µM doxorubicin for 24 hours. *The luciferase activity was measured, normalized against the renilla luciferase activity and calculated relative to the wild type F5 promoter. Mean values (n=10) and SD from two separate experiments were shown. Significant differences in comparison to negative control were marked with *(p≤0.05) or **(p≤0.001).*

In MDA-MB-231 cells, induction of p53 was verified by Cignal Finder p53 reporter which showed an increase in luciferase activity with approximately 2.5-fold with doxorubicin treatment compared to untreated cells (result not shown). A 17% reduction in relative luciferase activity with mutated p53 site 1 in comparison to wild type was shown (*P*=0.00006). Results for mutations in p53 site 2 and both p53 sites were not significant (Figure 48).

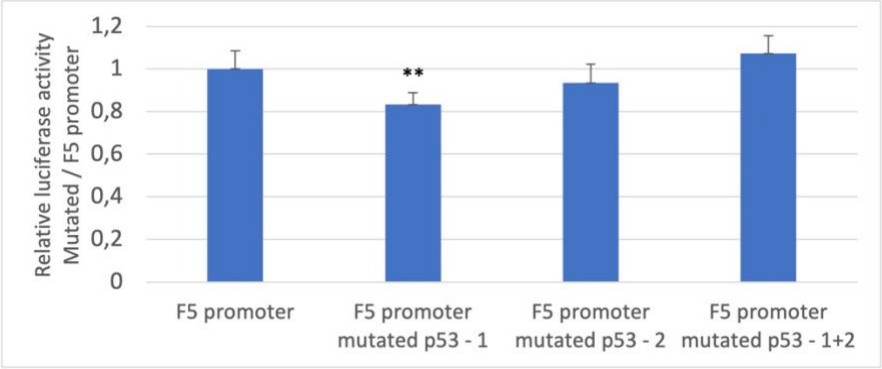

Figure 48: Relative luciferase activity for doxorubicin treated MDA-MB-231 cells transfected with plasmids with different mutation status in the two p53 half-sites in the F5 promoter. Cells were treated with 1 µM doxorubicin for 24 hours. *The luciferase activity was measured, normalized against the renilla luciferase activity and calculated relative to the wild type F5 promoter. Mean values (n=10) and SD from two separate experiments were shown. Significant differences in comparison to negative control were marked with **(p≤0.001).*

4.5 Functional effects of FV on apoptosis and proliferation

Based on the results in the clinical data material in the NeoAva and Osaka cohort which revealed an increased level in *F5* expression in responding tumors, it was interesting to study the functional effects of FV. A coagulation independent mechanism of FV was found in a mouse sepsis model where FV in complex with APC and PS had an anti-inflammatory effect through

inhibition of the TF-mediated activation of PAR2 (Liang et al., 2015). It was interesting to study if this mechanism was also involved in cancer and if FV had an antitumor effect through this mechanism.

In this thesis the functional effects of FV on apoptosis and proliferation were examined. The results in the clinical data material showed a predominance of the ER and PR negative status in tumors responding to neoadjuvant chemotherapy and therefore it was decided to do the experiments in the triple-negative MDA-MB-231 cells.

The effects of FV were studied using three approaches; 1) by transfection of FV overexpression plasmid, 2) by stimulation with recombinant FV and coagulation factors which were part of the PAR2 complex which the cells did not express and 3) by stimulation with FV deficient plasma and recombinant FV, APC and PS.

4.5.1 Effect of overexpression of FV

Overexpression of FV was performed to study the effect of FV in MDA-MB-231 cells. To ensure sufficient amounts of APC to generate the FV-APC-PS complex, FV overexpressing cells were also added APC in the proliferation experiments.

Overexpression of FV in MDA-MB-231 cells showed a 29% increase in apoptosis in cells transfected with the overexpression plasmid pMT2-FV in comparison to control cells (P=0.0002) (Figure 49A). No significant difference in proliferation was observed in cells transfected with pMT2-FV alone, but a 23% decrease in proliferation was shown in cells transfected with pMT2-FV together with APC (P=0.006) (Figure 49B). In summary, FV led to increased apoptosis and FV with APC led to decreased proliferation.

The functionality of pMT2-FV was verified by examining the FV protein level in cell media. In cells transfected with pMT2-FV, the protein level of FV increased by approximately 20-fold compared to empty plasmid control (P=0.04) (Figure 50).

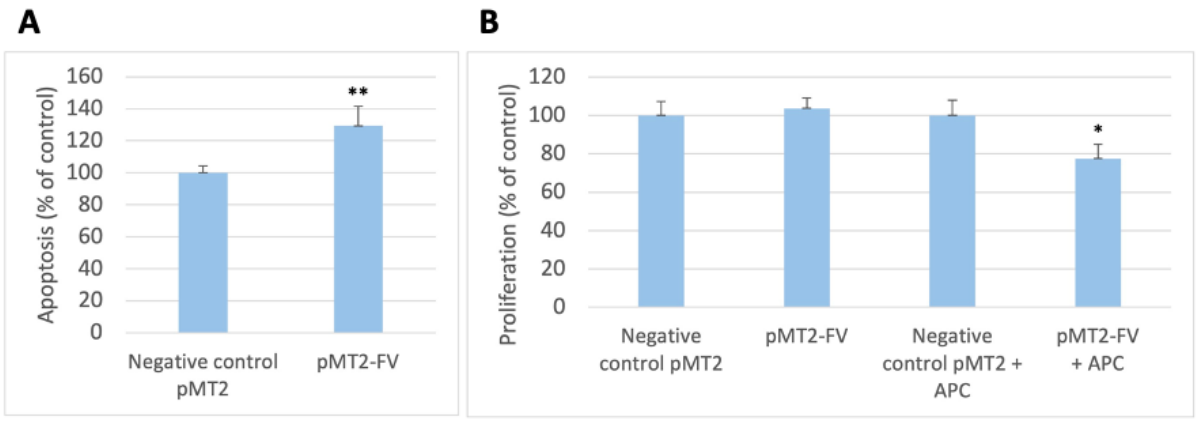

*Figure 49: Effect of overexpression of FV on apoptosis and proliferation in MDA-MB-231 cells after 48 hours. Apoptosis was calculated relative to negative control pMT2. Significant differences in comparison to negative control were marked with *(p≤0.05) or **(p≤0.001. A) Effect on apoptosis measured by DNA fragmentation. Mean values (n=6) and SD from two separate experiments were shown. B) Effect on proliferation, measured with WST-1. Mean values (n>12) and SD from two separate experiments were shown.*

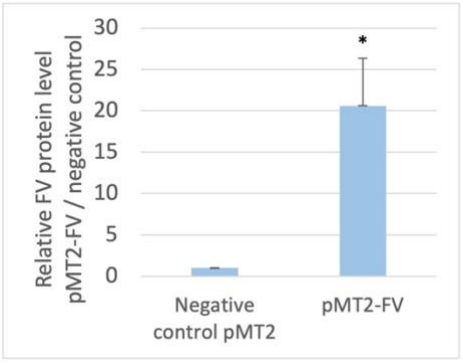

*Figure 50: Relative FV protein levels in cell media in MDA-MB-231 cells transfected with the FV overexpression plasmid; pMT2-FV and empty pMT2 after 48 hours. The FV protein levels were measured by FV ELISA and calculated relative to the negative control pMT2. Mean values (n=2) and SD from two separate experiments were shown. Significant differences in comparison to negative control were marked with *(p≤0.05.*

4.5.2 Effect of FV and coagulation factors

The effect of FV alone or together with coagulation factors which are a part of the TF-mediated PAR2 inhibition complex on apoptosis and proliferation were examined to study the suggested antitumor effect of FV. MDA-MB-231 cells were added the specified coagulation factors together with FV or activated FV (FVa).

In MDA-MB-231 cells a 57% decrease in apoptosis with APC, PS, FVIIa and FXa in comparison to control was observed (P=0.0007) (Figure 51A). For FVa together with the coagulation factors, it was observed a 214% increase in apoptosis in comparison to control (P=1.7*10^{-5}) (Figure 51B). The effect of coagulation factors on proliferation did not provide any significant results (result not shown). A small reduction in proliferation of approximately 5% was observed

in cells treated with PAR2 agonist for 24 hours (*P*=0.04) (result not shown). In summary, FVa and the coagulation factors led to increased apoptosis but no detectable effect on proliferation.

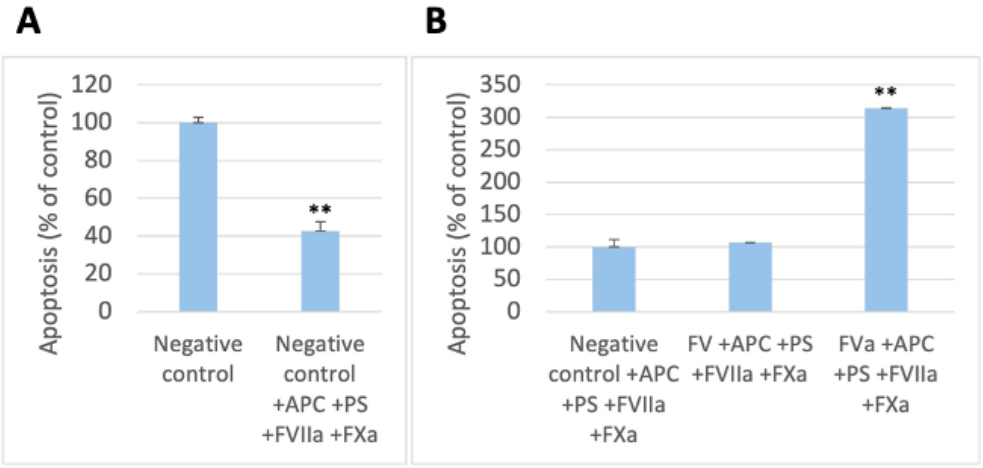

*Figure 51: Effect of coagulation factors on apoptosis in MDA-MB-231 cells after 48 hours measured by DNA fragmentation and calculated relative to negative control. Mean values (n=6) and SD from two separate experiments were shown. Significant differences in comparison to negative control were marked with **(p≤0.001). A) Effect of APC, PS, FVIIa and FXa. B) Effect of APC, PS, FVIIa and FXa with FV or FVa.*

4.5.3 Effect of FV and plasma

FV deficient plasma and APC were added in combination with FV or FVa to study the effects of the TF-mediated PAR2 inhibition complex on apoptosis and proliferation in the cells together with the salts, hormones, lipids, immunoglobulins, clotting factors (except from FV) and fibrinogen in the FV deficient plasma.

In MDA-MB-231 cells stimulated with FV deficient plasma and APC a 105% increase in apoptosis was observed in comparison to only FV deficient plasma (*P*=0.0001) (Figure 52A). When FV was added to the mixture a 64% decrease in apoptosis compared to plasma and APC control was shown ($P=8.5*10^{-6}$) (Figure 52B). The small increase in apoptosis for FVa was not significant. The effect of FV, coagulation factors and FV deficient plasma on proliferation did not provide any significant results (result not shown). In summary, FV and plasma led to decreased apoptosis but no detectable effect on proliferation.

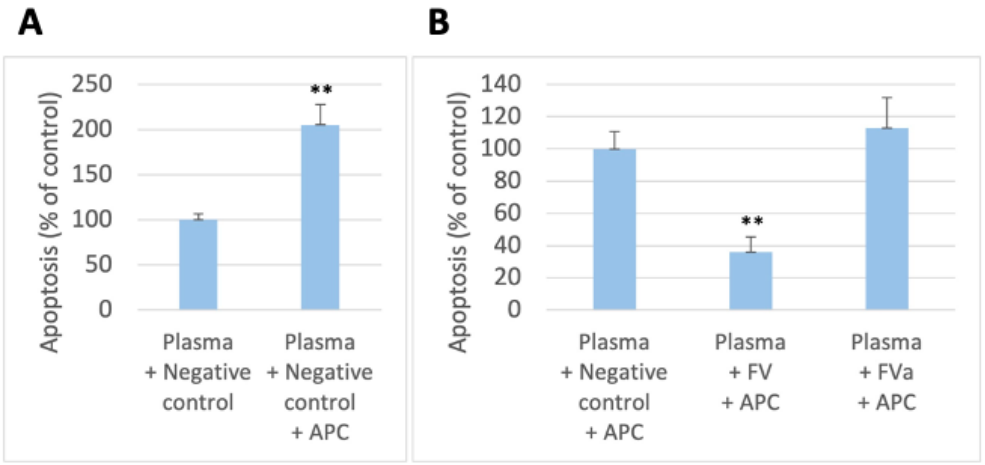

*Figure 52: Effect of coagulation factors and FV deficient plasma on apoptosis in MDA-MB-231 cells after 48 hours measured by DNA fragmentation and calculated relative to the negative control. Mean values (n=6) and SD from two separate experiments were shown. Significant differences in comparison to negative control were marked with **(p≤0.001). A) Effect of APC. B) Effect of FV and FVa.*

4.6 Influence of FV on the effects of doxorubicin

It was interesting to study if FV influenced the effect of doxorubicin on apoptosis and proliferation in triple negative breast cancer cells. This was studied using the same three approaches; 1) by transfection of FV overexpression plasmid, 2) by stimulation with recombinant FV and coagulation factors which were part of the PAR2 inhibition complex which the cells did not express and 3) by stimulation with FV deficient plasma and recombinant FV, APC and PS.

4.6.1 Influence of FV overexpression

To study if overexpression of FV influenced the effect of doxorubicin on apoptosis and proliferation the experiments were conducted in MDA-MB-231 cells treated with doxorubicin.

Overexpression of FV in doxorubicin treated MDA-MB-231 cells showed a 45% increase in apoptosis in cells transfected with the overexpression plasmid pMT2-FV in comparison to control cells (*P*=0.001) (Figure 53A). In cells transfected with the overexpression plasmid pMT2-FV a 9% decrease in proliferation were shown (*P*=0.002) (Figure 53B). No significant differences were observed in proliferation of the cells with pMT2-FV together with APC in comparison to control cells (Figure 53B). In summary, FV led to increased apoptosis and decreased proliferation.

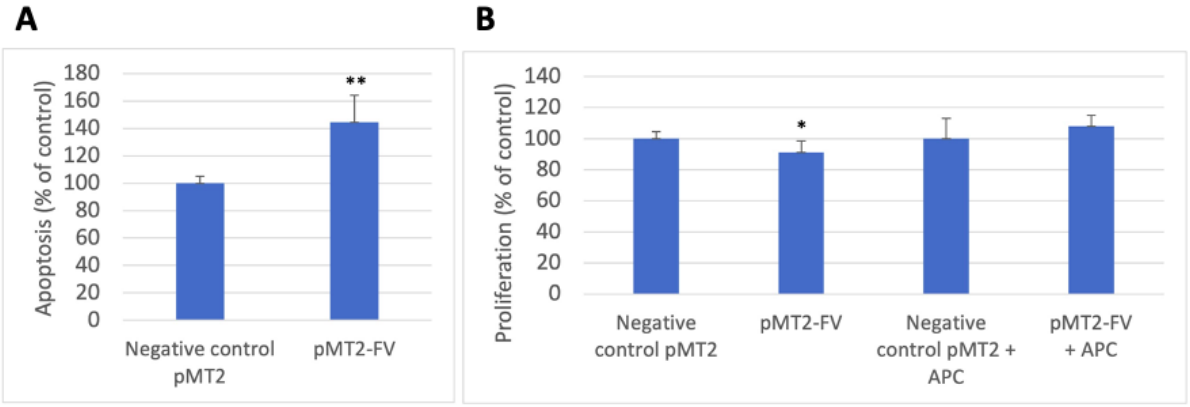

*Figure 53: Effect of overexpression of FV on apoptosis and proliferation in MDA-MB-231 cells treated with 1 µM doxorubicin for 48 hours. Values were calculated relative to negative control pMT2. Significant differences in comparison to negative control were marked with *(p≤0.05) or **(p≤0.001. A) Effect on apoptosis measured by DNA fragmentation. Mean values (n=6) and SD from two separate experiments were shown. B) Effect on proliferation, measured with WST-1. Mean values (n>12) and SD from two separate experiments were shown.*

4.6.2 Influence of FV and coagulation factors

To study if FV together with coagulation factors influenced the effect of doxorubicin on apoptosis and proliferation, the experiments were conducted in MDA-MB-231 cells treated with doxorubicin.

In doxorubicin treated MDA-MB-231 cells, a 47% reduction in apoptosis was observed when the cells were stimulated with APC, PS, FVIIa and FXa in comparison to control (P=7.6*10^{-5}) (Figure 54A). An increase in apoptosis of 20% was shown with the addition of recombinant FV (P=0.003) and an even larger increase of 162% with recombinant FVa (P=0.0006) in comparison to control (Figure 54B). The effect of FV and coagulation factors on proliferation did not provide any significant results (result not shown). A small reduction in proliferation of approximately 5% was observed in cells treated with PAR2 agonist for 24 hours (P=0.01), and a reduction of approximately 11% was observed after 48 hours (P=0.04) (result not shown). In summary, FV and the coagulation factors led to a small increase in apoptosis and this effect was much more increased with FVa. There was no detectable effect on proliferation.

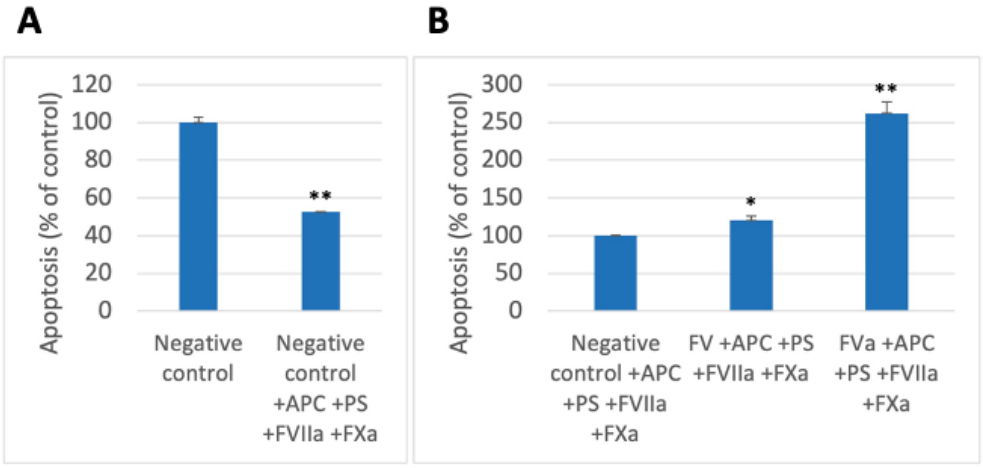

Figure 54: Effect of coagulation factors on apoptosis in MDA-MB-231 cells treated with 1 µM doxorubicin for 48 hours *measured by DNA fragmentation. Mean values (n=6) and SD from two separate experiments were shown. Significant differences in comparison to negative control were marked with *(p≤0.05) or **(p≤0.001). A) Effect of APC, PS, FVIIa and FXa. B) Effect of APC, PS, FVIIa and FXa with FV or FVa.*

4.6.3 Influence of FV and plasma

FV deficient plasma and APC were added in combination with FV or FVa in cells receiving doxorubicin treatment to study the influence on doxorubicin's effect on apoptosis and proliferation together with the salts, hormones, lipids, immunoglobulins, clotting factors (except from FV) and fibrinogen in the FV deficient plasma.

In doxorubicin treated MDA-MB-231 cells, an 89% increase in apoptosis was shown with stimulation of APC (P=0.0005) (Figure 55A). When FV was added to the incubation a 58% decrease in apoptosis was observed (P=1.1*10^{-5}), and incubation with FVa resulted in a small increase of 16% in apoptosis in comparison to control (P=0.0007) (Figure 55B). The effect of FV and the coagulation factors with FV deficient plasma on proliferation did not provide any significant results (result not shown). In summary, FV and plasma led to a decrease in apoptosis but in contrast FVa led to a small increase in apoptosis. There was no detectable effect on proliferation.

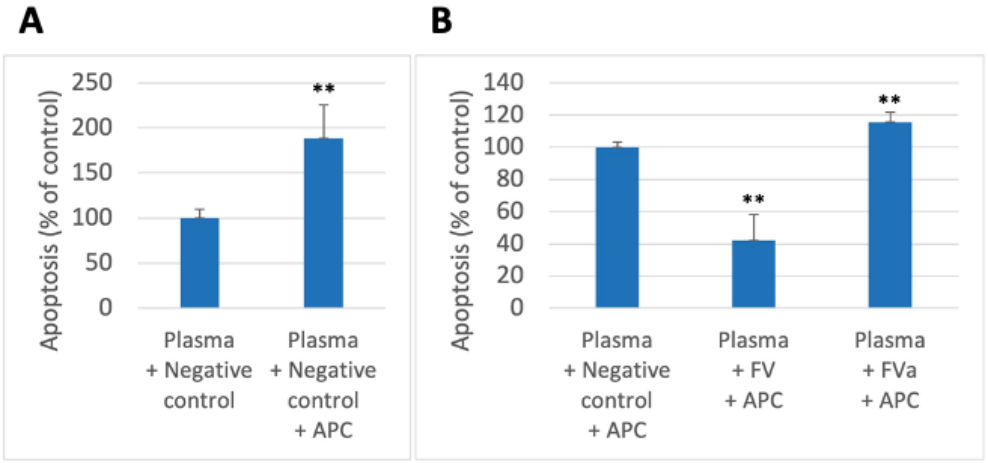

*Figure 55: Effect of coagulation factors and FV deficient plasma on apoptosis in MDA-MB-231 cells treated with 1 µM doxorubicin for 48 hours measured by DNA fragmentation. Mean values (n=6) and SD from two separate experiments were shown. Significant differences in comparison to negative control were marked with **(p≤0.001). A) Effect of APC. B) Effect of FV and FVa.*

5. DISCUSSION

The connection between cancer and increased risk for thrombosis has been long known. In addition, thrombosis is the second leading cause of death among cancer patients after the cancer itself. It has also been documented an association between coagulation factors and tumor progression.

In this thesis FV was studied in clinical data materials from breast cancer patients and in breast cancer cell lines. It has been shown that FV is expressed in cancer tumors, suggesting an association between FV and cancer (Tinholt et al., 2018). A study by Tinholt et al. (2014) revealed SNPs in the factor 5 gene (*F5*) which are associated with breast cancer. The *F5* SNPs and *F5* mRNA expression are also associated with clinicopathological tumor characteristics. Another study by Tinholt et al. (2018) illustrated that a higher expression of *F5* was associated with aggressive cancer subtypes, but also with increased survival. Nevertheless, the role of FV in the tumor tissue is still not determined.

A study performed by Liang et al. (2015) showed for the first time a coagulation independent effect of FV. They found that FV in complex with APC and PS had an anti-inflammatory effect on the TF-mediated PAR2 activation in a mouse sepsis model. This mechanism has not yet been studied in cancer.

The main aims of this thesis were to study if there was an association between FV and treatment response, study the *F5* expression in different breast cancer subtypes and hormone receptor status, study the viability of breast cancer cell lines during chemotherapy treatment, study the role of p53 in doxorubicin induced expression of *F5*, and study the functional effects of FV included if the coagulation independent mechanism of FV found by Liang et al. (2015) was also involved in breast cancer cells.

5.1 Analysis of *F5* expression and treatment response in breast cancer

In this thesis it was evaluated if there was an association between tumor gene **expression of *F5* and treatment response** in breast cancer. The patients were referred to as either responders or non-responders based on whether pCR was achieved or not. A significantly

higher tumor expression of *F5* in responders compared to non-responders to neoadjuvant chemotherapy was found, thereby suggesting that tumor expression of *F5* is associated with sensitivity to chemotherapy in breast cancer. In a study by Tinholt et al. (2020) it was revealed that a higher expression of *F5* was associated with increased overall survival, which supported the association between treatment response and elevated expression of *F5* observed in this thesis. It should be noted, however, that this was found in some of the cohorts. Of the nine cohorts, only three of them involved FEC treatment. The two cohorts showing significant results in *F5* expression where among these three cohorts. This may indicate that tumor expression of *F5* is associated with sensitivity to this specific drug treatment.

Treatment response according to *F5* in subgroups was also examined in this thesis. Breast cancer is a heterogeneous disease that can be divided into several subgroups that differ at the molecular and clinical level (Yersal & Barutca, 2014). Still, it was not shown that *F5* was associated with treatment response within the different pathological (ER/PRHER2 status) or molecularly defined subgroups (PAM50) of breast cancer in this thesis. Additionally, the number of observations in these subgroups may have been too small to provide sufficient statistical power.

There was examined if there was a difference in expression of *F5* in breast cancer subgroups. Differences in the expression of *F5* between PAM50 subgroups were observed. The expression of *F5* was highest in the basal followed by the normal-like subgroup and lower in the luminal B, luminal A and Her2 subtype respectively. In the study by Tinholt et al. (2018) similar result were observed in the basal, luminal A and luminal B subtype, but the expression of *F5* in the HER2 subtype were almost as high in the basal. The results for the *F5* expression in the HER2 tumors was among the subgroups with the lowest expression of *F5* in this thesis. In comparison, the study by Tinholt et al. (2018) showed that the HER2 subtype was among the subtypes with the highest expression of *F5*. The divergent results may be caused by low numbers of patients in the HER2 subgroup in this thesis. Also, it must be considered that this was a borderline result and that more data for the PAM50 subgroups would be desirable for a more statistical power. The results revealed by Tinholt et al. (2018) for the HER2 subtype was considered more reliable.

In a study by Haque et al. (2018), consisting of nearly 14.000 breast cancer patients, pCR rates for patients with different breast cancer molecular subtypes treated with neoadjuvant chemotherapy was investigated. The pCR rates in the subgroups were lowest for the luminal subtypes and highest for the basal and HER2 subtypes. Similar results were shown in a study by Carey et al. (2007). Considering that the expression of *F5* was highest in the basal subtype in this thesis and also in other studies (Tinholt et al., 2018), the suggested association between *F5* expression and treatment response is strengthen. In addition, the results in this thesis showed a low expression of *F5* in the luminal and normal subtype, which was also associated with low pCR rates (Carey et al., 2007; Haque et al., 2018). This strengthens the association between *F5* expression and treatment response further.

There was examined if there was a difference in expression of *F5* according to receptor status in breast cancer. A higher expression of *F5* in ER negative compared with positive tumors was found. Similar results were shown in a study conducted by Tinholt et al. (2018) where a higher expression of *F5* in ER negative compared with ER positive tumors were reported. The expression of *F5* was also higher in PR negative compared with PR positive tumors in this thesis. Similar results were not previously reported, but a higher expression of *F5* was found in tumors with a general negative hormone receptor status in the study by Tinholt et al. (2018) which still may support this result. Moreover, the distribution of the receptor negative compared with the positive status in the responding tumors revealed that over 70% was ER negative compared with ER positive, and over 80% was PR negative compared with PR positive. This may potentially be caused by the elevated expression in *F5* in these subtypes and support the indication of the postulated antitumor effect of FV.

Elevated expression of *F5* was found in ER and PR negative compared to the positive status in tumors examined in this thesis. The highest rates of pCR are in the hormone receptor negative breast cancer subtypes. In contrast, breast cancer subtypes associated with the lowest pCR rates, are hormone receptor positive (Carey et al., 2007; Haque et al., 2018). This may support the association between higher expression of *F5* and treatment response further.

Collectively, the results for the analysis of the clinical data material in this thesis indicated an association between elevated *F5* expression and treatment response with FEC treatment. To

determine whether this is a marker or have a direct effect, this was also tested functionally in this thesis.

5.2 Breast cancer cell lines

In this thesis MCF-7 and MDA-MB-231 breast cancer cell lines were used. Cell lines are beneficial as *in vitro* study models due to low cost, easy access and the advantage that they can be thawed and frozen on demand (Kaur & Dufour, 2012). Cell lines holds the property of potentially infinite cell division which enables culturing for long periods of time. When the cell lines are cultured to long, there is a risk for generation of mutations resulting in alterations of the cells. In culturing for long periods of time, it is also a risk for cross-contamination (Hughes et al., 2007).

To prevent this in the cell experiments, sterile conditions were strictly enforced. The cell lines depend on specific culturing conditions and are sensitive to even small changes in these conditions. Because of this the recommended culturing medium and serum were applied, and cells were incubated at 37°C in 5% CO_2 atmosphere.

In vitro studies enable examinations of cellular processes outside a living organism in a controlled environment, which does not recreate the same conditions of an organism (Katt et al., 2016). Considering this, *in vitro* studies should also be tested *in vivo* in animal models to study the overall effects of the experiment.

Different magnitude of response between similar experiments was observed in the *TP53* knockdown experiments in MCF-7 cells in this thesis. Microscopy and RNA concentration both revealed differences in cell density in the wells among these experiments. The variable responses observed can thus be explained by the importance of cell density for the transfection effectivity. The variation in response made it difficult to merge the results from the three similar experiments, and therefore one representative experiment was shown in this thesis.

5.3 Effect of chemotherapy treatment on FV

Based on the findings in the two cohorts in the clinical data material which showed an association between *F5* expression and treatment response, it was interesting to examine the mechanisms of the drugs used in these cohorts. The combination chemotherapy, FEC, was used in both cohorts. Bevacizumab was also used in combination with FEC in one of the cohorts.

To calculate the drug concentrations for the stimulation experiments, IC_{50} values for doxorubicin, epirubicin, 5-fluorouracil, cyclophosphamide and bevacizumab were determined using the WST-1 proliferation reagent in MDA-MB-231 and/or MCF-7 cells.

In WST-1 proliferation measurements, a formazan dye is generated by metabolically active cells. The method is sensitive, effective and simple to perform. The dye is generated quickly in comparison to other assays with measurements of metabolic activity like MTT, XTT and MTS. Because of interference of the strong color of doxorubicin and epirubicin, using a color independent assay would have been more accurate. Although more accurate assays for proliferation were available, WST-1 was appropriate in this case because it was used only for an indication of drug concentrations in upcoming experiments.

The IC_{50} value was found for all drugs except bevacizumab, which in contrary showed an increase in proliferation in the highest doses. Bevacizumab is an inhibitor of the VEGF-A pathway and is used in combination with chemotherapy or as a single agent for second-line treatment of cancer (Montero et al., 2012). The therapeutic effect of bevacizumab on tumor cells is through reduction in microvascular growth on tumor blood vessels resulting in limitation of blood supply to the tumor (Kanat & Ertas, 2019; Kazazi-Hyseni et al., 2010). The effect of bevacizumab may thus be difficult to detect in *in vitro* cell lines.

To study the effect of chemotherapy on *F5* expression, MDA-MB-231 and MCF-7 cells were treated with the drugs used in the two cohorts. In MDA-MB-231 cells, a 41-fold increase in *F5* expression was found after epirubicin treatment. An increase in *F5* expression after treatment with FEC and FEC-bevacizumab was also found which probably was caused by epirubicin because the other drugs did not have any effect alone. A slight decrease in *F5* expression was observed with FEC-bevacizumab compared with FEC, which probably was due to the toxicity in

DMSO which bevacizumab was dissolved in. The effect of epirubicin on *F5* expression in MDA-MB-231 cells was previously not known. However, an induction of *F5* after treatment with doxorubicin has been observed in MDA-MB-231 and MCF-7 cells in previous experiments in the research group. Doxorubicin and epirubicin are highly similar and only differs by an epimerization of a hydroxyl group (Khasraw et al., 2012). Therefore, the drugs function through the same mechanisms via p53 and were expected to have the same effect on *F5* expression.

In MCF-7 cells, a 15-fold increase in *F5* expression was found after 5-fluorouracil treatment. An increase in *F5* expression after treatment with FEC and FEC-bevacizumab was observed, which probably was caused by 5-fluorouracil because the other drugs did not have any up-regulating effect alone. A slight decrease in *F5* expression was observed with FEC-bevacizumab compared with FEC, which probably was due to the toxicity in DMSO which bevacizumab was dissolved in. The effect of 5-fluorouracil on the *F5* expression in MCF-7 cells were previously not known. Several studies have shown that 5-fluorouracil induces p53 (Cheng et al., 2012; Cho et al., 2020; Ju et al., 2007). Cyclophosphamide treatment resulted in a decrease in *F5* expression. This effect was previously not found, but still it has been shown in several studies that cyclophosphamide treatment alters gene expression also for other coagulation factors like FVIII, FIII, fibrinogen and vWF (Doloff & Waxman, 2015; El-Serafi et al., 2014; Hofmann et al., 2014). There was not found any *in vitro* studies that verified induction of p53 by cyclophosphamide in contrast to the other drugs.

Because of the similarity of doxorubicin and epirubicin and the previously findings in the research group, it was expected to observe an effect of epirubicin on *F5* expression in MCF-7 cells. Even though there was no effect of epirubicin on *F5* expression in MCF-7 cells in this experiment, induction of *F5* was shown by doxorubicin treatment in subsequent experiments in MCF-7 cells. In some of these experiments 48 hours of treatment were required to achieve the induction of *F5*. Therefore, experiments with treatment in longer periods of time would be appropriate. The effect of cyclophosphamide on *F5* expression, which was shown in MCF-7 cells, was not observed in MDA-MB-231 cells and treatment in longer periods of time could be appropriate.

The results obtained strengthen the indication that the drugs induced *F5* expression through a mechanism involving p53 in breast cancer. Therefore, it was interesting to study the regulation of FV by p53 further.

FV protein levels were examined in cell media and lysates in MCF-7 and MDA-MB-231 cells treated with doxorubicin to examine the effect of doxorubicin on FV protein production.

FV protein was induced by doxorubicin in both cell types. The results showed that FV protein was maintained in the cell lysates and was not secreted into the cell media. In contrast, it was shown that FV protein generated in untreated MDA-MB-231 cells transfected with the overexpression plasmid, secreted FV protein into the cell media. This may indicate that the FV protein have an intracellular role during doxorubicin treatment, which is not needed without any treatment. Alternatively, doxorubicin might have a function which inhibits the secretory pathway. It is known that doxorubicin treatment causes induction of autophagy in cells. Interestingly, it has been reported that inhibition of the doxorubicin-induced autophagy in cancer cell lines resulted in increased apoptosis (Cosan et al., 2010; Zhao et al., 2014). Considering the results in this thesis, which indicated an antitumor effect of FV, it had been interesting to examine whether the increased apoptosis during inhibition of autophagy was caused by the prevention of destruction of the FV protein leading to secretion of FV. For example, the protein levels of FV in cell lysates and media during doxorubicin treatment combined with inhibition of autophagy, could be examined in future experiments.

5.4 The interaction between *F5* and p53

5.4.1 The role of inhibition or knockdown of p53 on F5 expression

Based on the findings that some of the drugs, which were known to induce p53 activity, increased the *F5* expression, it was investigated if the lack of p53 induction had an effect in the drug-induced upregulation of *F5*. This was studied by inhibition by PFT-α or knockdown by siRNA-p53.

Experiments with inhibition of p53 by PFT-α in MCF-7 cells were previously performed by the research group and showed a reduction in the doxorubicin induced *F5* expression. In this thesis

the results for inhibition of p53 by PFT-α showed similar results in MDA-MB-231 cells, with a 46% reduction of doxorubicin induced *F5* expression during treatment with PFT-α. This indicated that p53 had an effect in the regulation of doxorubicin induced *F5* expression.

Based on the results from inhibition of p53 on the protein level, it was then interesting to inhibit *TP53* on the gene level by knockdown with siRNA. Similar to the experiments with PFT-α, also these experiments showed a 36% and 35-45% reduction in doxorubicin induced *F5* expression in MDA-MB-231 and MCF-7 cells respectively. This supported the indication that p53 was involved in the regulation of doxorubicin induced *F5* expression further.

5.4.2 The role of p53 in the F5 promoter

Inhibition and knockdown of p53/*TP53* resulted in a reduction in doxorubicin *F5* expression. Using the software PROMO with TRANSFAC, the research group had previously found two putative p53 half sites in the *F5* promoter. It was therefore interesting to study if p53 had an effect on the regulation of *F5* trough these half sites.

A luciferase vector containing the *F5* promoter was previously generated by the research group. The two putative p53 half-sites in the *F5* promoter were mutated to generate plasmids with mutation in one or both bindings sites. The luciferase plasmids were transfected in MDA-MB-231 and MCF-7 cells, and the cells were treated with doxorubicin to induce p53 activity.

In MDA-MB-231 cells transfected with the plasmids, a reduction in luciferase activity were observed when p53 site 1 was mutated and a further reduction when p53 site 2 and both sites were mutated. These results indicated that the two putative p53 sites were actual binding sites for p53, and that p53 may have a role in the doxorubicin induced upregulation of *F5*. In MCF-7 cells transfected with the plasmids a reduction in luciferase activity were observed when p53 site 1 was mutated. The results for mutation in p53 binding site 2 and both sites were not significant. This result indicated that p53 site 1 was an actual binding site for p53, and that p53 may have a role in the doxorubicin induced upregulation of *F5* in MCF-7 cells through this binding site.

The status for p53 is different in MCF-7 and MDA-MB-231 cells. MCF-7 cells have the *TP53* wildtype whereas MDA-MB-231 cells have a mutation in *TP53*, though still with a partial function. Because these experiments were based on the generation of the host cells own p53 protein, the variation in the results may be due to the variations in the p53 protein in the two cell types. Still, a significant reduction was observed in both binding sites in at least one cell type, which indicated that both bindings sites had a role in the regulation of *F5* by p53.

Considering all the results for the effect of p53 inducing drugs, p53 inhibition, *TP53* knockdown and mutation of p53 bindings sites in the *F5* promoter, these results strongly supported that p53 is one mechanism in the doxorubicin induced upregulation of *F5* in MDA-MB-231 and MCF-7 cells. Still, it should be considered that doxorubicin, in addition to p53, also induces a numerous other transcription factors (Daigeler et al., 2008; Kudoh et al., 2000). Therefore, other factors may also be involved in this mechanism in addition to p53. In the experiments in this thesis, doxorubicin induced *F5* expression were reduced with only 35-46% and although p53 and *TP53* were not either fully inhibited or knock downed, it is likely that there are other regulators of *F5* as well. For example, the research group have found other binding sites in the *F5* promoter and untranslated regions (UTRs) like for estrogen receptor alpha and microRNA (miRNA), which also suggest other regulators of *F5*.

5.5 Functional effects of FV on apoptosis and proliferation in breast cancer cells

Based on the findings in the clinical data material, which showed an increased expression of *F5* in responders compared with non-responders to neoadjuvant chemotherapy, and the *in vitro* experiments, which showed an induction of *F5* during treatment with chemotherapy drugs, it was interesting to study the functional effects of FV in breast cancer cells. A study conducted by Liang et al. (2015) revealed a coagulation independent mechanism of FV in a mouse sepsis model where FV in complex with APC and PS had an anti-inflammatory effect through inhibition of the TF-mediated activation of PAR2 signaling. TF-mediated PAR2 signaling has been shown to induce protumor effects like stimulation of proliferation, migration, angiogenesis and anti-apoptosis (Ruf et al., 2011; Schaffner & Ruf, 2009; Wojtukiewicz et al., 2015). A tumor suppressor function of FV has previously been suggested in a study by Tinholt et al. (2018).

Therefore, it was interesting to study if this mechanism was also involved in cancer and if FV had an antitumor effect through inhibition of PAR2.

The results in the clinical data material showed a predominance of the ER and PR negative status in tumors responding to neoadjuvant chemotherapy, and therefore it was decided to do the functional experiments in the triple-negative MDA-MB-231 cells. The effect of FV was studied using three approaches: 1) by transfection of FV overexpression plasmid, 2) by stimulation with recombinant FV and coagulation factors which were part of the PAR2 inhibition complex and were not expressed by the cells and 3) by stimulation by recombinant FV and APC together with FV deficient plasma. The functional effects were studied on apoptosis and proliferation.

Overexpression of FV resulted in a 29% increase in apoptosis in the cells without any coagulation factors added. APC was necessary in combination with FV to detect an effect on proliferation which was reduced by 23%. This might be due to insufficient sensitivity of the WST-1 method used to measure proliferation. Also, there might not have been sufficient amounts of APC in the cells naturally to generate a detectable effect of the postulated inhibition complex, with FV overexpression alone. Considering the postulated PAR2 inhibition complex, adding more APC might lead to increased formation of the inhibition complex, resulting in a greater effect on both proliferation and apoptosis. APC was not added in apoptosis experiments, and thus this possible effect could not be confirmed. Nevertheless, the results for overexpression of FV supported the postulated antitumor effect of FV in breast cancer.

The effects of recombinant FV and coagulation factors involved in the postulated TF-mediated PAR2 inhibition complex were then studied. To verify the activity of PAR2 in the cells, proliferation was measured with a PAR2 agonist which resulted in a significant reduction. The coagulation factors in the TF-mediated PAR2 activating complex, resulted in a 57% reduction in apoptosis. With the postulated TF-mediated PAR2 inhibition complex, a substantial 215% increase in apoptosis was observed with recombinant FVa and no effect on apoptosis was observed with recombinant FV. The study by Liang et al. (2015) showed that FV cleaved by APC at Arg506, and not thrombin cleaved FVa, was an essential cofactor in the inhibition complex.

This may indicate a PAR2 independent mechanism of FVa. No detectable effects of recombinant FV or FVa and the coagulation factors on proliferation were observed. The results on apoptosis supported the antitumor properties of FVa in breast cancer and indicated that the effect was through a PAR2 independent mechanism. Further studies are necessary to determine if PAR2 is involved in the effect of FV, for example by inhibition of PAR2 with antibodies or studying downstream factors for PAR2 like Interleukin-8 (IL-8). To determine which of the coagulation factors were necessary to achieve an effect together with FV/FVa, several combinations of these must be tested.

The third approach was stimulation of cells with FV deficient plasma combined with FV and APC to include more natural elements in the cells like all coagulation factors, salts, hormones, lipids, immunoglobulins and fibrinogen. In contrast to the two previous approaches, only APC with plasma increased apoptosis. In combination with recombinant FV there was a decrease in apoptosis. No detectable effects on proliferation were observed. These results then did not support the postulated antitumor effect of FV in breast cancer cells. It should be considered that the use of plasma also leads to less control over the cellular processes occurring, and although it may provide a more complex overview, there are still many components missing to recreate the complexity of the natural system. Moreover, it was necessary to use hirudin to prevent clotting, which may also have unknown effects in the cells.

The WST-1 method used to measure proliferation in the studies of the functional effects of FV and the influence of FV on the effects of doxorubicin (discussed in section *5.6*) might not have been the most suitable method, and potential effects could have been detected with more sensitive methods. In the FV overexpression experiments for the effect on proliferation the reduction in proliferation, especially in doxorubicin treated cells, were minor. In the experiments with the stimulation of recombinant coagulation factors there were not observed any effect on proliferation. Considering that the effect on apoptosis in these experiments were substantial, an effect on proliferation were also expected. Therefore, the WST-1 method used for measuring proliferation might not have been sensitive enough. In WST-1 proliferation measurements, a formazan dye is generated by metabolically active cells. The method is cheap, effective and simple to perform. The dye is generated quickly in comparison to other assays with measurements of metabolic activity like MTT, XTT and MTS. In some cases, more accurate

methods are required. For example, assays for detecting specific proliferation-dependent antigens are popular in cancer research and are accurate and reliable, but the results can be subjective. Quantification of the ATP concentrations are also a possible measure on proliferation due to the linear relationship between number of living cells and ATP. ATP assays are performed with bioluminescent luciferase and its substrate luciferin and are highly sensitive. The most accurate method for detecting proliferation in the laboratory is through detecting DNA synthesis by incubation with radiolabeled 3H-thymedine. Thereafter the radiolabels incorporated in newly synthetized DNA can be detected. The method is highly sensitive, replicable and accurate, but on the other hand it is expensive, time-consuming and in addition the radioactive materials are hazardous (Madhavan, 2007; Riss et al., 2016).

Apoptosis can be measured in a series of different mechanisms and can be detected in the induction phase to early, intermediate and late stage of apoptosis. The methods includes detection of membrane alterations, DNA fragmentation, mitochondrial damage, cytochrome c release, mitochondrial membrane potential, flow and laser scanning cytometry and mechanism based assays (Banfalvi, 2017). ELISA was used for detection of apoptosis in the studies of the functional effects of FV and the influence of FV on the effects of doxorubicin (discussed in section *5.6*) in this thesis. The ELISA method is based on detection of the early stage of apoptosis by detection of nucleosomes. Since it was observed significant changes in apoptosis in this thesis, it was assumed that this method was sensitive enough for this purpose.

Among the three approaches used to examine the effect of FV on apoptosis and proliferation, two of them supported the postulated antitumor effect of FV in breast cancer. Considering the uncertainty in the plasma experiments, it was legitimate to rely more on the other two experiments. The result for the two first approaches was also supported by the findings by Tinholt et al. (2020), which showed an increased overall survival with a higher expression of *F5*.

Whereas the antitumor effect of FV acts through the postulated complex for inhibition of TF-mediated PAR2 activation, was not proven according to the results in this thesis. In FV overexpression experiments, FV alone had an antitumor effect, while other experiments showed an antitumor effect together with APC and other coagulation factors. Moreover,

overexpression experiments gave an increase in apoptosis of 29%, while in comparison an increase in apoptosis of 214% was observed in the experiments with recombinant FVa and the coagulation factors involved in the postulated TF-mediated PAR2 inhibition complex. The results cannot determine which mechanisms are involved in the functional effects of FV in breast cancer cells, but the effect with FV, APC and PS may indicate that the postulated inhibition complex for TF-mediated PAR2 activation might be involved. The apoptotic effect observed with FVa, may also indicate that coagulation dependent mechanisms could be involved. Further experiments are needed to confirm the exact mechanisms involved in the functional effects of FV in breast cancer.

5.6 The influence of FV on the effect of doxorubicin

The three approaches used to examine the effect of FV on apoptosis and proliferation were also used to study if FV influenced doxorubicin effect in the triple negative breast cancer cells MDA-MB-231.

Overexpression of FV in doxorubicin treated cells resulted in a 45% increase in apoptosis and a 9% decrease in proliferation. In contrast to untreated cells, APC was not necessary to reduce proliferation. This might be due to the doxorubicin induced thrombomodulin which facilitates the activation of protein C to APC (Todorova et al., 2020). The results indicated that FV facilitated the effect of doxorubicin on apoptosis in the cells.

The effect of recombinant FV and coagulation factors involved in the postulated TF-mediated PAR2 inhibition complex was studied. The coagulation factors in the TF-mediated PAR2 activating complex resulted in a 47% reduction in apoptosis. With the postulated TF-mediated PAR2 inhibition complex, a 20% increase in apoptosis was observed with recombinant FV and a substantial larger increase of 162% was observed with recombinant FVa. No detectable effects of FV and the coagulation factors on proliferation were observed. The results indicated that recombinant FV, and especially recombinant FVa, facilitated the effect of doxorubicin on apoptosis in the cells.

The effect of FV deficient plasma combined with FV and APC was studied to include more natural elements in the cells like all coagulation factors, salts, hormones, lipids, immunoglobulins and fibrinogen. In opposite to the two previous approaches, only APC with plasma increased apoptosis by 89%. In combination with recombinant FV there was a 58% decrease in apoptosis and recombinant FVa led to a small increase of 16% in apoptosis. The results indicated that recombinant FV decreased the effect of doxorubicin on apoptosis while FVa increased the effect combined with the plasma factors. The apoptotic effect of FVa might indicate that coagulation dependent mechanisms are involved.

The lack of detection of effects on proliferation may be caused by the sensitivity of the WST-1 method used and was previously discussed in section *5.5*. The decreased reliability to the experiments with FV combined with plasma was also discussed in that section and was also applicable to these experiments.

Essentially, two of the three approaches showed that FV led to an increased in apoptosis and thus facilitated the effect of doxorubicin. Nevertheless, it should be taken into account that a similar pattern was observed in untreated cells, and it was legitimate to assume that the apoptotic effect of FV acted directly on the cells regardless of doxorubicin treatment. However, these results supported the postulated antitumor effect of FV in breast cancer and may be involved in the association between treatment response and elevated expression of *F5* which was found in the clinical data material in this thesis.

6. CONCLUSION

Through understanding the molecular mechanisms of the role of coagulation factors in promoting and inhibiting cancer progression, it may be possible to provide a more individualized treatment for both cancer and thrombosis in cancer patients. Moreover, it can contribute to attenuate cancer progression. The aim in this thesis was to study the expression, regulation and functional effects of FV during treatment with chemotherapy. This was studied in clinical data materials and in *in vitro* breast cancer cell lines.

The statistical analyses in the clinical data materials showed an association between *F5* expression and treatment response. The expression of *F5* differed in different breast cancer subtypes. The expression of *F5* was elevated in tumors with the ER/PR negative status compared to the positive status and a large amounts of ER/PR negative receptor status were present in responders to neoadjuvant chemotherapy. In the PAM50 subtypes the highest level of *F5* was in the basal subtype which was also associated with increased survival in other studies. Collectively, these results indicated that a higher expression of *F5* was associated with treatment response and suggested an antitumor effect of *F5* in breast cancer.

The *in vitro* experiments in breast cancer cell lines, MDA-MB-231 and MCF-7 revealed that chemotherapy treatment with epirubicin, doxorubicin and 5-fluorouracil resulted in an increased expression of *F5*. Epirubicin, doxorubicin and 5-fluorouracil are known to induce p53 activity, which indicated a role of p53 in the induction of *F5* for these drugs. Studies of p53 were conducted by p53 inhibition, *TP53* knockdown and *F5* promoter bindings sites for p53. The results for all of these approaches strongly indicated a role of p53 as a transcriptional regulator of the doxorubicin induced upregulation of the expression of *F5*. Functional studies of FV on apoptosis and proliferation in MDA-MB-231 cells revealed an increase in apoptosis with FV alone and a decrease in proliferation with FV together with APC. The results indicated an antitumor effect of FV, and a possible mechanism for these effects may be through inhibition of TF-mediated PAR2 activation. Simultaneously, FVa, and not FV, was a necessary cofactor to generate this effect, indicating a coagulation dependent mechanism. FV facilitated the doxorubicin effect in breast cancer cells further and this may be involved in the association

between treatment response and elevated expression of *F5* which was found in the clinical data material in this thesis.

The antitumor effect of FV was confirmed by the large major of the results in this thesis. This verifies that FV is associated with treatment response in certain chemotherapy treatments, is induced by several cytostatica and seems to be a cancer suppressor by increasing apoptosis with and without doxorubicin treatment. Also, it was indicated that the antitumor effect FV may function through the FV-APC-PS complex by inhibition of TF-mediated PAR2 activation, but the results also indicated that a coagulation dependent mechanism was involved in the antitumor effect of FV.

7. REFERENCES

Adams, R. L. C. & Bird, R. J. (2009). Review article: Coagulation cascade and therapeutics update: Relevance to nephrology. Part 1: Overview of coagulation, thrombophilias and history of anticoagulants. *Nephrology*, 14 (5): 462-470. doi: 10.1111/j.1440-1797.2009.01128.x.

Alberts, B., Johnson, A., Lewis, J., Morgan, D., Raff, M., Roberts, K. & Walter, P. (2015). *Molecular Biology of the Cell* 6th ed. New York: Garland Science.

Aniogo, E. C., George, B. P. A. & Abrahamse, H. (2017). Phthalocyanine induced phototherapy coupled with Doxorubicin; a promising novel treatment for breast cancer. *Expert review of anticancer therapy*, 17 (8): 693-702.

Arruebo, M., Vilaboa, N., Sáez-Gutierrez, B., Lambea, J., Tres, A., Valladares, M. & González-Fernández, Á. (2011). Assessment of the Evolution of Cancer Treatment Therapies. *Cancers (Basel)*, 3 (3): 3279-3330. doi: 10.3390/cancers3033279.

Asselta, R., Tenchini, M. L. & Duga, S. (2006). Inherited defects of coagulation factor V: the hemorrhagic side. *Journal of Thrombosis and Haemostasis*, 4 (1): 26-34. doi: 10.1111/j.1538-7836.2005.01590.x.

Banfalvi, G. (2017). Methods to detect apoptotic cell death. *Apoptosis*, 22 (2): 306-323.

BC Cancer Agency Cancer Drug Manual©. (2013). *Cyclophosphamide*: Provincial Health Services Authority. Available at: http://www.bccancer.bc.ca/health-professionals/clinical-resources/cancer-drug-manual/drug-index#c-content.

Beckman Coulter. (2017). *CleanSEQ*. Available at: https://labplan.ie/product/cleanseq/ (accessed: 26.09.2020).

BioLegend, I. (2008). *VEGF Pathway*. Available at: https://www.biolegend.com/en-us/vegf-pathway (accessed: 25.02.21).

Blandino, G., Levine, A. J. & Oren, M. (1999). Mutant p53 gain of function: differential effects of different p53 mutants on resistance of cultured cells to chemotherapy. *Oncogene*, 18 (2): 477-485.

Breastcancer.org. (2020). *Molecular Subtypes of Breast Cancer*. Available at: https://www.breastcancer.org/symptoms/types/molecular-subtypes (accessed: 01.10.2020).

Caminiti, M. F., El-Rabbany, M., Jeon, J. & Bradley, G. (2020). 5-Fluorouracil Is Associated With a Decreased Recurrence Risk in Odontogenic Keratocyst Management: A Retrospective Cohort Study. *Journal of Oral and Maxillofacial Surgery*.

CancerResearchUK. (2020). *How chemotherapy works*. Available at: https://www.cancerresearchuk.org/about-cancer/cancer-in-general/treatment/chemotherapy/how-chemotherapy-works (accessed: 08.09.2020).

Carey, L. A., Dees, E. C., Sawyer, L., Gatti, L., Moore, D. T., Collichio, F., Ollila, D. W., Sartor, C. I., Graham, M. L. & Perou, C. M. (2007). The triple negative paradox: primary tumor chemosensitivity of breast cancer subtypes. *Clinical cancer research*, 13 (8): 2329-2334.

Carthew, R. W. & Sontheimer, E. J. (2009). Origins and mechanisms of miRNAs and siRNAs. *Cell*, 136 (4): 642-655.

Carvalho, C., Santos, R. X., Cardoso, S., Correia, S., Oliveira, P. J., Santos, M. S. & Moreira, P. I. (2009). Doxorubicin: the good, the bad and the ugly effect. *Current medicinal chemistry*, 16 (25): 3267-3285.

Cheng, M., He, B., Wan, T., Zhu, W., Han, J., Zha, B., Chen, H., Yang, F., Li, Q. & Wang, W. (2012). 5-Fluorouracil nanoparticles inhibit hepatocellular carcinoma via activation of the p53 pathway in the orthotopic transplant mouse model. *PloS one*, 7 (10): e47115.

Cho, Y.-H., Ro, E. J., Yoon, J.-S., Mizutani, T., Kang, D.-W., Park, J.-C., Kim, T. I., Clevers, H. & Choi, K.-Y. (2020). 5-FU promotes stemness of colorectal cancer via p53-mediated WNT/β-catenin pathway activation. *Nature communications*, 11 (1): 1-13.

Corrie, P. G. (2007). Cytotoxic chemotherapy: clinical aspects. *Medicine*, 36 (1): 24-28. doi: 10.1016/j.mpmed.2007.10.012.
Cosan, D., Soyocak, A., Tekedereli, I., Gacar, G., Karaoz, E. & Ozpolat, B. (2010). *Doxorubicin-induced autophagy functions as a pro-survival pathway in breast cancer cells*: AACR.
Crawley, J. T. B. (2011). *The Coagulation Cascade and Its Regulation*. 1st ed. Boston, MA: Boston, MA: Springer US. pp. 357-370.
Creative Diagnostics. *P53 Signaling Pathway*. Available at: https://www.creative-diagnostics.com/p53-signaling-pathway.htm (accessed: 04.10.2020).
Czeczuga-Semeniuk, E., Wołczyński, S., Dabrowska, M., Dziecioł, J. & Anchim, T. (2004). The effect of doxorubicin and retinoids on proliferation, necrosis and apoptosis in MCF-7 breast cancer cells. *Folia histochemica et cytobiologica*, 42 (4): 221-227.
Daigeler, A., Klein-Hitpass, L., Chromik, A. M., Müller, O., Hauser, J., Homann, H.-H., Steinau, H.-U. & Lehnhardt, M. (2008). Heterogeneous in vitro effects of doxorubicin on gene expression in primary human liposarcoma cultures. *BMC cancer*, 8 (1): 1-17.
Doloff, J. C. & Waxman, D. J. (2015). Transcriptional profiling provides insights into metronomic cyclophosphamide-activated, innate immune-dependent regression of brain tumor xenografts. *BMC cancer*, 15 (1): 1-21.
Dumont, P., Leu, J.-J., Della Pietra, A. C., George, D. L. & Murphy, M. (2003). The codon 72 polymorphic variants of p53 have markedly different apoptotic potential. *Nature genetics*, 33 (3): 357-365.
ECACC. (2017a). *Cell line profile MCF-7*. England. Available at: https://admin.phe-culturecollections.org.uk/media/130237/mcf7-cell-line-profile.pdf (accessed: 31.05.2021).
ECACC. (2017b). *Cell line profile MDA-MB-231*. England. Available at: https://www.phe-culturecollections.org.uk/media/133182/mda-mb-231-cell-line-profile.pdf (accessed: 31.05.2021).
El-Serafi, I., Abedi-Valugerdi, M., Potácová, Z., Afsharian, P., Mattsson, J., Moshfegh, A. & Hassan, M. (2014). Cyclophosphamide alters the gene expression profile in patients treated with high doses prior to stem cell transplantation. *PLoS One*, 9 (1): e86619.
Esmon, C. T. (2000). Regulation of blood coagulation. *Biochimica et biophysica acta, Protein structure and molecular enzymology*, 1477 (1-2): 349-360. doi: 10.1016/s0167-4838(99)00266-6.
Estevezj. (2012). *File:Sanger-sequencing.svg*: Wikipedia. Available at: https://en.wikipedia.org/wiki/File:Sanger-sequencing.svg (accessed: 25.09.2020).
Falanga, A., Marchetti, M. & Vignoli, A. (2013). Coagulation and cancer: biological and clinical aspects. *Journal of Thrombosis and Haemostasis*, 11 (2): 223-233.
Fennerty, A. (2006). Venous thromboembolic disease and cancer. *Postgraduate medical journal*, 82 (972): 642-648.
Fernandes, C. J., Morinaga, L. T., Alves, J. L., Castro, M. A., Calderaro, D., Jardim, C. V. & Souza, R. (2019). Cancer-associated thrombosis: the when, how and why. *European Respiratory Review*, 28 (151).
Fragomeni, S. M., Sciallis, A. & Jeruss, J. S. (2018). Molecular subtypes and local-regional control of breast cancer. *Surgical Oncology Clinics*, 27 (1): 95-120.
Fritsche, M., Haessler, C. & Brandner, G. (1993). Induction of nuclear accumulation of the tumor-suppressor protein p53 by DNA-damaging agents. *Oncogene*, 8 (2): 307-318.
GmbH, I. (2015). *WST-1 CTLL-2 cell proliferation Kit (ready-to-use)*. Hamburg, Germany.
Hanahan, D. & Weinberg, R. (2015). *Chapter 2 : Hallmarks of Cancer : An Organizing Principle for Cancer Medicine*.
Haque, W., Verma, V., Hatch, S., Klimberg, V. S., Butler, E. B. & Teh, B. S. (2018). Response rates and pathologic complete response by breast cancer molecular subtype following neoadjuvant chemotherapy. *Breast cancer research and treatment*, 170 (3): 559-567.

Hofmann, E., Weibel, S. & Szalay, A. A. (2014). Combination treatment with oncolytic Vaccinia virus and cyclophosphamide results in synergistic antitumor effects in human lung adenocarcinoma bearing mice. *Journal of translational medicine*, 12 (1): 1-14.
Hollstein, M., Soussi, T., Thomas, G., Von Brevern, M.-C. & Bartsch, H. (1997). P53 gene alterations in human tumors: perspectives for cancer control. *Risk and Progression Factors in Carcinogenesis*: 369-389.
Hughes, P., Marshall, D., Reid, Y., Parkes, H. & Gelber, C. (2007). The costs of using unauthenticated, over-passaged cell lines: how much more data do we need? *Biotechniques*, 43 (5): 575-586.
Ju, J., Schmitz, J. C., Song, B., Kudo, K. & Chu, E. (2007). Regulation of p53 expression in response to 5-fluorouracil in human cancer RKO cells. *Clinical cancer research*, 13 (14): 4245-4251.
Kanat, O. & Ertas, H. (2019). Existing anti-angiogenic therapeutic strategies for patients with metastatic colorectal cancer progressing following first-line bevacizumab-based therapy. *World journal of clinical oncology*, 10 (2): 52.
Kastan, M. B., Onyekwere, O., Sidransky, D., Vogelstein, B. & Craig, R. W. (1991). Participation of p53 protein in the cellular response to DNA damage. *Cancer research*, 51 (23 Part 1): 6304-6311.
Katt, M. E., Placone, A. L., Wong, A. D., Xu, Z. S. & Searson, P. C. (2016). In vitro tumor models: advantages, disadvantages, variables, and selecting the right platform. *Frontiers in bioengineering and biotechnology*, 4: 12.
Kaur, G. & Dufour, J. M. (2012). *Cell lines: Valuable tools or useless artifacts*: Taylor & Francis.
Kazazi-Hyseni, F., Beijnen, J. H. & Schellens, J. H. (2010). Bevacizumab. *The oncologist*, 15 (8): 819.
Khasraw, M., Bell, R. & Dang, C. (2012). Epirubicin: is it like doxorubicin in breast cancer? A clinical review. *The Breast*, 21 (2): 142-149.
Khleif, S. N., Rixe, O. & Skeel, R. T. (2016). *Skeel's Handbook of Cancer Therapy*. [9th ed.]. ed. Philadelphia, Pennsylvania: Wolters Kluwer.
Khorana, A. A., Francis, C. W., Culakova, E., Kuderer, N. M. & Lyman, G. H. (2007). *Thromboembolism is a leading cause of death in cancer patients receiving outpatient chemotherapy*. [Oxford] :. pp. 632-634.
Kudoh, K., Ramanna, M., Ravatn, R., Elkahloun, A. G., Bittner, M. L., Meltzer, P. S., Trent, J. M., Dalton, W. S. & Chin, K.-V. (2000). Monitoring the expression profiles of doxorubicin-induced and doxorubicin-resistant cancer cells by cDNA microarray. *Cancer research*, 60 (15): 4161-4166.
Kuter, D. J. (2015). Managing thrombocytopenia associated with cancer chemotherapy. *Oncology*, 29 (4): 282-282.
Kvolik, S., Jukic, M., Matijevic, M., Marjanovic, K. & Glavas-Obrovac, L. (2010). An overview of coagulation disorders in cancer patients. *Surgical oncology*, 19 (1): e33-e46.
Kwaan, H. C. & Vicuna, B. (2007). Thrombosis and bleeding in cancer patients. *Oncology Reviews*, 1 (1): 14-27.
Königsbrügge, O., Pabinger, I. & Ay, C. (2014). Risk factors for venous thromboembolism in cancer: novel findings from the Vienna Cancer and Thrombosis Study (CATS). *Thromb Res*, 133: S39-S43. doi: 10.1016/S0049-3848(14)50007-2.
Lam, W. & Moosavi, L. (2020). *Physiology, Factor V*. Treasure Island (FL): StatPearls Publishing LLC. Available at: https://www.ncbi.nlm.nih.gov/books/NBK544237/ (accessed: 15.09.2020).
Leibniz Institute. *MCF-7*. Germany: DSMZ-German Collection of Microorganisms and Cell Cultures. Available at: https://www.dsmz.de/collection/catalogue/details/culture/ACC-115 (accessed: 30.09.2020).
Liang, H. P. H., Kerschen, E. J., Basu, S., Hernandez, I., Zogg, M., Jia, S., Hessner, M. J., Toso, R., Rezaie, A. R., Fernandez, J. A., et al. (2015). Coagulation factor V mediates inhibition of tissue factor signaling by activated protein C in mice. *Blood*, 126 (21): 2415-2423. doi: 10.1182/blood-2015-05-644401.
Longley, D. B., Harkin, D. P. & Johnston, P. G. (2003). 5-fluorouracil: mechanisms of action and clinical strategies. *Nature reviews cancer*, 3 (5): 330-338.
Lowe, S. W. & Jacks, T. (1997). p53 and treatment of bladder cancer. *Nature*, 385 (6612): 124-125.

Madhavan, H. (2007). Simple Laboratory methods to measure cell proliferation using DNA synthesis property. *Journal of stem cells & regenerative medicine*, 3 (1): 12.
Mitsis, T., Efthimiadou, A., Bacopoulou, F., Vlachakis, D., Chrousos, G. P. & Eliopoulos, E. (2020). Transcription factors and evolution: an integral part of gene expression. *World Academy of Sciences Journal*, 2 (1): 3-8.
Momenimovahed, Z. & Salehiniya, H. (2019). Epidemiological characteristics of and risk factors for breast cancer in the world. *Breast Cancer (Dove Med Press)*, 11: 151-164. doi: 10.2147/bctt.s176070.
Montero, A. J., Escobar, M., Lopes, G., Glück, S. & Vogel, C. (2012). Bevacizumab in the treatment of metastatic breast cancer: friend or foe? *Current oncology reports*, 14 (1): 1-11.
Neuenschwander, P. F. (2006). COAGULATION CASCADE | Factor V. In *Encyclopedia of Respiratory Medicine*, pp. 490-494. University of Texas Health Center, Tyler, TX, USA: Academic Press.
Ogino, M. H. & Tadi, P. (2020). Cyclophosphamide. *StatPearls [Internet]*.
Palta, S., Saroa, R. & Palta, A. (2014). Overview of the coagulation system. *Indian J Anaesth*, 58 (5): 515-523. doi: 10.4103/0019-5049.144643.
Pan, L., Yu, Y., Yu, M., Yao, S., Mu, Q., Luo, G. & Xu, N. (2019). Expression of flTF and asTF splice variants in various cell strains and tissues. *Molecular medicine reports*, 19 (3): 2077-2086.
Parker, A. L., Newman, C., Briggs, S., Seymour, L. & Sheridan, P. J. (2003). Nonviral gene delivery: techniques and implications for molecular medicine. *Expert reviews in molecular medicine*, 5 (22): 1.
Perou, C. M., Sørlie, T., Eisen, M. B., van de Rijn, M., Jeffrey, S. S., Rees, C. A., Pollack, J. R., Ross, D. T., Johnsen, H., Akslen, L. A., et al. (2000). Molecular portraits of human breast tumours. *Nature*, 406 (6797): 747-52. doi: 10.1038/35021093.
PHARMACY. (2016). *Cytotoxic Agents*. Available at: https://basicmedicalkey.com/cytotoxic-agents/ (accessed: 01.09.2020).
Phillips, T. (2008). Regulation of Transcription and Gene Expression in Eukaryotes. *Nature Education*, 1 (1).
Pilco-Ferreto, N. & Calaf, G. M. (2016). Influence of doxorubicin on apoptosis and oxidative stress in breast cancer cell lines. *International journal of oncology*, 49 (2): 753-762.
Pollen, I. (2014). *Characterization of TFPIalpha and TFPIbeta on growth, adhesion and migration in breast cancer cells*: Norwegian University of Life Sciences, Ås.
Promega. *pGL3 Luciferase Reporter Vectors*: Promega. Available at: https://no.promega.com/products/luciferase-assays/genetic-reporter-vectors-and-cell-lines/pgl3-luciferase-reporter-vectors/?catNum=E1751 (accessed: 13.11.20).
Promega. *pRL Renilla Luciferase Control Reporter Vectors*. Available at: https://no.promega.com/products/luciferase-assays/genetic-reporter-vectors-and-cell-lines/prl-renilla-luciferase-control-reporter-vectors/?catNum=E2231 (accessed: 13.11.2020).
Pulverer, B. (2005). Sequence-specific DNA-binding transcription factors. *Nature Milestones*. doi: 10.1038/nrm1800.
Riss, T. L., Moravec, R. A., Niles, A. L., Duellman, S., Benink, H. A., Worzella, T. J. & Minor, L. (2016). Cell viability assays. *Assay Guidance Manual [Internet]*.
Roche. (2016). *Cell Death Detection ELISAPLUS, Version 15*.
Ruf, W., Disse, J., CARNEIRO-LOBO, T. C., Yokota, N. & Schaffner, F. (2011). Tissue factor and cell signalling in cancer progression and thrombosis. *Journal of Thrombosis and Haemostasis*, 9: 306-315.
Ruf, W. (2014). FXa takes center stage in vascular inflammation. *Blood, The Journal of the American Society of Hematology*, 123 (11): 1630-1631.
Rusch, V., Klimstra, D., Venkatraman, E., Oliver, J., Martini, N., Gralla, R., Kris, M. & Dmitrovsky, E. (1995). Aberrant p53 expression predicts clinical resistance to cisplatin-based chemotherapy in locally advanced non-small cell lung cancer. *Cancer research*, 55 (21): 5038-5042.

Schaffner, F. & Ruf, W. (2009). Tissue factor and PAR2 signaling in the tumor microenvironment. *Arteriosclerosis, thrombosis, and vascular biology*, 29 (12): 1999-2004.
Scientific, T. F. (2018). *Product Information: Thermo Scientific GeneRuler DNA Ladder Mix, ready-to-use*. Available at: https://assets.thermofisher.com/TFS-Assets/LSG/manuals/MAN0013015_GeneRuler_DNALadder_RTU_50ug_UG.pdf (accessed: 09.10.2020).
Segers, K., Dahlbäck, B. & Nicolaes, G. A. (2007). Coagulation factor V and thrombophilia: background and mechanisms. *Thrombosis and haemostasis*, 98 (09): 530-542.
Smith, S. A. (2009). The cell-based model of coagulation. *J Vet Emerg Crit Care (San Antonio)*, 19 (1): 3-10. doi: 10.1111/j.1476-4431.2009.00389.x.
Soff, G. (2019). *Thrombosis and Hemostasis in Cancer*. 1st ed. 2019. ed., vol. 179. Cham: Springer International Publishing : Imprint: Springer.
Stavik, B., Skretting, G., Aasheim, H.-C., Tinholt, M., Zernichow, L., Sletten, M., Sandset, P. M. & Iversen, N. (2011). Downregulation of TFPI in breast cancer cells induces tyrosine phosphorylation signaling and increases metastatic growth by stimulating cell motility. *Bmc Cancer*, 11 (1): 1-14.
Su, S., Li, Y., Luo, Y., Sheng, Y., Su, Y., Padia, R., Pan, Z., Dong, Z. & Huang, S. (2009). Proteinase-activated receptor 2 expression in breast cancer and its role in breast cancer cell migration. *Oncogene*, 28 (34): 3047-3057.
Sullivan, A., Syed, N., Gasco, M., Bergamaschi, D., Trigiante, G., Attard, M., Hiller, L., Farrell, P. J., Smith, P. & Lu, X. (2004). Polymorphism in wild-type p53 modulates response to chemotherapy in vitro and in vivo. *Oncogene*, 23 (19): 3328-3337.
Sun, H. (2015). Factor V: an active player in inflammation. *Blood, The Journal of the American Society of Hematology*, 126 (21): 2352-2353.
Sørlie, T., Perou, C. M., Tibshirani, R., Aas, T., Geisler, S., Johnsen, H., Hastie, T., Eisen, M. B., van de Rijn, M., Jeffrey, S. S., et al. (2001). Gene expression patterns of breast carcinomas distinguish tumor subclasses with clinical implications. *Proc Natl Acad Sci U S A*, 98 (19): 10869-74. doi: 10.1073/pnas.191367098.
Tacar, O., Sriamornsak, P. & Dass, C. R. (2013). Doxorubicin: an update on anticancer molecular action, toxicity and novel drug delivery systems. *Journal of pharmacy and pharmacology*, 65 (2): 157-170.
Thermo Fisher Scientific. *How TaqMan Assays Work*. Available at: https://www.thermofisher.com/no/en/home/life-science/pcr/real-time-pcr/real-time-pcr-learning-center/real-time-pcr-basics/how-taqman-assays-work.html (accessed: 19.09.2020).
Thermo Fisher Scientific. *Luciferase Reporters*. Available at: https://www.thermofisher.com/no/en/home/life-science/protein-biology/protein-biology-learning-center/protein-biology-resource-library/pierce-protein-methods/luciferase-reporters.html (accessed: 27.10.2020).
Thermo Fisher Scientific. *Overview of ELISA*. Available at: https://www.thermofisher.com/no/en/home/life-science/protein-biology/protein-biology-learning-center/protein-biology-resource-library/pierce-protein-methods/overview-elisa.html (accessed: 19.09.2020).
Tinholt, M., Viken, M. K., Dahm, A. E., Vollan, H. K. M., Sahlberg, K. K., Garred, Ø., Børresen-Dale, A.-L., Jacobsen, A. F., Kristensen, V. & Bukholm, I. (2014). Increased coagulation activity and genetic polymorphisms in the F5, F10 and EPCRgenes are associated with breast cancer: a case-control study. *Bmc Cancer*, 14 (1): 845.
Tinholt, M., Garred, Ø., Borgen, E., Beraki, E., Schlichting, E., Kristensen, V., Sahlberg, K. & Iversen, N. (2018). Subtype-specific clinical and prognostic relevance of tumor-expressed F5 and regulatory F5 variants in breast cancer: the CoCaV study. *Journal of Thrombosis and Haemostasis*, 16 (7): 1347-1356.

Tinholt, M., Stavik, B., Tekpli, X., Garred, Ø., Borgen, E., Kristensen, V., Sahlberg, K. K., Sandset, P. M. & Iversen, N. (2020). Coagulation factor V is a marker of tumor-infiltrating immune cells in breast cancer. *OncoImmunology*, 9 (1): 1824644.

Todorova, V. K., Hsu, P.-C., Wei, J. Y., Lopez-Candales, A., Chen, J. Z., Su, L. J. & Makhoul, I. (2020). Biomarkers of inflammation, hypercoagulability and endothelial injury predict early asymptomatic doxorubicin-induced cardiotoxicity in breast cancer patients. *American Journal of Cancer Research*, 10 (9): 2933.

Vossen, C. Y., Hoffmeister, M., Chang-Claude, J. C., Rosendaal, F. R. & Brenner, H. (2011). Clotting Factor Gene Polymorphisms and Colorectal Cancer Risk.

Wattel, E., Preudhomme, C., Hecquet, B., Vanrumbeke, M., Quesnel, B., Dervite, I., Morel, P. & Fenaux, P. (1994). p53 mutations are associated with resistance to chemotherapy and short survival in hematologic malignancies.

Weinberg, R. A. (2014). *The biology of cancer*. 2nd ed. New York: Garland science.

Weller, M. (1998). Predicting response to cancer chemotherapy: the role of p53. *Cell and tissue research*, 292 (3): 435-445.

WHO. (2019). *International Agency for Research on Cancer*: GLOBOCAN 2018. Available at: http://gco.iarc.fr/today (accessed: 08.09.2020).

Wojtukiewicz, M. Z., Hempel, D., Sierko, E., Tucker, S. C. & Honn, K. V. (2015). Protease-activated receptors (PARs)—biology and role in cancer invasion and metastasis. *Cancer and Metastasis Reviews*, 34 (4): 775-796.

Xu, Y., Yao, L., Ouyang, T., Li, J., Wang, T., Fan, Z., Lin, B., Lu, Y. & Xie, Y. (2005). p53 Codon 72 polymorphism predicts the pathologic response to neoadjuvant chemotherapy in patients with breast cancer. *Clinical Cancer Research*, 11 (20): 7328-7333.

Yersal, O. & Barutca, S. (2014). Biological subtypes of breast cancer: Prognostic and therapeutic implications. *World journal of clinical oncology*, 5 (3): 412.

Zhan, Q., Carrier, F. & Fornace, A. (1993). Induction of cellular p53 activity by DNA-damaging agents and growth arrest. *Molecular and cellular biology*, 13 (7): 4242-4250.

Zhang, X., Li, Q., Zhao, H., Ma, L., Meng, T., Qian, J., Jin, R., Shen, J. & Yu, K. (2017). Pathological expression of tissue factor confers promising antitumor response to a novel therapeutic antibody SC1 in triple negative breast cancer and pancreatic adenocarcinoma. *Oncotarget*, 8 (35): 59086.

Zhao, D., Yuan, H., Yi, F., Meng, C. & Zhu, Q. (2014). Autophagy prevents doxorubicin-induced apoptosis in osteosarcoma. *Molecular medicine reports*, 9 (5): 1975-1981.

APPENDIX

APPENDIX A

Contains tables of instruments, kits, reagents, drugs, coagulation factors, disposables and software used in this thesis.

Table A 1: Software with suppliers.

Software:	Supplier:
SeqScape™ v4.0	Applied Biosystems
Sequence Scanner Software 2.0	Applied Biosystems
RStudio	RStudio, PBC
SoftMax® Pro 6.4	Molecular Devices
ImageQuant™ TL ID v8.1	Cytiva

Table A 2: Instruments with suppliers.

Instrument:	Supplier:
ABI 3730 DNA Analyzer	Applied Biosystems
BioMek FX	Beckman Coulter
Forma™ 370 Steri-Cycle™ CO_2 Incubator	Thermo Scientific
NanoDrop® ND-1000	Thermo Scientific
Nikon Eclipse TE 300	Nikon
Veriti™ 96 well Thermal Cycler	Applied Biosystems
NucleoCounter® NC-100™	ChemoMetec A/S
Incubator	Termaks A/S
2720 Thermal Cycler	Applied Biosystems
1296-003 DELFIA® Plateshake	PerkinElmer
GloMax 96 Microplate Luminometer	Promega
VersaMax™ Microplate Reader	Molecular Devices
Nikon Eclipse -FTL	Nikon
ImageQuant™ LAS 4000	Cytiva
QuantStudio 12K Flex	Thermo Fisher
Microfuge® 22R Centrifuge	Beckman Coulter™
Power Pac 300	Bio-Rad

Sub-cell® GT	Bio-Rad

Table A 3: Disposables with suppliers.

Disposable:	Supplier:
NucleoCasette™	ChemoMetec
Nunc™ Cell Culture Treated Multidishes (96- 24- and 12 well)	Thermo Fisher Scientific
Microplate, 96 well, half area, µclear®, white, med. binding	Greiner bio-one GmbH
MicroAmp™ Optical 384-Well Reaction Plate with Barcode	Thermo Fisher Scientific
0.2ml Non-skirted 96-well PCR Plate	Thermo Fisher Scientific
T75, T175 and T225 EasYFlask, TC Surface, Filter Cap	Thermo Fisher Scientific
Acrodisc® 32mm Syringe Filter 0.2µm Supor Membrane Non-Pyrogenic	Pall
Cell scraper 240 mm TPP – blade 13 mm	TPP Techno Plastic Products
BD Microlance™ 3 0.8mm*50mm	Fisher Scientific
Omnifix® 2ml Luer Solo	B. Braun Medical
BD Falcon™ Petri Dish	Sigma-Aldrich®

Table A 4: Kits with suppliers and catalogue numbers.

Kit:	Supplier:	Catalogue no:
Zyppy™ Plasmid Miniprep Kit (Ver. 1.2.6).	Zymo Reasearch	D4019
ZymoPURE™ II Plasmid Maxiprep Kit	Zymo Reasearch	D4202
BigDye®Terminator v3.1 Cycle Sequencing Kit	Applied Biosystems	4337455
Lipofectamine™ 3000 Transfection Reagent	Invitrogen™	L3000015
CleanSEQ® Kit	Agencourt®	A29161
Dual-Luciferase® Reporter Assay System	Promega	E1960
Monarch® Total RNA Miniprep Kit	NEB	T2010S
High-Capacity cDNA Reverse Transcription Kit	Applied Biosystems	4368814
Pierce™ BCA Protein Assay Kit	Thermo Fisher Scientific	23225
MycoAlert® Mycoplasma Detectioin Kit	Lonza	LT07-218
TaqMan™ Gene Expression Master Mix	Thermo Fisher Scientific	4370074
Cell Death Detection ELISA^{PLUS} Kit	Sigma-Aldrich®	11774425001
Human Factor V ELISA Kit	Abcam	ab137976

Table A 5: Chemicals and reagents with suppliers and catalogue numbers.

Chemical / reagent:	Supplier:	Catalogue no:
Ampicillin, Sodium Salt	Calbiochem®	171254
Fetal Bovine Serum	Biowest	Si86H-500
Dulbecco´s phosphate-buffered Saline (DPBS)	Thermo Fisher Scientific	14190250
S.O.C Medium	Invitrogen™	1749148
Trypsin-EDTA (0.05%)	Lonza	CC-5012
imMedia™ Growth Medium, agar, ampicillin	Invitrogen™	Q60120
GeneRuler DNA Ladder Mix, ready-to-use	Thermo Fisher Scientific	SM0334
Opti-MEM® Reduced Serum Medium	Thermo Fisher Scientific	31985062
Reagent A100 Lysis buffer	Chemometec	910-0003
Reagent B Stabilizing buffer	Chemometec	910-0002
Dulbecco´s Modified Eagle Medium (DMEM)	Thermo Fisher Scientific	
Cell proliferation reagent WST-1	Sigma-Aldrich®	11644807001
RIPA buffer	Sigma-Aldrich®	R0278
Tryptone	Sigma-Aldrich®	119311000
Yeast extract	Sigma-Aldrich®	Y1625
Agar-agar	Sigma-Aldrich®	101614
Halt™ Protease and Phosphatase Inhibitor Cocktail	Thermo Fisher Scientific	78441
TaqMan™ Gene Expression Master Mix	Applied Biosystems	43369016
GelRed Nucleic Acid Gel Stain	VWR	730-2958
Lipofectamine®RNAiMax	Invitrogen	13778150
OptiMem™ Reduced Serum Medium	Thermo Fisher Scientific	31985062
Dimethyl sulfoxide (DMSO)	Sigma-Aldrich®	D2650
50x TAE Buffer	Bio-Rad	161-0743
Seakem® LE Agarose	Lonza	50004
Factor V deficient plasma	Nordic Diagnostica	FV-ID
PAR-2 agonist	Sigma-Aldrich®	539109-1MG

Table A 6: Drugs with suppliers and catalogue numbers.

Drug:	Supplier:	Catalog no:
Adriamycin®	Pfizer	505875
Epirubicin medac 2 mg/ml	Medac	147842
Cyclophosphamide Monohydrate	Sigma-Aldrich®	239785
Fluorouracil Accord 50 mg/ml	Accord	548357
Bevacizumab (VEGF Inhibitor, VI – Calbiochem)	Sigma-Aldrich®	676495-1MG
Hirudin	Sigma-Aldrich®	H0393-100UN

Table A 7: Factors with suppliers and catalog numbers.

Factor:	Supplier:	Catalog no:
Human FV	Nordic Diagnostica	HCV-0100
Human FVa	Nordic Diagnostica	HCV-0110
Human APC	Nordic Diagnostica	HCAPC-0080
Human protein S	Nordic Diagnostica	HCPS-0090
Human FXa	Nordic Diagnostica	HCXA-0060
Human FVIIa	Nordic Diagnostica	HCVIIA-0031

Table A 8: siRNA with suppliers and catalog numbers.

siRNA:	Supplier:	Catalog no:
siRNA p53	Thermo Fisher Scientific	4390824
siRNA p53 negative control	Thermo Fisher Scientific	AM4642

Table A 9: Plasmids with suppliers and catalog numbers.

Plasmid:	Supplier:	Catalog no:
pMT2-FV-wt (corrected version of pMT2-V)	ATCC	40515
pMT2-negative control (empty vector - version of pMT2-V)	ATCC	40515
Cignal Finder p53 (from Cignal Reporter Assay Kit p53)	QIAGEN	CCS-004L

APPENDIX B

Contains table with the sequence of the complete F5 promoter in plasmids used in this thesis.

Table B 1: F5 promoter sequence.

F5 promoter sequence 2145bp:
TTATAGTAGTCATCTTGTCTCTGTAAAATGTAATTAAATAAATATGTCATGTACACTGTATATACATAAGCAAACATGCAA ATAAAAAAGCAGCCTACTCAAAGGTTACAATAATGTTGCAACAATTCTGGTAGTAACCTTGGGATTTAGGGACACAGTG CTTTCAAAACGTTTCTCTGATACACTGCCAGTAGCATCTCTGACTGCTTATTTAAATGTCAATCAGTAGGCTAGGTGTTCT AGGACTTTGGTCTCAACCCTGTTTCCTGAGTCAGAATCTACATTTTGTAAAAGTTCCCCTGGGAATTCTGATGGTCTGCC AACTTTGGGAGACACTGATAATATTGTAGATAAAGAAGTGTAAGCAACTGTTCAGTTAGGGAGACAATAGATACCTGCA TGGAATAACAAAAGGTAATTAACATGATTATATAATTTGAATAGTGTTGTAATAGTTCATAAAATGGAAAAGCCAATTTG AGCCCAGAATCTGGGAGATAGGCAGAACTCTGGACTGTAAAGAATGGCCCAGCAAAGAGGAAGAAAATGGGCATTCT AAGTTGGTGCAATAATATCAGCACAGGAGAAAAGACAGAATATTGGGGGGAGTGGGGAGGGAGGAAGAGGCTGTTG ATGAGCCTGATATCATTAACAGAGACCTCATGTGAGGTGCCAGATTACAATTTATTGAATGTACTGAATGCATAAAGCAT AAGACAGAAACCTGGAGCCATGCAGATACAGGGAACCCAGGACAAGTCATTATGATGCCTCAGACAATATAATTCGCA GATTCTCTATCAATAGCAAAGTAAGATTTAAGGTGCTGTGAAACAGTCAGATCCTTCAAGAAAAACAAGAATACAAGGG GTCCTGGAGACAGGAAAATATGATCATAATAATAAATTTGTGATTCCTTCTTTCTCTCTTTTTCTCTTTCTTTCTTTTTCTTT CTTTCTTTTTTTTTTTTGATGGAGTTTTGCTCTCGTTGCCCAGGCTGGAGTAAAATGGCATGATATCAGCTCACTGCAAAC TCCACCTTCCAGGTTCAAGCAATTCTCTTGCCTCAATCTCTCGAGTAGGTGGGATTACAGGTGTCCACCACAACGCCCGG CTAATTTTTTATATTTTTAGTAGAGAAGGGTTTCACCATGTTGGCCAGGCTGGTCTTGAACTCCTGACCTCAGGTGATTCA CCCGCCTTGGCCTCCCAAAGTACTGGGATTACAGGCGTGAGCCACTGCGCCTAGCCTCTGTGTGTTAAGTGCTGGAACTA TAGTTTACAGTAGCATTTTATCCTCCCAACATACCCTATCAGGAAAAATTATTATTGTCATCCTTATTTCACAGATGTCAA AACTGAACAGAGAGGTACAGTAACTTGCCCAAGACAACACAGCTAGTAAGTGAAACTGAAATCTGGACAACTGATTTTT TTCAGCCAAGCTCTTCAAGCCCGCTGCTATGCTGCAGCTTAGCTGGCGACAGGCCCTTATCAAGGCAGAACTGTGCCTT GATAGAGGCCAGGAAGGCGATTCAGAGCAGTAGGCCTTGTCCATGTGTTTGTTCCCTGCTTCTTCACCACTTGAAAATA GTGTTTCAGTGCCCAGTAACAGGGCACAATACTCTTTTCCTCAGATTAAAAGGGGAGCCATCTGCTTAAGGTGGTTGGG TGCCACTGCACTGCACAGAAGGTTCTCCAAGTGTGAGCTTGGACCCAGGCAGGCCTCAGGTCAGTGGTAACGGACGAC TGCTTCCGTGGTGTTGGCAGGTGGAAATGGAGGGATACAGCTTTGTCCGGCTCATGAATCCCTGGGCATTGTCCCGCCT GCTAGAGCCTCTGATCTCTGCCCCTTCTTCACCTGCAGTAAAACAGTCACTAGTTTGGTTGCTCTCCCTAATACCTCTGGT CACTGGGAGCTGTGATCTCACCAAACCCCTGCCAGGAAAAGCCCCAGAAAAAGCGGAGGGAGTGAGAGCCAGAGGCT GCTGCTGCCGTTTGCAAGAACTGCAGGGGAGGAGGACGCTGCCACCCACAGCCTCTAGAGCTCATTGCAGCTGGGACA GCCCGGAGTGTGGTTAGCAGCTCGGCAAGCGCTGCCCAGGTCCTGGGGTGGTGGCAGCCAGCGGGAGCAGGAAAGG AAGCATG *

* Green markers indicate putative *p53* sites, grey markers indicate putative *p53* sites and pink markers indicates the chosen primers.

APPENDIX C

Contains recipes for solution used in this thesis.

Lysogeny Broth (LB) medium:

10 g tryptone

10 g NaCl

5 g yeast extract

900 mL MQ-H_2O

pH adjusted to 7.0 using 12 M HCl

Volume adjusted to 1 L using MQ-H_2O

Autoclave solution

1% Agarose gel:

0.5 g Seakem® LE Agarose

50 ml 1x TAE Electrophoresis buffer

Boil for 30 seconds and add 5 µl GelRed Nucleic Acid Gel Stain

RIPA lysis buffer with inhibitor:

100x Halt™ Protease & Phosphatase Inhibitor cocktail diluted 1:100 in

1x RIPA buffer

APPENDIX D

Contains standard curves and figures used in this thesis.

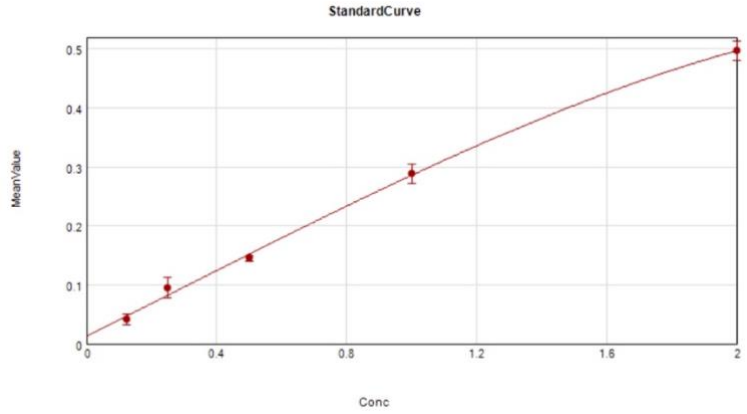

Figure D1: Standard curve for albumin (0-2mg/ml) at 562nm absorbance. *The standard curve was used to calculate total protein levels in cell lysates in MCF-7 and MDA-MB-231 cells.*

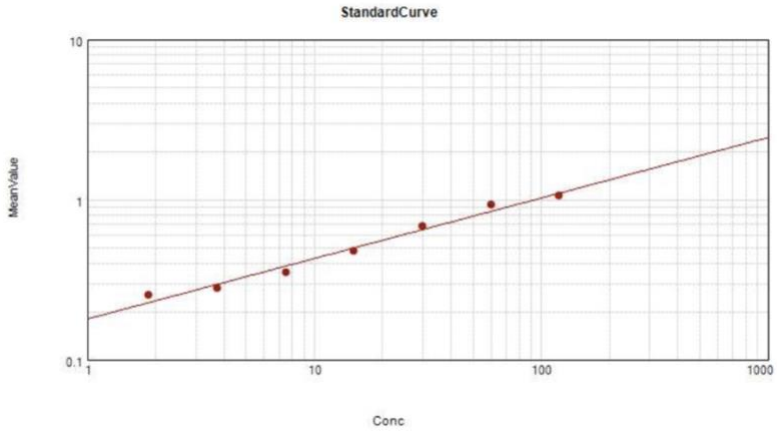

Figure D2: Standard curve for FV concentrations (0-120 ng/ml) at 450 nm absorbance. *The standard curve was used to calculate FV levels in cell lysates in MCF-7 and MDA-MB-231 cells*

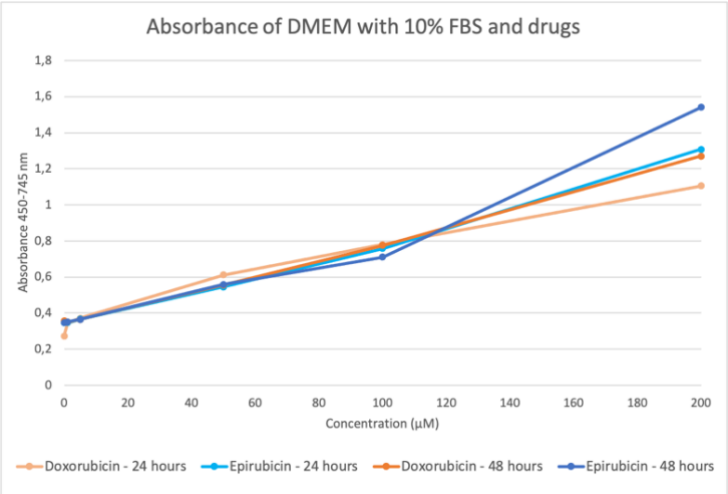

Figure D3: Absorbance (450-745 nm) of DMEM with 10% FBS, doxorubicin or epirubicin and WST-1. *The absorbance was measured after 24 and 48 hours. The curve was used in IC_{50} calculations to correct for the absorbance of the strong dye.*

Norges miljø- og biovitenskapelige universitet
Noregs miljø- og biovitskapelege universitet
Norwegian University of Life Sciences

Postboks 5003
NO-1432 Ås
Norway